# Characterizing the neurochemical basis of hypoxia signaling in the zebrafish gill

**Maddison Reed**

Thesis submitted to the University of Ottawa
in partial fulfillment of the requirements for the
Doctorate in Philosophy Degree in Biology

Department of Biology
Faculty of Science
University of Ottawa

## ACKNOWLEDGEMENTS

This thesis represents the culmination of *years* of research, countless hours of work, and far too many cups of coffee. It would not have been possible without the support, encouragement, and occasional well-timed distractions from many individuals.

First and foremost, I would like to thank my supervisor, Dr. Michael Jonz, for his unwavering guidance throughout this journey. Michael, your ability to simultaneously challenge and support me has been instrumental in this process. Thank you for never questioning my sanity (out loud) and for always providing constructive feedback—even when I may have secretly been hoping for a compliment instead. Your mentorship has been invaluable, and I hope we have the opportunity to work together again.

To my thesis advisory committee, Dr. Katie Gilmour and Dr. Jan Mennigen. Thank you for the time and effort you put into every committee meeting. You both brought unique perspectives that improved the quality of this thesis beyond what I could have imagined.

To the physiology professors who supported me just as much in non-academic ways as they did academically – John Lewis, Tuan Bui, and Emily Standen. I can only hope to one day be as patient as John, as curious as Em, and as funny as Tuan.

To Mary Upshall and Steph Gaudreau, my grad school queens. Thank you for being here. Between our endless coffee chats, post-experiment drinks, and conference adventures, the two of you made this time unforgettable.

To my partner, Bryson Perrin, whose support kept me sane (or at least *mostly* sane) throughout this entire process. You've been my rock, my sounding board, and my personal therapist—sometimes all in the same day. Thank you.

To my parents, Rick and Janette Reed, who have supported me from day one.
To Kaley Madigan, who knew I could do this long before I ever did. And to my amazing friends near and far, who despite having no idea what I was doing these past five years (including my personal favourite – studying glow in the dark fish) supported me in every way anyway. I am so lucky to have had such a wonderful, albeit slightly chaotic, support network.

Thank you.

**Play the Eras tour intro song here**

## ABSTRACT

Oxygen sensing and the physiological responses to hypoxia are essential for survival in aquatic environments. In teleost fish, the gills act as the primary site for detecting oxygen levels and initiating compensatory responses. Neuroepithelial cells (NECs) in the gills are key peripheral oxygen sensors in aquatic vertebrates and share morphological features with mammalian oxygen chemoreceptors, such as those in the carotid body. Upon detecting hypoxia, NECs inhibit background $K^+$ channels, leading to membrane depolarization and neurotransmitter release. This cascade activates sensory pathways in the gills projecting to higher order centers, resulting in physiological responses like hyperventilation. Despite the extensive research on vertebrate ventilatory responses to hypoxia, the specific neurotransmitters, receptors, and afferent pathways that mediate these responses in fish remain poorly understood. Using an isolated gill preparation from *Tg(elavl3:GCaMP6s)* zebrafish, we measured hypoxia-induced changes in intracellular $Ca^{2+}$ concentration ($[Ca^{2+}]_i$) in both NECs and postsynaptic chain neurons (ChNs). Our results show that both NECs and ChNs exhibit hypoxia-induced increases in $[Ca^{2+}]_i$. Importantly, we found that a functional NEC-ChN synapse is required for the hypoxia-induced increase in $[Ca^{2+}]_i$ in ChNs, and that these postsynaptic responses are modulated by presynaptic dopamine through dopamine $D_2$ receptors ($D_2$Rs). Additionally, we show that acetylcholine (ACh) plays a vital excitatory role in activating ChNs and extrabranchial nerves involved in reflex hyperventilation via nicotinic ACh receptors. We further identify two distinct populations of neurosecretory cells in the gill—ACh-positive and 5-HT-positive—that transmit hypoxic signals to different postsynaptic neurons. Our findings provide the first direct evidence of neurotransmission at the NEC-ChN synapse in the gill and suggest that the modulatory role of

dopamine and the excitatory role of ACh in oxygen sensing are evolutionarily conserved features that emerged early in vertebrate evolution.

# Résumé

La détection de l'oxygène et les réponses physiologiques à l'hypoxie sont essentielles à la survie dans les environnements aquatiques. Chez les poissons téléostéens, les branchies agissent comme le site principal de détection des niveaux d'oxygène et d'initiation des réponses compensatoires. Les cellules neuroépithéliales (NEC) des branchies sont des capteurs périphériques clés de l'oxygène chez les vertébrés aquatiques et partagent des caractéristiques morphologiques avec les chémorécepteurs de l'oxygène des mammifères, comme ceux du corps carotidien. Lors de la détection de l'hypoxie, les NEC inhibent les canaux $K^+$ de fond, entraînant une dépolarisation de la membrane et la libération de neurotransmetteurs. Cette cascade active les voies sensorielles dans les branchies projetant vers des centres de plus haut niveau, entraînant des réponses physiologiques telles que l'hyperventilation. Malgré les recherches approfondies sur les réponses ventilatoires des vertébrés à l'hypoxie, les neurotransmetteurs spécifiques, les récepteurs et les voies afférentes qui médiatisent ces réponses chez les poissons restent mal compris. En utilisant une préparation de branchies isolées de poisson-zèbre Tg(*elavl3:*GCaMP6s), nous avons mesuré les changements induits par l'hypoxie dans la concentration intracellulaire de $Ca^{2+}$ ($[Ca^{2+}]_i$) à la fois dans les NEC et dans les neurones de la chaîne postsynaptique (ChN). Nos résultats montrent que les NEC et les ChN présentent une augmentation induite par l'hypoxie de $[Ca^{2+}]_i$. Il est important de noter que nous avons trouvé qu'une synapse fonctionnelle NEC-ChN est nécessaire pour l'augmentation induite par l'hypoxie de $[Ca^{2+}]_i$ dans les ChN, et que ces réponses postsynaptiques sont modulées par la dopamine présynaptique via les récepteurs $D_2$ de la dopamine ($D_2$Rs). De plus, nous montrons que l'acétylcholine (ACh) joue un rôle excitateur essentiel dans l'activation des ChN et des nerfs extrabranchiaux impliqués dans l'hyperventilation réflexe via les récepteurs nicotiniques de

l'ACh. Nous identifions en outre deux populations distinctes de cellules neurosecrétrices dans les branchies - positives pour l'ACh et positives pour la 5-HT - qui transmettent les signaux hypoxiques à différents neurones postsynaptiques. Nos résultats fournissent la première preuve directe de la neurotransmission à la synapse NEC-ChN dans les branchies et suggèrent que le rôle modulateur de la dopamine et le rôle excitateur de l'ACh dans la détection de l'oxygène sont des caractéristiques conservées évolutivement qui sont apparues tôt dans l'évolution des vertébrés.

## TABLE OF CONTENTS

## LIST OF FIGURES

## LIST OF TABLES

## LIST OF ABBREVIATIONS

| | |
|---|---|
| AC | Adenyl cyclase |
| ACh | Acetylcholine |
| ASR | Aquatic surface respiration |
| ATP | Adenosine triphosphate |
| $Ca^{2+}$ | Calcium ion |
| $CaCl_2$ | Calcium chloride |
| CNS | Central nervous system |
| $CO_2$ | Carbon dioxide |
| ChNs | Chain neurons |
| $D_2R$ | Dopamine 2 receptors |
| DAPI | 4′,6-diamidino-2-phenylindole |
| DAT | Dopamine active transporter |
| dpf | Days post fertilization |
| eFa | Efferent filament artery |
| ECS | Extracellular solution |
| $F_v$ | Ventilation frequency |
| GFP | Green fluorescent protein |
| h | Hour |
| $H^+$ | Proton |
| HVR | Hypoxic ventilatory response |

| | |
|---|---|
| KCl | Potassium chloride |
| $KH_2PO_4$ | Potassium phosphate monobasic |
| $K^+$ | Potassium ion |
| mAChRs | Muscarinic acetylcholine receptors |
| mM | Milimolar |
| $MgCl_2$ | Magnesium chloride |
| mm | Millimeter |
| mmHg | Millimeter of mercury |
| $Na_2HPO_4$ | Sodium phosphate dibasic |
| NaCl | Sodium chloride |
| NECs | Neuroepithelial cells |
| NEBs | Neuroepithelial bodiesn |
| nAChRs | Nicotinic acetylcholine receptors |
| $O_2$ | Oxygen |
| PBS | Phosphate buffered solution |
| $PO_2$ | Partial pressure of oxygen |
| RT-PCR | Reverse transcription polymerase chain reaction |
| s | Second |
| SV2 | Synaptic vesicle protein 2 |
| TH | Tyrosine hydroxylase |
| Tg | Transgenic |
| Vmat2 | Vesicular monoamine transporter 2 |
| VAChT | Vesicular acetylcholine transporter |

| | |
|---|---|
| µl | Microliter |
| µm | Micrometer |
| µM | Micromolar |

# Chapter 1

# General Introduction

This chapter includes material from the following article:

Reed, M., & Jonz, M. G. (2022). Neurochemical Signalling Associated With Gill Oxygen Sensing and Ventilation: A Receptor Focused Mini-Review. *Frontiers in Physiology*, *13*, 940020.

## 1.1 Introduction

Adequate oxygen delivery to tissue is important for maintaining cellular processes and homeostasis. Thus, an animal's ability to detect low oxygen, and respond appropriately, is crucial for survival. Vertebrate respiratory chemoreceptors detect such chemical changes in the environment, or arterial blood supply, and upon stimulation initiate corrective autonomic reflexes, such as the hyperventilatory response (HVR) to hypoxia (Perry et al., 2009; Nurse, 2010; Jonz, 2018). The most well described vertebrate chemoreceptors are the type 1 (or glomus) cells of the mammalian carotid body. Hypoxic activation of these cells involves the modulation of $K^+$ conductance, membrane depolarization, and resulting $Ca^{2+}$-dependent neurotransmitter release to act on sensory terminals of the carotid sinus nerve (Lopez-Barneo et al., 1988; Gonzalez et al., 1994; Nurse, 2010; Kumar and Prabhakar, 2012).

The neurochemistry involved in transmitting the hypoxic signal in the carotid body is well characterized. Adenosine triphosphate (ATP) is released by type 1 cells to act on afferent terminal purinergic P2X3 receptors, and is one of the main excitatory neurotransmitters involved in hypoxic signalling (Zhang et al., 2000; Nurse, 2005). Adenosine, produced by the breakdown of extracellular ATP, acts on adenosine A2a receptors to further enhance the hypoxic response by type 1 cells (Nurse, 2014). Acetylcholine (ACh), co-released with ATP, is also largely responsible for excitatory signalling in the carotid body *via* postynaptic nicotinic receptors (Zhang et al., 2000). Dopamine, acting on $D_2$ receptors, plays a modulatory role in mediating the response to hypoxia in the carotid body (Benot and López-Barneo, 1990; Iturriaga and Alcayaga, 2004). Additionally, embedded within the respiratory epithelium of neonatal mammals lie clusters of chemosensory neuroepithelial bodies (NEBs), of which serotonin (5-

hydroxytryptamine, 5-HT) is the major neurotransmitter released during hypoxia (Fu et al., 2002).

In contrast, remarkably little is known about the receptors and afferent pathways mediating HVR in fishes. However, since zebrafish would share a common ancestor with mammals. studying zebrafish systems allows us a unique look into the evolutionary origin of oxygen sensing and how oxygen regulation has evolved across different animals and environments. In this chapter, I will review gill oxygen chemoreceptors, gill innervation, and summarize the available evidence that has linked specific receptor types in the gills to neurochemical signalling associated with $O_2$ sensing in fish.

### 1.2 Fish Oxygen Chemoreceptors

Neuroepithelial cells (NECs) were first identified in the gill by Dunel-Erb et al. (1982), who noted a similar morphology to mammalian pulmonary chemoreceptors. NECs were characterized by the presence of dense-cored vesicles and contained the monoamine, serotonin (5-hydroxytrymptamine, 5-HT; Dunel Erb et al., 1982). Due to the homology between the carotid body and the first gill arch in fish, NECs were believed to be homologues of type 1 cells (Milsom and Burleson, 2007). More recent evidence has suggested they may have a closer evolutionary link to pulmonary NEBs (Hockman et al., 2017).

The first direct evidence for the involvement of gill NECs in $O_2$ chemoreception came from studies using zebrafish (*Danio rerio*; Jonz et al., 2004). Using whole-cell patch-clamp recordings of NECs isolated from the gills, it was shown that NECs responded to a decreased $PO_2$ by inhibition of background $K^+$ channels and membrane depolarization. Subsequent studies showed similar $O_2$ sensitivity of gill NECs in channel catfish (*Ictalurus punctatus*; Burleson et

al., 2006), and isolated NECs from adult goldfish (*Carassius auratus*) responded to hypoxia by $Ca^{2+}$-dependent vesicular recycling (Zachar et al., 2017), which is consistent with neurotransmitter release and activation of sensory nerve fibres to initiate the hypoxic response. Previously there is no direct evidence of the neurotransmitters released during hypoxia and the receptors they act on remain uncharacterized.

### 1.3 Gill Structure and Innervation

Teleost fish gills have a complex and highly efficient structure designed for physiological functions such as gas exchange and osmoregulation. The gills are made up of four paired arches on each side of the pharynx (Wilson & Laurent, 2002). Each gill arch supports two rows of gill filaments that extend plate-like structures, called the respiratory lamellae. The structure of the lamellae greatly increases the surface area for gas exchange and are designed with a thin epithelium surrounding a well-vascularized core supported by pillar cells (Laurent, 1984; Hughes, 1984; Laurent, 1989). The epithelial layer of the gills is a complex structure composed of several specialized cell types including chemosensory neuroepithelial cells, pavement cells, mitochondria-rich cells, mucous cells, and pillar cells (Wilson & Laurent, 2002).

Fish gills are innervated by branches of cranial nerves, primarily the glossopharyngeal (IX) and vagus (X) nerves (Burleson, 2009). Chemosensory NECs in fish gills, which function as oxygen sensors, receive innervation from both intrabranchial and extrabranchial sources (Jonz and Nurse, 2003). This dual innervation pattern suggests a complex sensory pathway for oxygen chemoreception in fish gills. NECs are distributed throughout the gill filaments and respiratory lamellae, forming an extensive network of oxygen-sensitive cells. The innervation of NECs

allows them to communicate changes in oxygen levels to the central nervous system, triggering adaptive cardiorespiratory reflexes to maintain oxygen uptake (Jonz and Nurse, 2008).

### 1.4 Receptor Control of Oxygen Sensing and Ventilation

Despite the lack of receptor characterization in the gill, there are numerous studies identifying neurotransmitters and neuroendocrine factors that may be associated with $O_2$ sensing in the gills of fish (recently reviewed by Porteus et al., 2012; Pan and Perry, 2020). The following sections will summarize the major candidate receptor subtypes suggested to play a role in facilitating and mediating the ventilatory responses to hypoxia. Reviewing this part of the literature helped to establish my approach for the subsequent research chapters.

#### 1.4.1 Serotonergic Receptors

Serotonergic receptors are divided into seven distinct classes, 5-$HT_{1-7}$, largely based on their structural and operational characteristics within the serotonergic system (Peroutka and Howell, 1994; Hoyer et al., 2002). 5-HT receptors belong to the G-protein-coupled receptor (GPCR) superfamily, with the exception of the 5-$HT_3$ receptor, which is a ligand-gated ion channel (Hoyer et al., 2002). Of the seven distinct classes, there are also a number of different 5-$HT_{1-7}$ receptor subtypes, each having a distinct pattern of distribution and function in the nervous system, giving rise to many different signalling capabilities (reviewed by Barnes and Sharp, 1999). Some postsynaptic 5-HT receptor subtypes are known to cause neuronal depolarization (5-$HT_{2A}$, 5-$HT_{2C}$, 5-$HT_3$ and 5-$HT_4$ receptors) leading to excitatory signalling, or neuronal hyperpolarization (5-$HT_{1A}$ receptor) inhibiting signalling (Barnes and Sharp, 1999).

As NECs characteristically contain 5-HT, it has been long hypothesized that 5-HT is involved in the neurotransmission of the hypoxic signal. Early evidence of this came from isolated gills of rainbow trout (*Oncorhynchus mykiss*), where 5-HT elicited a modest transient burst of chemoreceptor activity (Burleson and Milsom, 1995a). Additionally, rainbow trout intra-arterial injections of 5-HT also caused an elevation in gill ventilation and heart rate (Burleson and Milsom, 1995b).

Pharmacological studies targeting specific 5-HT receptor subtypes have revealed a potential excitatory role of 5-$HT_2$ and 5-$HT_3$ receptors. In the European eel (*Anguilla anguilla*), intravenous administration of 5-HT elicited a large increase in ventilatory frequency and amplitude (Janvier et al., 1996). Janvier et al. also showed the 5-HT-induced hyperventilatory response could be mimicked by the 5-$HT_3$ receptor agonist, 1-phenylbiguanide, and blocked by the 5-$HT_3$ receptor antagonist, metoclopramide. In the Gulf toadfish (*Opsanus beta*), injection with the 5-$HT_2$ receptor agonist, α-methyl-5-HT, increased ventilation amplitude and this response was attenuated by the 5-$HT_2$ receptor antagonist, ketanserin (McDonald et al., 2010). Similarly, 5-HT mimicked hypoxia by increasing ventilation frequency of 7 days post-fertilization (d.p.f) zebrafish larvae, and subsequent addition of ketanserin reversibly reduced ventilation frequency (Shakarchi et al., 2013). In zebrafish larvae, 5-$HT_3$ receptor blockade with tropanyl 3,5-dichlorobenzoate (MDL 72222) also reduced the hyperventilatory response to acute hypoxia (Jonz et al., 2015). These results suggest an excitatory role for 5-$HT_2$ and 5-$HT_3$ receptors; however, it is unknown if these effects were limited to the gills, as whole animal experiments do not exclude potential targets in the central nervous system (CNS). Additionally, in the gills of the Antarctic fish (*Pagothenia borchgrevinki*), branchial vasoconstriction was mediated by 5-$HT_2$ receptors (Sundin et al., 1998); and previous studies demonstrated the

innervation of the filament arteries by serotonergic neurons in trout and zebrafish (Bailly et al., 1989; Jonz and Nurse, 2003). Given the effects of hypoxia on blood flow in the gills (Booth, 1979), an additional role of 5-$HT_2$ receptors in controlling vascular responses to hypoxia is conceivable.

Recent single-cell transcriptomic analysis of chemosensory NECs and other cell types of the gills of adult zebrafish has begun to provide compelling evidence for potential actions of these receptor types by localizing them to, and within, the gill. The gene encoding 5-$HT_{3A}$-like receptors shows highest expression in gill neurons (Pan et al., 2022). As NECs are innervated by at least one population of intrabranchial neurons, as well as extrabranchial nerve fibres (Jonz et al., 2004), there is a plausible mechanism for chemotransduction *via* 5-$HT_{3A}$ receptors in the gill. This would be similar to the carotid body, where postsynaptic excitation during hypoxia is mediated primarily by ionotropic 5-$HT_3$ receptors and, to a lesser extent, 5-$HT_2$ (Zhong et al., 1999; Nurse, 2005). Further work localizing 5-$HT_{3A}$ receptors to the specific neuronal population innervating NECs would be needed to confirm this.

Interestingly, the gene encoding the inhibitory 5-$HT_{1A}$ receptor, *htr1ab*, was found to be most abundant in NECs above any other cell type in the gill (Pan et al., 2022). This may suggest a specific $O_2$-sensing role for these receptors, possibly through negative feedback or autoreceptor mechanism, which has not yet been explored pharmacologically.

### 1.4.2 Cholinergic Receptors

Cholinergic receptors are subdivided into nicotinic and muscarinic types. Nicotinic receptors (nAChRs) are ligand-gated ion channels formed by the assembly of five transmembrane subunits and mediate fast neurotransmission in the central and peripheral

nervous systems (Ho et al., 2020). Many different nAChR subtypes exist, each consisting of a specific combination of subunits (α1-10, β1-4, γ, δ, and ε; Kalamida et al., 2007). Muscarinic receptors (mAChRs) are G-protein coupled receptors, of which five main subtypes exist (M1-5), and have actions in the central and peripheral nervous systems (Caulfield, 1993).

A role for ACh in gill neurotransmission is not as clear as in the mammalian carotid body. Non-serotonergic, NEC-like cells containing the vesicular ACh transporter, VAChT, have been identified in zebrafish (Shakarchi et al., 2013; Zachar et al., 2017) and mangrove rivulus (*Kryptolebias marmoratus*; Regan et al., 2011), though it is currently unclear if these cells function as $O_2$ chemoreceptors. Ventilatory responses to ACh and nicotine have been reported in several species (Burleson and Milsom, 1995b; Shakarchi et al., 2013). The effects of muscarine, however, appear to be more uncertain. In rainbow trout, muscarine elicited moderate afferent nerve activity in gill arch preparations and increased ventilation frequency in whole animal experiments. The muscarinic antagonist, atropine, prevented stimulation by hypoxia; however, it had no effect on ventilation (Burleson and Milsom, 1995a; 1995b). Similarly, atropine had no effect on ventilatory responses to hypoxia in the Adriatic sturgeon (*Acipenser naccarii;* McKenzie et al., 1995) or the channel catfish (Burleson and Smatresk, 1990). In zebrafish, atropine abolished the ventilatory response to hypoxia, but only at very high concentrations (Rahbar et al., 2016). Administration of atropine also abolished the hypercarbia-induced ventilatory responses observed in Pacific spiny dogfish (*Squalus acanthias*; McKendry et al., 2001).

Additionally, there appears to be a time-dependent emergence of cholinergic control of ventilation during development. Exogenous application of ACh did not affect ventilation frequency in early-stage zebrafish larvae (7–10 d.p.f); however, in late-stage larvae (14–21 d.p.f)

ACh had a stimulatory effect on ventilation frequency. The nicotinic ACh receptor antagonist, hexamethonium, did not inhibit hypoxia-induced hyperventilation at 10 d.p.f. but did after 12 d.p.f. (Shakarchi et al., 2013).

In the Asian catfish (*Heteropneustes fossilis*) the nicotinic receptor α7 subunit is expressed in the NECs and mucous cells in the gill and respiratory air sac (Lauriano et al., 2021). In addition, semi-quantitative PCR detected low expression of the AChR γ-like subunit in the gills of adult transparent *Pristella maxillaris* (Ma et al., 2021). RNA sequencing of the adult zebrafish gills has further narrowed down potential ACh receptor subunit targets within the gill. The nicotinic receptor α2b subunit gene, *chrna2b*, was highly expressed in NECs and neurons; whereas the α6 subunit gene (*chrna6*) and β3a subunit gene (*chrnb3a*) were expressed primarily in NECs, and the β4 subunit gene (*chrnb4*) was mainly present in neurons (Pan et al., 2022). The location of these subunits supports a model in which VAChT-positive cells release ACh during hypoxic stimulation, leading to excitatory postsynaptic or paracrine effects on ACh receptors of neurons or NECs (Pan et al., 2022). Like NECs, VAChT-positive cells of the zebrafish gills are closely opposed to nerve fibres (Zachar et al., 2017).

### 1.4.3 Purinergic Receptors

There are two families of purinergic receptors—P1 (adenosine) receptors, including four subtypes (A1, A2a, A2b and A3), and P2 (ATP) receptors, which are further subdivided into ionotropic P2X (P2X1-7) and metabotropic P2Y (P2Y1-12) receptors (reviewed by Burnstock, 2018). ATP is a major excitatory neurotransmitter in the mammalian carotid body (Zhang et al., 2000; Nurse, 2005), and adenosine, produced by the extracellular breakdown of ATP, enhances the excitatory response (Nurse, 2014). Such a role in the gills of fish has been less explored.

The broad-spectrum purinergic agonist, ATPγS, elicited a hyperventilatory response in zebrafish larvae. Further, the purinergic receptor antagonist, PPADS, which targets purinergic P2X2 and P2X3 receptors, inhibited the hyperventilatory response to hypoxia (Coe et al., 2017). Immunohistochemical staining of P2X3 receptors showed co-localization with NECs and 5-HT-positive neurons (Rahbar et al., 2016). P2X3 receptors were also found in 5-HT-positve cells in the tips of zebrafish lamellae (Jonz and Nurse, 2003).

In the common carp (*Cyprinus carpio*), purinergic blockade with aminophylline, an A1 and A2 receptor antagonist, reversed the increases in respiration rate that occurred with the onset of hypoxia (Stecyk and Farrell, 2006). Adenosine injection initiated a biphasic response in ventilation frequency (a decrease followed by an increase) in the epaulette shark (*Hemiscyllium ocellatum*), which was also blocked by aminophylline (Stensløkken et al., 2004). Moreover, in zebrafish, the A2a receptor antagonist, SCH58261, inhibited the ventilatory response to hypoxia (Coe et al., 2017).

The above studies provide evidence for an excitatory role of P2X2/3 and A1/2 receptors in control of the hyperventilatory response to hypoxia in fish. Further, these results suggest a similar mechanism to the carotid body, where pre- and postsynaptic A2a receptors are believed to enhance the response to hypoxia (Nurse, 2014).

### 1.4.4 Dopaminergic Receptors

Dopamine receptors are G-protein coupled and include the $D_1$-like receptor subtypes ($D_1$ and $D_5$) which activate adenylyl cyclase, and the $D_2$-like subfamily ($D_2$, $D_3$, and $D_4$) which inhibit adenylyl cyclase and activate $K^+$ channels (reviewed by Martel and Gatti McArthur, 2020). Dopamine is an important inhibitory neuromodulator in carotid body hypoxia signalling

(Nurse, 2010). Dopamine released by type 1 cells has an autocrine-paracrine action on dopaminergic $D_2$ receptors located on type 1 cells to inhibit $Ca^{2+}$ channels, leading to negative feedback regulation of further neurotransmitter release during hypoxia (Benot and López-Barneo, 1990).

Early evidence for a role of dopamine in the gills was shown in isolated gills of rainbow trout, where dopamine caused a small and brief burst in chemoreceptor activity followed by a mild inhibition of receptor discharge (Burleson and Milsom, 1995a). In zebrafish larvae, exogenous application of dopamine has been shown to decrease ventilation frequency as early as 7 d.p.f. (Shakarchi et al., 2013). RNA sequencing of the adult zebrafish gill detected dopamine receptors in the $D_2$-like family, including *drd4a* in NECs and *drd3* highly expressed in neurons (Pan et al., 2022). This recent work using zebrafish suggests an inhibitory dopaminergic mechanism in the gill, possibly via $D_2$-like receptors, and is an area for potential future developments. Pharmacologically targeting the specific dopamine receptor subtypes controlling the ventilatory responses to hypoxia may be an interesting extension of this work.

**Table 1.1** Summary of receptor types reported to effect ventilation amplitude and/or frequency and their location within the gill.

| Receptor type | Effect on ventilation* | Location within gill | Reference |
|---|---|---|---|
| **Serotonergic receptors (5-HT)** | | | |
| α-methyl-5-HT (5-$HT_2$ receptor agonist) | ↑ | - | McDonald et al. (2010) |
| Ketanserin (5-$HT_2$-R antagonist) | ↓ | - | McDonald et al. (2010), Shakarchi et al. (2013) |
| 1-phenylbiguanide (5-$HT_3$ receptor agonist) | ↑ | - | Janvier et al. (1996) |
| Metoclopramide (5-$HT_3$ receptor antagonist) | ↓ | - | Janvier et al. (1996) |

| | | | |
|---|---|---|---|
| MDL72222 (5-$HT_3$ receptor antagonist) | ↓ | - | Jonz et al. (2015) |
| SCL (gene encoding $5HT_{3A}$-like receptors) | - | Neurons | Pan et al. (2022) |
| *htr1ab* (gene encoding 5-$HT_{1A}$) | - | NECs | Pan et al. (2022) |
| **Cholinergic receptors (ACh)** | | | |
| Nicotine (nicotinic ACh receptor agonist) | ↑ | - | Burleson and Milsom (1995a) |
| Hexamethonium (nicotinic ACh receptor antagonist) | ↓ | - | Shakarchi et al. (2013) |
| Muscarine (muscarinic ACh receptor agonist) | ↑ | - | Burleson and Milsom (1995a) |
| Atropine (muscarinic ACh receptor antagonist) | No effect | - | Burleson and Milsom (1995a), McKenzie et al. (1995), Burleson and Smatresk (1990) |
| | ↓ | - | Rahbar et al. (2016) |
| *chrna7* (gene encoding nicotinic ACh receptor subunit α7) | - | NECs | Lauriano et al. (2021) |
| *chrna2b* (gene encoding nicotinic ACh receptor subunit α2b) | - | NECs/ neurons | Pan et al. (2022) |
| *chrna6* (gene encoding nicotinic ACh receptor subunit α6) | - | NECs | Pan et al. (2022) |
| *chrnb3a* (gene encoding nicotinic ACh receptor subunit β3a) | - | NECs | Pan et al. (2022) |
| *chrnb4* (gene encoding nicotinic ACh receptor subunit β4) | - | Neurons | Pan et al. (2022) |
| **Purinergic receptors** | | | |
| ATPγS (broad spectrum purinergic receptor agonist) | ↑ | - | Coe et al. (2017) |
| PPADS (purinergic P2X2/3 receptor antagonist) | ↓ | - | Coe et al. (2017) |
| P2X3 immunolabelling | - | NECs/ neurons | Rahbar et al. (2016) |
| Aminophylline (adenosine A1/2 receptor antagonist) | ↓ | - | Stecyk and Farrel (2006), StenslØkken et al. (2004) |
| SCH58261 (adenosine A2a receptor antagonist) | ↓ | - | Coe et al. (2017) |
| **Dopamine receptors** | | | |

| | | | |
|---|---|---|---|
| DA | ↓ | - | Shackarchi et al. (2013) |
| *drd4a* (gene encoding dopamine $D_2$-like family $D_4$ receptor) | - | NECs | Pan et al. (2022) |
| *drd3* (gene encoding dopamine $D_2$-like family $D_3$ receptor) | - | Neurons | Pan et al. (2022) |

*Effect on ventilation measured as amplitude or frequency.

## 1.5 Thesis Objectives

The goal of this doctoral thesis was to identify and characterize the neurochemical signalling pathways involved in gill oxygen sensing and the regulation of ventilation zebrafish. The objectives of the subsequent research chapters are outlined below:

***Chapter 2****:* The goal of this study was to evaluate a potential role for dopamine in hypoxia signaling in zebrafish by establishing a site for the synthesis and storage of dopamine in the gill and characterizing the distribution of $D_2$ receptors.

***Chapter 3*****:** The goal of this study was to delineate a mechanism by which presynaptic $D_2$Rs provide a feedback mechanism that attenuates the chemoreceptor response to hypoxia.

***Chapter 4****:* The goal of this final study was to elucidate the role of ChNs in ventilatory responses to hypoxia and to uncover the neurochemical basis of excitatory NEC-ChN signalling.

The objectives of this research were accomplished through a multi-faceted approach combining experimental techniques. Given the numerous potential receptor types implicated in hypoxia signaling outlined in this chapter, my initial task was to identify which receptors are active in the gill. To achieve this, I employed molecular biology techniques, specifically mRNA expression analysis of genes encoding these receptors, in isolated gill tissue as an initial screening tool. This allowed me to pinpoint which receptors are present in the gill. To further

investigate these gill receptors, I utilized immunohistochemistry to localize these receptors and their respective neurotransmitter synthesis sites, with a focus on their relationship to oxygen-sensing NECs in the gill. While these methods provided insight into potential signaling pathways, the pivotal aspect of this research involved calcium imaging to examine the physiological responses within the gill. Since $Ca^{2+}$ influx in NECs plays a critical role in hypoxia activation, $Ca^{2+}$ imaging proved to be a valuable tool for assessing *in situ* responses to hypoxia, both with and without manipulations of dopaminergic, cholinergic, and serotonergic systems.

By integrating molecular biology, confocal microscopy, and calcium imaging throughout the following research chapters, I propose a model where excitatory signaling in NECs is mediated through cholinergic and serotonergic pathways, with modulation by presynaptic dopamine. This combination of techniques forms the foundation for understanding the complex signaling mechanisms involved in hypoxia detection in the gill.

# Chapter 2

## A role for dopamine in control of the hypoxic ventilatory response via $D_2$ receptors in the zebrafish gill

This chapter includes material from the following article:

Reed, M., Pan, W., Musa, L., Arlotta, S., Mennigen, J. A., & Jonz, M. G. (2024). A role for dopamine in control of the hypoxic ventilatory response via $D_2$ receptors in the zebrafish gill. *The Journal of Comparative Neurology*, *532*(2), e25548. Co-authors: Wen Pan, Lina Musa, and Stefania Arlotta.

My contributions: Manuscript written by me and data for figures 2.1, 2.6, 2.7, 2.8, 2.9, and 2.10 were collected by me.

## 2.1 Abstract

Dopamine is a neurotransmitter involved in $O_2$ sensing and control of reflex hyperventilation. In aquatic vertebrates, $O_2$ sensing occurs in the gills via chemoreceptive neuroepithelial cells (NECs), but a mechanism for dopamine in autonomic control of ventilation has not been defined. We used immunohistochemistry and confocal microscopy to map the distribution of tyrosine hydroxylase (TH), an enzyme necessary for dopamine synthesis, in the gills of zebrafish. TH was found in nerve fibers of the gill filaments and respiratory lamellae. We further identified dopamine active transporter (*dat*) and vesicular monoamine transporter (*vmat2*) expression in neurons of the gill filaments using transgenic lines. Moreover, TH and *dat*-positive nerve fibers innervated NECs. In chemical screening assays, domperidone, a $D_2$-receptor antagonist, increased ventilation frequency in zebrafish larvae in a dose-dependent manner. When larvae were confronted with acute hypoxia, the $D_2$ agonist, quinpirole, abolished the hyperventilatory response. Quantitative PCR confirmed expression of *drd2a* and *drd2b* (genes encoding $D_2$ receptors) in the gills, and their relative abundance decreased following acclimation to hypoxia for 48 h. We localized $D_2$ receptor immunoreactivity to NECs in the efferent gill filament epithelium, and a novel cell type in the afferent filament epithelium. We provide evidence for the synthesis and storage of dopamine by sensory nerve terminals that innervate NECs. We further suggest that $D_2$ receptors on pre-synaptic NECs provide a feedback mechanism that attenuates the chemoreceptor response to hypoxia. Our studies suggest that a fundamental, modulatory, role for dopamine in $O_2$ sensing arose early in vertebrate evolution.

## 2.2 Introduction

An animal's ability to detect low oxygen, or hypoxia, and respond appropriately is crucial for survival. The hypoxic ventilatory response (HVR) in vertebrates is an important physiological response to low partial pressure of oxygen ($PO_2$), which involves compensatory changes in ventilation to raise arterial $PO_2$ (Powell et al., 1998; Perry et al., 2009). In the mammalian carotid body, dopamine is an important neuromodulator involved in oxygen sensing and control of reflex hyperventilation. Hypoxic activation of carotid body oxygen chemosensory type 1 (glomus) cells involves the modulation of $K^+$ conductance, membrane depolarization, and resulting $Ca^{2+}$-dependent neurotransmitter release to act on sensory terminals of the carotid sinus nerve (Nurse, 2010; López-Barneo et al., 1988; González et al., 1994; Kumar & Prabhakar, 2012). Dopamine, released by type 1 cells, has been shown to have autocrine-paracrine actions on carotid body activation in many species via G-protein coupled dopamine $D_2$-receptors on both pre-synaptic type 1 cells and postsynaptic afferent terminals (Nurse, 2010). At the pre-synaptic type 1 cell, the inhibitory actions of dopamine act to decrease further neurotransmitter release, thereby mediating carotid body hypoxia signaling (Benot & López-Barneo, 1990). A role for dopamine in mediating the ventilatory responses to hypoxia in aquatic vertebrates is less understood; however, since zebrafish would share a common ancestor with mammals, studying zebrafish systems allows us a unique look into the evolutionary origin of such an important physiological response and how it has evolved across different environments.

In fish, oxygen sensing occurs in the gills via chemoreceptive neuroepithelial cells (NECs; Fig. 1). As water flows through the gill basket during breathing, NECs sense changes in oxygen and initiate HVR during hypoxia (Perry et al., 2009). NECs are found in the filament epithelium near the efferent filament artery and respond to a decrease in $PO_2$ by inhibition of

background $K^+$ channels, membrane depolarization and $Ca^{2+}$-dependent vesicular recycling (Jonz et al., 2004; Zachar et al., 2017a). The latter is consistent with neurotransmitter release into the synaptic cleft, which may lead to activation of sensory nerve fibers. NECs are polymodal, such that they are sensitive to changes in $O_2$, $CO_2$, and $H^+$ (Jonz, 2018; Qin et al., 2010; Abdallah et al., 2015a) and are characterized by immunoreactivity to serotonin (5-hydroxytryptamine, 5-HT) and synaptic vesicle protein, SV2 (Jonz & Nurse, 2003). Due to these characteristics, and the homology between the site of the carotid body and the first gill arch in fish, NECs are believed to be structurally and functionally similar to type 1 cells (Milsom & Burleson, 2007; Zachar & Jonz, 2012). Recent evidence, however, suggests that NECs may be homologues of oxygen-sensitive pulmonary neuroepithelial bodies (NEBs; Hockman et al., 2017).

In contrast to the well-described neurochemistry of the carotid body (Nurse, 2010), currently there is no direct evidence for which neurotransmitters are released within the gill during hypoxia, and the receptors they act on remain uncharacterized. 5-HT, the most abundant neurotransmitter in gill NECs, and acetylcholine have both been suggested as excitatory neurotransmitters in the gills (Jonz & Nurse, 2003; Porteus et al., 2012; Zachar et al., 2017). Early evidence for a role of dopamine in the gills was shown in isolated gills of rainbow trout (*Oncorhynchus mykiss*), where dopamine caused a small, brief burst in chemoreceptor activity followed by a mild inhibition of receptor discharge (Burleson & Milsom, 1995). In live, whole-animal experiments using zebrafish larvae, application of dopamine decreased ventilation frequency, suggesting inhibitory effects of dopamine on ventilation (Shakarchi et al., 2013). Recent single-cell RNA-sequencing in zebrafish indicated expression of $D_2$-like receptors in gill cells, including NECs (Pan et al., 2022); however, a mechanism for control of ventilation during hypoxia via an inhibitory dopaminergic pathway in the gill has not been defined.

The goal of the present study was to evaluate a potential role for dopamine in hypoxia signaling in zebrafish by establishing a site for the synthesis and storage of dopamine in the gill and characterizing the distribution of $D_2$ receptors. We identify the presence of tyrosine hydroxylase (TH) and the dopamine active transporter (DAT), involved in the synthesis or transport of dopamine, in sensory nerve fibers using immunohistochemistry and transgenic lines. In addition, we co-localize dopamine $D_2$ receptors with oxygen-sensitive NECs and provide evidence for pre-synaptic $D_2$ receptors in the modulation of the hyperventilatory response to hypoxia.

## 2.3 Methods

### 2.3.1 Ethics statement

All wild-type and transgenic zebrafish were bred and maintained at the Laboratory for the Physiology and Genetics of Aquatic Organisms, University of Ottawa. Zebrafish were kept at 28°C on a 14:10-h light:dark cycle (Westerfield, 2007). Larvae were obtained by breeding from 12-month old adults and maintained in 150-mm Petri dishes until 2 days post-fertilization (d.p.f.). All procedures for animal use were carried out in accordance with institutional guidelines according to protocol BL-3666, and guidelines provided by the Canadian Council on Animal Care. Adult zebrafish were euthanized by concussion and decapitated. Larvae were euthanized by hypothermic shock by immersion in an ice bath for 20 min.

### 2.3.2 Immunohistochemistry and antibody characterization

Techniques for tissue extraction and immunolabeling were carried out as previously described (Jonz & Nurse, 2003). Whole gill baskets were removed and immersed in phosphate-

buffered solution (PBS) containing (mM): NaCl 137, $Na_2HPO_4$ 15.2, KCl 2.7, and $KH_2PO_4$ 1.5 at pH 7.8 (Bradford et al., 1994). Gill baskets were fixed by immersion in 4% paraformaldehyde in PBS overnight at 4°C. Tissues were removed and rinsed in PBS three times at 3 min before permeabilization for 24 h at 4°C. Permeabilizing solution (PBS-TX) contained 2% Triton X-100 in PBS (pH 7.8). After 3 rinses in PBS, gill baskets were then separated into individual arches. Gill arches were incubated in primary antibodies for 24 h at 4°C, rinsed with PBS three times at 3 min, and immersed in secondary antibodies for 1 h at room temperature in darkness. Dissection and removal of gill arches are illustrated in Figure 1a–c.

NECs, neurons and nerve fibers were identified using antibodies against serotonin (5-HT), the synaptic vesicle protein SV2, or the zebrafish-specific neuronal marker, zn-12. Polyclonal anti-5-HT was raised in rabbit against a 5-HT creatinine sulfate complex conjugated with bovine serum albumin (manufacturer specifications; cat. no. S5545, Sigma-Aldrich, Oakville, ON, Canada; RRID: AB_477522). These antibodies were used at 1:250 and localized with goat anti-rabbit secondary antibodies conjugated with fluorescein isothiocyanate (FITC, 1:50, cat. no. 111-095-003, Cedarlane, Burlington, ON, Canada). zn-12 and SV2 antibodies were monoclonal and raised in mouse (RRID: AB_2315387 and RRID: AB_531908; Developmental Studies Hybridoma Bank, University of Iowa, IA, USA). zn-12 targets membrane fractions from adult zebrafish CNS and recognizes an HNK-1-like epitope (manufacturer specifications). Western blot analysis demonstrated that zn-12 and HNK-1 antibodies label similar bands ranging in molecular weight from 60 to 248 kDa (see Metcalfe et al., 1990). SV2 antibodies were raised against synaptic vesicles from the elasmobranch electric organ and bind to a transmembrane glycoprotein of ~95 kDa on the cytoplasmic side of synaptic vesicles in endocrine and neurosecretory cells (Buckley & Kelly, 1985; manufacturer

specifications). SV2 and zn-12 were used at 1:100 and targeted by goat anti-mouse secondary antibodies conjugated with Alexa 594 at 1:100 (cat. no. A11005, Invitrogen, Burlington, ON, Canada). Labeling by these antibodies in the zebrafish gill has been previously characterized (Jonz & Nurse, 2003).

Cells and nerve fibers of the filament epithelium expressing $D_2$ receptors were identified using polyclonal antibodies at 1:100 that targeted amino acids 24–34 near the ligand binding domain of rat $D_2$ receptor (Tomé et al., 2004; cat. no. AB1558, Millipore, Burlington, MA, USA; RRID: AB_90775). Prior to antibody incubation, antigen retrieval was performed to facilitate anti-$D_2$ binding. Gill baskets were immersed in buffer containing 10 mM sodium citrate, 0.05% Tween 20 at pH 6.0 and incubated for 10 min at 98°C. $D_2$ receptor immunoreactivity was observed using goat anti-rabbit secondary antibodies conjugated with FITC (1:50). To control for the specificity of $D_2$ in our preparation, we generated a custom peptide corresponding to the immunogen sequence (GSEGKADRPHY, Millipore). Pre-adsorption of the control peptide with the $D_2$ antibodies blocked all immunolabeling in gill tissue. Monoclonal anti-TH (1:200; Developmental Studies Hybridoma Bank; RRID: AB_528490) was raised in mouse and directed against a complex of recombinant TH amino acids 60-368 and β galactosidase fusion protein of molecular mass 63 kDa (Fauquet & Ziller, 1989; manufacturer specifications). Alexa 594 or 488 was used as secondary antibodies. All antibodies were diluted using PBS-TX. Gill arches were rinsed with PBS, mounted onto glass microscope slides with Prolong Diamond antifade mountant (Thermo Fisher Scientific, Burlington, ON, Canada) and covered with a 1.2 mm glass coverslip. In some experiments, $D_2$-positive cells were further stained with the nuclear dye, 4′,6-diamidino-2-phenylindole (DAPI).

### 2.3.3 Transgenic lines

Two lines of transgenic zebrafish were used in the present study. The Tg(*dat:tom20 MLS-mCherry*) line was used to visualize dopaminergic neurons. In this line, the regulatory elements of the dopamine transporter gene (*dat*) were targeted to a reporter, mCherry, after fusion with the mitochondrial localizing signal (MLS) of Tom20 (Noble et al., 2015). Transgenic ET(*vmat2:GFP*) zebrafish were previously described by Wen et al. (2008) and were obtained from the Becker Laboratory at the University of Edinburgh. ET(*vmat2:GFP*) zebrafish contained a reporter gene for green fluorescent protein (GFP) under the expression of the vesicular monoamine transporter (*vmat2* also known as *slc18a2*), and was used to visualize NECs (Pan et al., 2021). VMAT2 is an integral membrane protein that mediates storage of monoamines, such as dopamine and 5-HT, into synaptic vesicles. To determine the distribution of dopaminergic expression relative to serotonergic NECs in these lines, adult homozygous Tg(*dat:tom20 MLS-mCherry*) fish were crossed with homozygous adults from ET(*vmat2:GFP*) to generate double transgenic offspring containing both mCherry and GFP reporter genes. Double transgenic fish were raised to 3 months before harvesting gill tissue. Complete gill arches were mounted onto microscopic slides without additional staining.

### 2.3.4 Confocal microscopy

Whole-mount preparations were examined using an upright microscope platform (FN1, Nikon, Japan; or, H101A ProScan, Olympus, Canada) with motorized XYZ control and a confocal scanning system (A1RsiMP, Nikon; or, FV100 BX61 LSM, Olympus) equipped with continuous laser lines at 405 nm, 488 nm and 561 nm. Images were viewed and captured with confocal imaging software, NIS Elements (Nikon). Each image is presented as a composite

projection of multiple optical sections, each separated by 0.5–1.0 μm and combined to produce a total tissue thickness of 20–60 μm. Processing of images was made through the open-source software, Fiji (RRID: SCR_002285; Schindelin et al., 2012) and Corel Draw 10 (RRID: SCR_014235; Corel Corp., Austin, TX, USA). Signals from red fluorescence markers were converted to magenta.

### 2.3.5 Chemical screening

Chemical screening assays were carried out as previously described (Rhabar et al., 2016; Coe et al., 2017). Larvae ranged from 14–16 d.p.f. At this age, zebrafish have fully functional NECs and display an adult-like ventilatory response to hypoxia (Jonz & Nurse, 2005; Shakarchi et al., 2013). Larvae were lightly anaesthetized with tricaine (MS 222, Aqualife TMS, Syndel Laboratories, Vancouver, Canada) at 0.04 mg $ml^{-1}$ and transferred individually to the wells of a multi-well plate (Greiner Cellstar, Sigma-Aldrich, Oakville, ON, Canada). The volume of each well was reduced to ~100 μl by pre-filling with Sylgard (Dow Corning Corporation, Midland, MI, USA). 50 μl of 1% methylcellulose and 0.04 mg $ml^{-1}$ tricaine were then added to each well to minimize movement of larvae. For all treatment groups, ventilation frequency ($f_v$) was recorded by placing the plate upon the stage of a stereomicroscope (M6, Leica, Wetzlar, Germany) and capturing 10-s videos using Leica Application Suite (RRID: SCR_016555). Videos were analyzed *post hoc* and $f_v$ was calculated by manually counting breaths and converting values to breaths $min^{-1}$. All sample sizes are indicated in the figures.

Normoxic $f_v$ was obtained after larvae had settled for 10 min. Larvae were exposed to hypoxic solution, the addition of 50 μl of a test drug, or a combination of hypoxia and drug. All solutions contained 0.04 mg $ml^{-1}$ tricaine. For hypoxia, the plate was placed in a hypoxic

incubator (Forma 3110, Thermo Fisher Scientific) for 7 min, into which 100% $N_2$ was injected to reduce $O_2$ levels to 1% (8 mmHg). $PO_2$ was measured with a built-in thermal conductivity $O_2$ sensor. In other experiments, the $D_2$ antagonist, domperidone (cat. no. D122; Sigma-Aldrich), or the $D_2$ agonist, quinpirole (cat. no. Q102, Sigma-Aldrich), were tested. Domperidone was applied at concentrations from 50–300 μM for 2 min; whereas quinpirole was co-administered with hypoxia at concentrations from 10–200 μM. Both drugs target $D_2$ receptors in the mammalian carotid body (Tomares et al., 1994; Carroll et al., 2005). Domperidone and quinpirole are poorly soluble in water and were therefore first dissolved in dimethyl sulfoxide (DMSO) and diluted to produce a final concentration of <0.5% DMSO. For controls, we included 0.5% DMSO in solution when hypoxia was tested alone (see Fig. 5C). We previously showed that DMSO at or below this concentration had no effect upon $f_v$ (Coe et al., 2017). For recovery, each larva was transferred to a new well in normal solution and $f_v$ was recorded after 5 min.

Analysis of variance (ANOVA) with repeated measures was used to compare $f_v$ between control, treatment and recovery at each concentration. A Bonferroni *post hoc* test was then used to determine whether mean $f_v$ was significantly different between control and treatment groups ($P < 0.05$). Curves for dose vs. response were prepared to display concentration-dependent trends and to estimate the effective concentration of each drug that gave a half-maximal $f_v$ response ($EC_{50}$). Percent maximum $f_v$ for domperidone (at 300 μM), and percent maximum inhibition for quinpirole (at 150 μM), were calculated to normalize the data following procedures described in Rahbar et al. (2016) and Coe et al. (2017). For estimation of $EC_{50}$, a line constrained from the origin at zero to the maximal response was fit to the data using a non-linear

ligand binding model with least squares following the equation: $y=b_{max}\cdot x^h/(k_d{}^h + x^h)$ (Prism v5.0, RRID: SCR_002798; GraphPad Software Inc., La Jolla, CA, USA).

### 2.3.6 Acclimation to chronic hypoxia

A total of 64 adult zebrafish were used in acclimation experiments. Groups of 8 zebrafish were placed in 2.5-l tanks and acclimated to hypoxia (35 mmHg) for 24 h, 48 h, 72 h or 7 days. Groups of 8 control zebrafish were simultaneously maintained in identical tanks at normoxia (~160 mmHg) for the same periods of time. For acclimated fish, water $PO_2$ was gradually lowered over 8 h at a rate of ~16 mmHg $h^{-1}$ by introducing a mixture of compressed air and 100% $N_2$ from a gas mixer (Pegas 4000 MF, Columbus Instruments, Columbus, OH, USA) and delivered through a porous air stone. Water temperature was kept at 28°C by placing tanks in a temperature-controlled water bath, and 50% water changes were performed in each tank every other day.

### 2.3.7 Aquatic surface respiration assays

Experiments assessing the effects of hypoxic acclimation on aquatic surface respiration (ASR) behavior were performed following Abdallah et al. (2015b). After 24 h, 48 h, 72 h or 7 d acclimation to hypoxia (see section 2.6), fish were allowed to recover in normoxic water for 1 h. A 1-l test chamber was marked with gradations on the outside measuring the distance (in mm) from the bottom to the air–water interface, or surface. 100% $N_2$ was delivered to the test chamber via polyethylene tubing and a porous stone until the desired water $PO_2$ was achieved. Water $PO_2$ ranged from ~160 mmHg to 10 mmHg and was verified before and after each trial with an $O_2$ meter (Model 550A, YSI, Yellow Springs, OH, USA). Individual zebrafish were

introduced into the test chamber and were allowed to recover from handling stress for 5 min. A 5-min trial was then performed, after which zebrafish were transferred to a normoxic tank for an additional 5 min for recovery. Zebrafish were reintroduced to the test chamber after recovery and an additional trial was performed at a lower $PO_2$. In this manner, zebrafish were exposed to successive bouts of progressively more severe acute hypoxia (100 mmHg, 50 mmHg, 30 mmHg, and 15 mmHg). Fish taking on a posture in which the dorsal aspect of the head lied just at or below the surface with the body at a slight angle (as described by Kramer & McClure, 1982; Timmerman & Chapman, 2004; Perry et al., 2009) were considered to be performing ASR. Videos were analyzed blindly by observation *post hoc* and the cumulative time (s) spent in ASR at each level of hypoxia was counted manually.

### 2.3.8 Quantitative polymerase chain reaction

Whole gill baskets were removed from zebrafish acclimated to hypoxia or normoxic controls after 48 h, as described in section 2.6, and immediately frozen on dry ice. Total RNA from gill baskets was extracted using Trizol reagent (Life Technologies, Carlsbad, CA, USA) and quantified using a NanoDrop 2000c UV-Vis Spectrophotometer (Thermo-Fisher Scientific). cDNA was generated using 1,000 ng of RNA from whole gill baskets using QuantiTect Reverse Transcription Kit (Qiagen, Toronto, ON, Canada) following manufacturers protocol. To check for genomic DNA contamination, a no-template negative control and a no reverse transcriptase negative control were included.

mRNA gene expression of dopamine receptor-2 (*drd2a* and *drd2b*) in the gill was assessed by real time reverse transcription quantitative PCR (RT-qPCR) using SsoAdvanced Universal SYBR Green Supermix (Bio-Rad, Missisauga, ON, Canada). Expression of reference

gene, elongation factor 1a (*ef1a*), was stable between gill baskets of normoxia and hypoxia groups and was therefore used to normalize *drd2a* and *drd2b* mRNA expression. Standard curves were generated using a serial dilution of pooled cDNA to optimize primer reaction conditions. qPCR reactions included 1 µl cDNA, 1 µl specific forward primer, 1 µl specific reverse primer, 7 µl nuclease-free water, and 10 µl Universal SYBR Green Supermix for a total reaction volume of 20 µl. Each reaction included an initial step at 98°C to activate the enzymes in the mix, followed by 40 repeats of a denaturation step at 95°C and an annealing/extension step at the optimized temperature for each primer pair (Table 1). A melt step from 66°C to 95°C in 0.5°C increments was included at the end of the reaction to check the specificity of the amplicon produced. Each biological sample was run in triplicate, and the relative abundance of mRNA was calculated using the ΔΔCt method (Livak & Schmittgen, 2001). Amplification efficiencies and $R^2$ values are included in Table 1. Statistical analysis was carried out using the Mann-Whitney U Test with Prism software.

## 2.4 Results

### 2.4.1 Dopaminergic innervation in the zebrafish gills

Gills were removed from zebrafish and prepared as whole mounts to observe NECs and associated innervation (Fig. 1d, e). Immunohistochemical labeling with anti-TH indicated extensive localization of the enzyme throughout the nerve supply in the gills (Fig. 2). TH-positive nerve fibers issued from the gill arches and coursed through the gill filaments via superficial and deep nerve bundles, located above and below the efferent filament artery (eFA), respectively (arrowheads, Fig. 2a, b, d, e). These nerves formed a plexus in the filaments that encircled the eFA and extended to the interlamellar regions and the respiratory lamellae (Fig. 2d,

e). In addition, TH-positive nerve fibers were closely associated with 5-HT-positive NECs of the filaments and lamellae (arrows, Fig. 2a, c, d, f). To confirm whether the identified TH-positive nerve fibers were similar to those previously identified in the zebrafish gills, which are predominantly of extrabranchial origin (Jonz & Nurse, 2003), we used the zebrafish-specific neuronal antibody, zn-12. TH-positive nerve fibers of the filaments and lamellae were co-labeled with both markers (arrowheads, Fig. 3). Chain neurons (ChN; see Jonz & Nurse, 2003), as part of the intrabranchial deep nerve bundle, were also visible and were both TH- and zn-12-positive.

In order to further examine dopaminergic activity in the gills, we produced a line of transgenic zebrafish by crossing the Tg(*dat:tom20 MLS-mCherry*) and ET(*vmat2:GFP*) lines (Fig. 4). This allowed visualization of cells or nerve fibers expressing *dat* (Noble et al., 2015) and *vmat2* (Pan et al., 2021). Nerve fibers expressing *dat* were observed in the gill filaments, including the interlamellar regions (arrowheads, Fig. 4a,b,d,e) and surrounding the eFA (Fig. 4g,h). The pattern of *dat* expression in nerve fibers was punctate. This may have been due to restriction of the reporter gene, *mCherry*, to mitochondria in cells that express *dat* (Noble et al., 2015). Mitochondria may be highly concentrated in sensory nerve terminals, including those that innervate oxygen chemoreceptors (González et al., 1994; Bollé et al., 2000). *dat* expression was not detected in nerve fibers of the lamellae. NECs of the gill filaments and lamellae expressed *vmat2*, but only NECs of the filaments came in close contact with *dat* nerve fibers (arrows, Fig. 4a,c,d,f). Intrabranchial ChNs were also found to have *vmat2* expression (Fig. 4d,f,g,i). Notably, we did not observe expression of *dat* in intrabranchial neurons.

### 2.4.2 Targeting dopamine $D_2$ receptors affected the ventilatory response

Chemical screening assays were used to assess $D_2$ receptors as putative targets of endogenous dopamine release. Exposure of zebrafish to domperidone to block $D_2$ receptors had no effect at low concentrations, but significantly increased $f_v$ at higher concentrations, with a ~1.6-fold change above control values at 200 and 300 μM (ANOVA, Bonferroni, $P < 0.05$; Fig. 5a). The effects of domperidone were dose dependent with an estimated $EC_{50}$ of 30 μM (Fig. 5b). Since $D_2$ blockade caused an increase in $f_v$, as does hypoxia (Rahbar et al., 2016), we hypothesized that activation of $D_2$ receptors would have the opposite effect. We therefore administered quinpirole while animals were exposed to acute hypoxia. Zebrafish displayed a robust ventilatory response to hypoxia alone (with 0.5% DMSO included for control), where $f_v$ was significantly elevated from 36.8 ± 6.4 to 92.4 ± 12.5 breaths $min^{-1}$ following acute exposure (ANOVA, Bonferroni, $P < 0.05$; Fig. 5c). At all concentrations tested, quinpirole abolished the hyperventilatory response to acute hypoxia, and even suppressed $f_v$ below control values at 150 and 200 μM (Fig. 5c). The $EC_{50}$ for quinpirole was estimated to be <10 μM (Fig. 5d).

### 2.4.3 Acclimation to hypoxia reduced $D_2$ gene expression

Previous studies from single-cell RNA-sequencing in zebrafish indicated expression of $D_2$-like receptors in gill cells, including NECs (Pan et al., 2022). In the present study, we sought to determine whether acclimation to hypoxia would change expression of paralogous genes encoding $D_2$ receptors (*drd2a* and *drd2b*), thereby implicating these receptors in the hypoxic response. To first determine a relevant time point of hypoxia acclimation to evaluate such changes in gene expression, we exposed hypoxia-acclimated and control zebrafish to progressive bouts of acute hypoxia and evaluated the amount of time spent performing ASR behaviour (Fig. 6). Acclimation to hypoxia for 48 h significantly reduced mean ± S.E.M. cumulative time spent

performing ASR during acute hypoxic exposure, compared with unacclimated zebrafish, at $PO_2$ values below 30 mmHg (Mann-Whitney U Test; $P<0.01$; Fig. 6). This reduction was not significant in fish acclimated to hypoxia for less than 48 h acclimation, thereby highlighting 48 h as a physiologically relevant time point of hypoxia exposure to evaluate changes in gene expression. Zebrafish were then exposed to hypoxia (35 mmHg) for 48 h, and qPCR was used to evaluate relative changes in *drd2a* and *drd2b* expression (Fig. 7). We found a significant reduction by 3.08-fold in *drd2a* compared to control fish (Mann-Whitney U Test, $P < 0.01$; Fig. 7), as well as a significant reduction by 3.04-fold in *drd2b* (Mann-Whitney U Test, $P < 0.01$; Fig. 7). Expression of the reference gene, *ef1a*, was stable between gill baskets of normoxia and hypoxia groups (Fig. 7).

### 2.4.4 Immunohistochemical localization of $D_2$ receptors in the gills

Immunohistochemical labeling of anti-$D_2$-R revealed localization of the receptor primarily to NECs of the efferent gill epithelium, and to nerve fibers of the lamellae (Fig. 8). $D_2$-R labeling was combined with anti-SV2 and zn-12 in order to simultaneously observe co-localization of $D_2$-R with NECs and nerve fibers, respectively. Although NECs and nerves were both labeled by antibodies raised in mouse (and appear in magenta), their markedly different morphology allowed them to be easily distinguished from each other. $D_2$-R co-localized with SV2 in NECs along the efferent filament epithelium (arrows, Fig 8a–c). Transverse optical sectioning and rotation of confocal images showed $D_2$-R-positive NECs were located superficially to, and in close apposition with, the eFA (Fig. 8d–i). Co-labeling with these antibodies also revealed sparse $D_2$-R/zn-12-positive nerve fibers of the filament and prominent $D_2$-R/zn-12-positive nerve fibers of the lamellae (arrowheads, Fig. 8a–c).

Co-application of anti-$D_2$-R with the nuclear marker, DAPI, identified $D_2$-R labeling of cells of the afferent gill epithelium (Fig. 9a,b). $D_2$-R-expressing cells surrounded the afferent filament artery (aFA) in transverse optical section (Fig. 9c,d). No labelling of SV2 was observed in the afferent filament epithelium (not shown).

**Figure 2-1 Illustration of the whole-mount gill preparation in zebrafish and organization of the structures involved in oxygen sensing.** Illustration of the whole-mount gill preparation in zebrafish and organization of the structures involved in oxygen sensing. **(**a) Gill baskets were removed ventrally from zebrafish, as shown. Rostral is at the top of the image and the gill filaments of gill arches 1–4 are labeled. E, eye; PF, pectoral fin. The scale bar represents 0.5 mm and applies panels (b) and (c). An isolated gill basket is shown in (b), and a single gill shown in (c). GA, gill arch. The dashed box indicates a typical region of a gill filament (F) that was studied using confocal microscopy and is represented as a schematic in (d). (d) In this simplified representation, oxygen-sensitive neuroepithelial cells (NECs, green) are located along the filament (F) and receive sensory innervation (red). Nerve fibres form a plexus (not shown) around NECs, extend laterally to the secondary lamellae (L, small arrows), and large nerve bundles (large arrow) extend toward the gill arch. (e) Extrabrancial (left) and intrabranchial (right) innervation of filament NECs arise from the branchial nerve (BN) or superficial and deep proximal neurons (SPN and DPN), respectively. E is modified from Jonz & Nurse (2008), with permission from the authors.

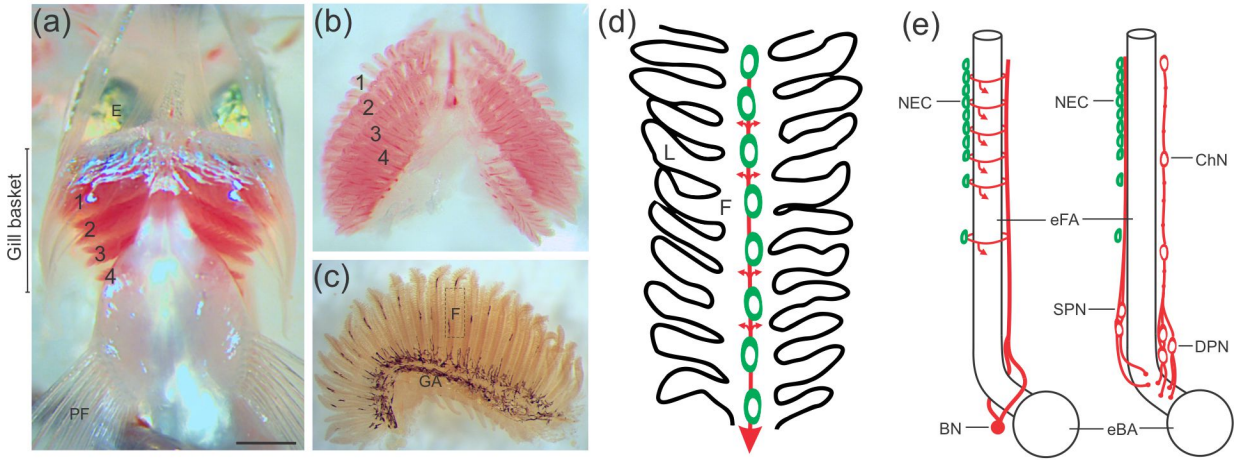
(a)
Gill basket
E
1
2
3
4
PF
(b)
1
2
3
4
(c)
F
GA
(d)
L
F
(e)
NEC
NEC
ChN
eFA
SPN
DPN
BN
eBA

Figure 2.1

**Figure 2-2 Confocal imaging of immunohistochemical localization of tyrosine hydroxylase (TH) positive nerve fibers associated with serotonergic neuroepithelial cells (NECs).** (a) NECs (arrows) labeled with anti-serotonin (5-HT, green) were closely associated with a plexus of nerve fibers (arrowheads) labeled by anti-TH (magenta) in the filaments (F) and lamellae (L). (b, c) TH and 5-HT labelling shown separately. (d–f) Images of gill filaments and lamellae are shown at higher magnification (upper panels) and tilted back 90° (lower panels). In the latter, the transverse optical section revealed the close association between NECs and nerve fibers, and that the nerve fibers surrounded the efferent filament artery (eFA). Scale bar in A = 20 μm and applies to b and c. Scale bar in d = 20 μm and applies to e and f.

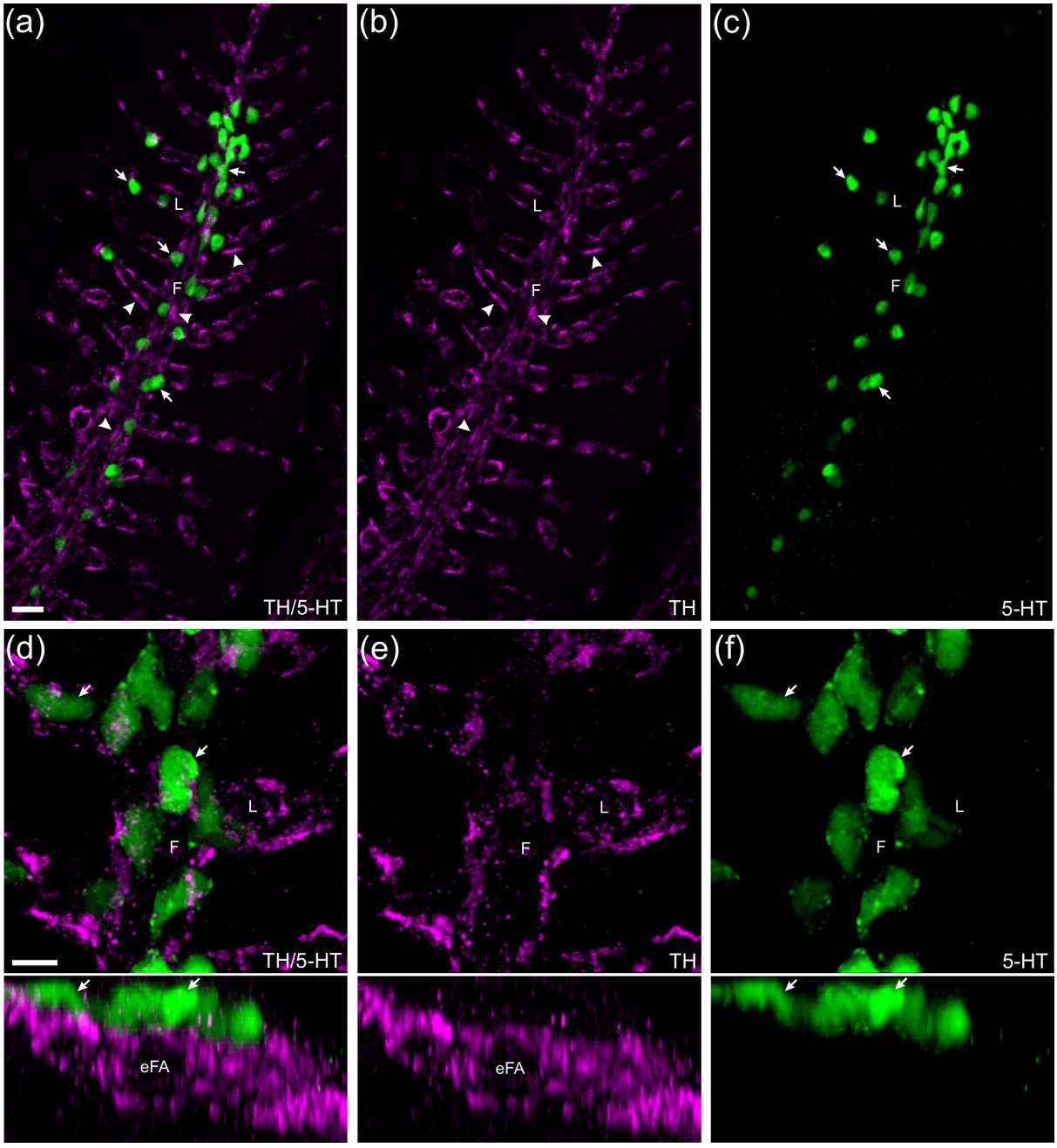


Figure 2.2

**Figure 2-3 Confocal imaging of immunohistochemical co-localization of tyrosine hydroxylase (TH) with a zebrafish-specific neuronal marker.** (a) Labelling with anti-TH (green) co-localized with nerve fibers labeled with zn-12 (magenta). (b, c) TH and zn-12 labeling shown separately. Both nerve bundles of the central filament (F) and all zn-12-positive nerve fibers (arrowheads) of the filaments and lamellae (L) were also TH-positive. Some labeling by anti-TH did not co-localize with zn-12. An intrabranchial chain neuron (ChN) is indicated that was labeled with both markers. Scale bar in a = 10 μm and applies to all panels.

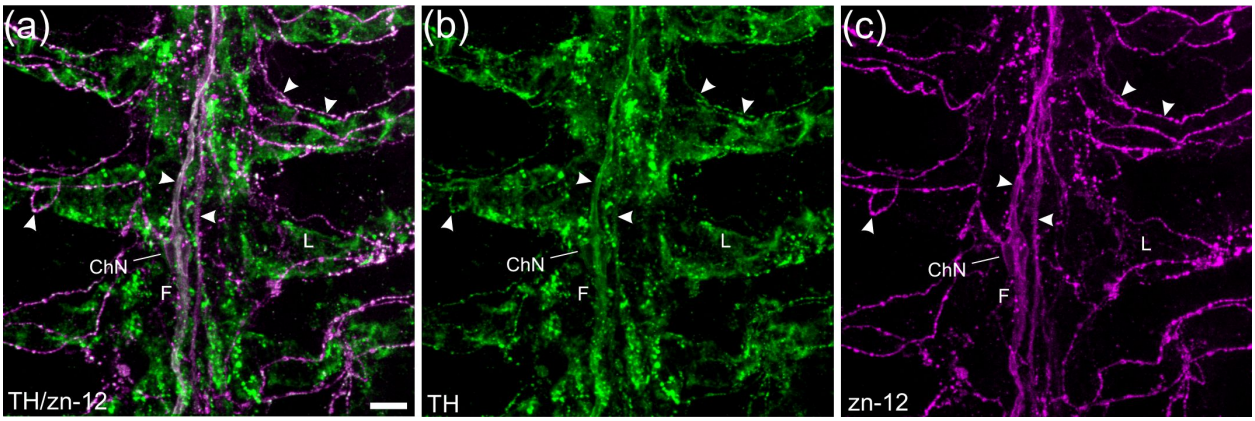

Figure 2.3

**Figure 2-4 Confocal imaging of nerve fibers expressing the dopamine active transporter (dat) and associated neuroepithelial cells (NECs) expressing the vesicular monoamine transporter (vmat2) in gills of the Tg(dat:mCherry)/ET(vmat2:GFP) line**. (a) dat expression (mCherry, magenta) was observed in nerve fibers (arrowheads) that formed a plexus along the center of the gill filaments (F). Nerves were closely opposed to vmat2-positive NECs (green), labeled by GFP and indicated by arrows. L = lamellae. (b, c) dat and vamt2 expression shown separately. (d–f) At higher magnification, the dat-positive nerve plexus extended across the filament epithelium and reached the interlamellar regions. A chain neuron (ChN) and associated axons was labeled and is indicated. (g–i) Images from d–f tilted back 45° (upper panels) and 90° (lower panels). Rotation demonstrates the relationship between the dat-expressing nerve fibers and NECs in a transverse optical section. The plexus of dat nerve fibers wrapped around the efferent filament artery (eFA) and was closely associated with NECs. The ChN was located beneath the eFA, as part of the deeper nerve bundle that is comprised by intrabranchial neurons. Scale bar in a = 25 μm and applies to b and c. Scale bar in d = 10 μm and applies to e–i.

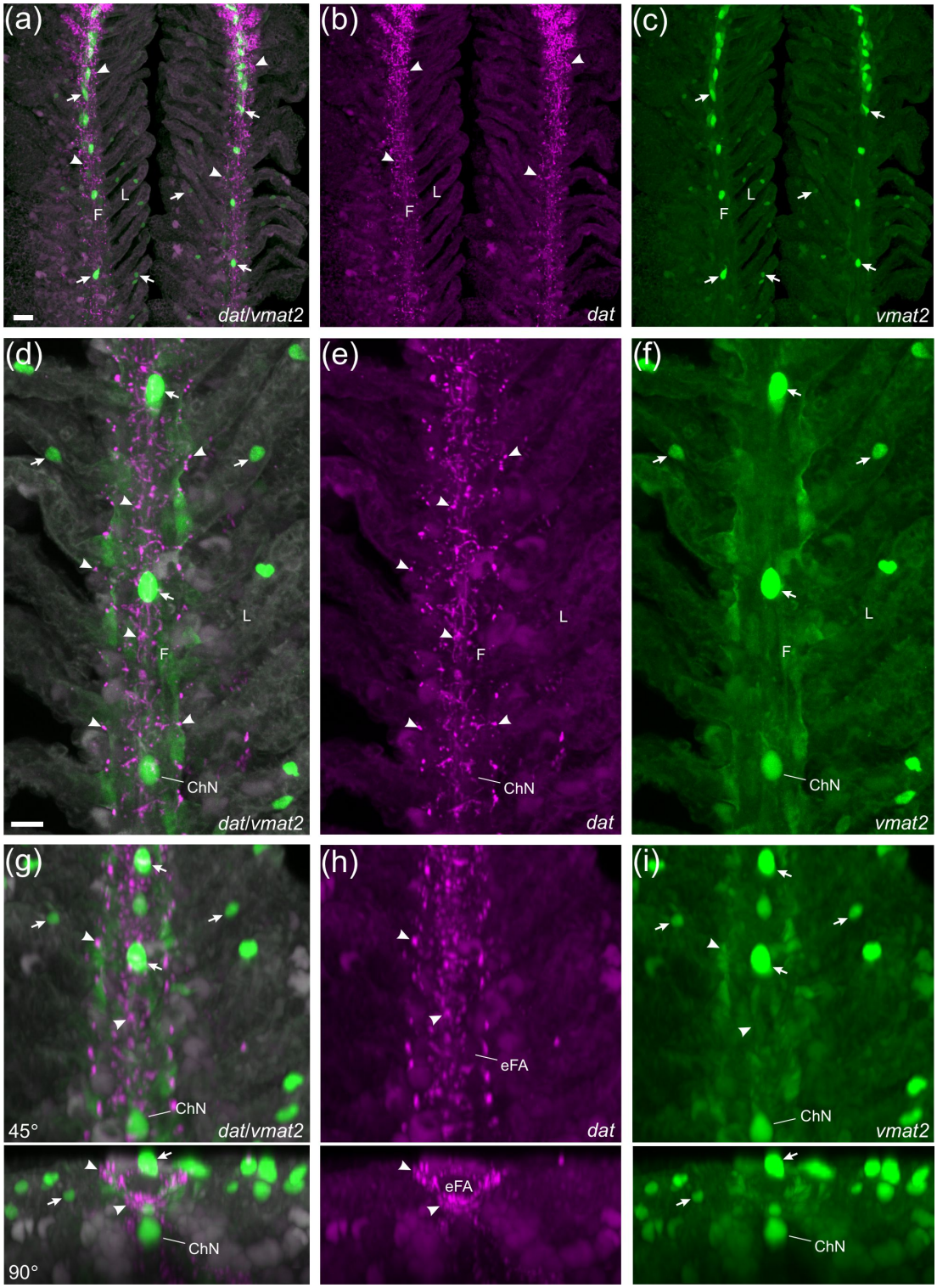
(a)
L
F
dat/vmat2
(b)
L
F
dat
(c)
L
F
vmat2
(d)
L
F
ChN
dat/vmat2
(e)
L
F
ChN
dat
(f)
L
F
ChN
vmat2
(g)
ChN
45°
dat/vmat2
ChN
90°
(h)
eFA
dat
eFA
(i)
ChN
vmat2
ChN

Figure 2.4

**Figure 2-5 In chemical screening assays, domperidone (a dopamine D2 receptor antagonist) increased breathing frequency (fv), and quinpirole (a dopamine D2 receptor agonist) abolished the hyperventilatory response to hypoxia.** fv (in breaths min-1) was measured in zebrafish larvae at 14–16 days post-fertilization (d.p.f.). (a) Mean $f_v$ ± SEM is shown for controls (C), after application of 50, 100, 200 or 300 μM domperidone, and after recovery (R). Asterisks denote a significant increase in $f_v$ compared to controls ($P < 0.05$; ANOVA with repeated measures and Bonferroni post-test; N = 11, 10, 11 and 10 for each concentration, respectively). (b) A plot of concentration vs. percent maximum $f_v$ response was fit with a non-linear ligand binding model with least squares following the equation: $y=b_{max}\cdot x^h/(k_d^h + x^h)$. The effective half-maximal concentration ($EC_{50}$) for domperidone was 30 μM. (c) Mean $f_v$ ± SEM for larvae exposed to hypoxia alone (including 0.5% DMSO for control; left panel) or hypoxia combined with 50, 150 or 200 μM quinpirole. N = 15 for hypoxia, and 12, 11 and 12 for each concentration, respectively. (d) A plot of the concentration vs. percent maximum inhibition of the $f_v$ response was fit with the same equation as in (b). The $EC_{50}$ for quinpirole could not be reliably determined but was estimated at <10 μM.

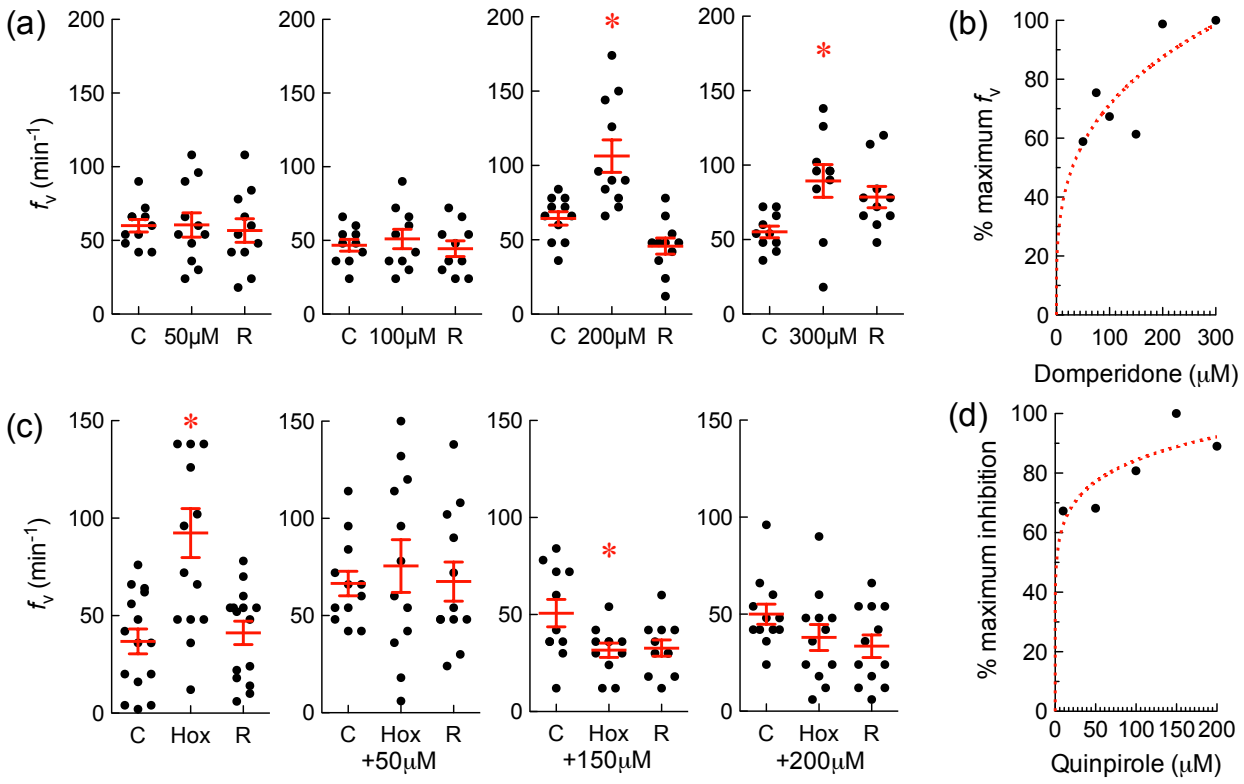
(a)
$f_V$ (min$^{-1}$)
C 50μM R
C 100μM R
C 200μM R
C 300μM R
(b)
% maximum $f_V$
Domperidone (μM)
(c)
C Hox R
+50μM
+150μM
+200μM
(d)
% maximum inhibition
Quinpirole (μM)

Figure 2.5

**Figure 2-6 Acclimation to chronic hypoxia reduced the aquatic surface respiration (ASR) response to acute hypoxia.** Adult zebrafish previously acclimated to hypoxia for various time points (24 h, 48 h, 72 h, or 7 d) were exposed to successive bouts of progressively more severe acute hypoxia (100 mmHg, 50 mmHg, 30 mmHg, and 15 mmHg). Data points for all groups were connected with a continuous line for clarity. Acclimation to hypoxia for 48 h, 72 h and 7 d significantly reduced mean ± SEM cumulative time in ASR during acute hypoxic exposure (squares) at $PO_2$ values below 30 mmHg, compared with unacclimated zebrafish (circles; Mann-Whitney U Test; $P<0.01$; N = 8 in control and acclimated groups for each $PO_2$ and each period of acclimation).

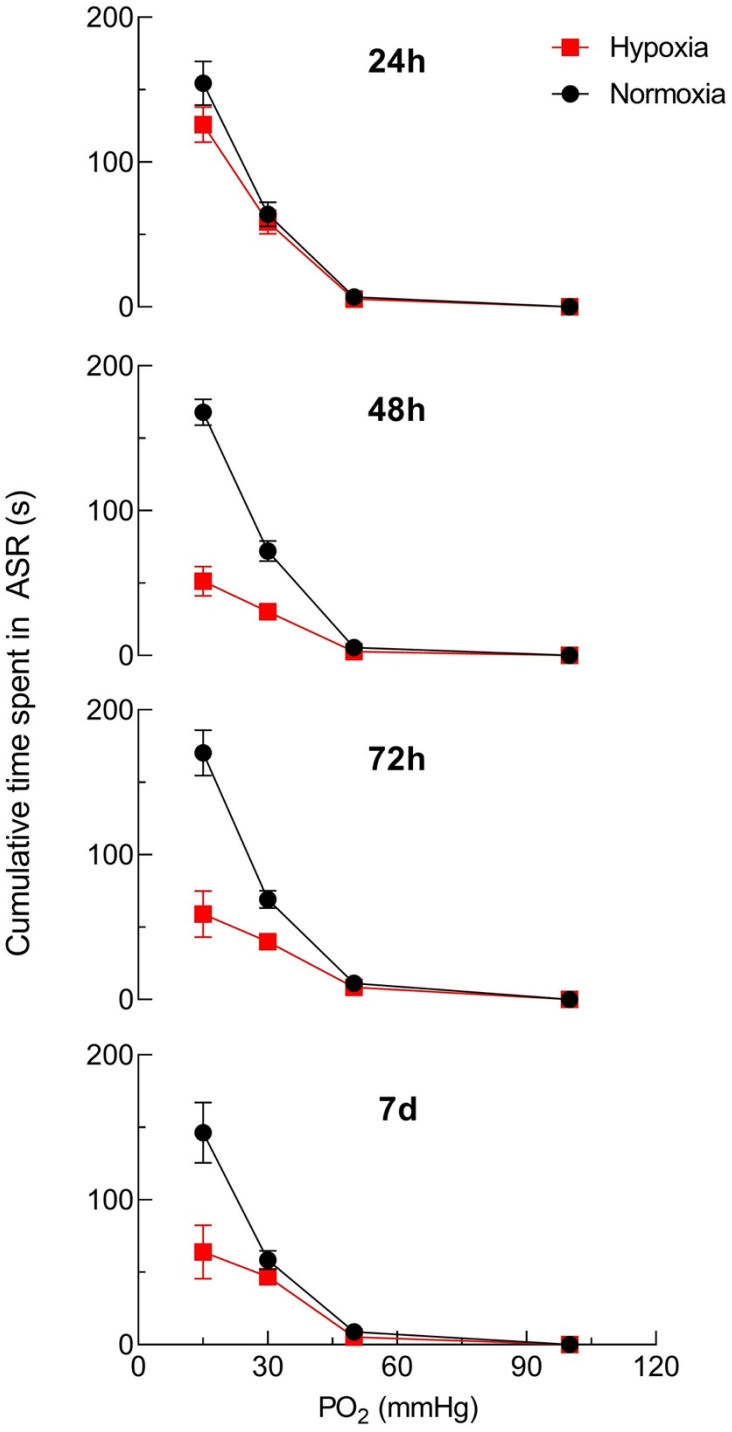
24h
48h
72h
7d
Hypoxia
Normoxia
Cumulative time spent in ASR (s)
200
100
0
0
30
60
90
120
PO2 (mmHg)

Figure 2.6

**Figure 2-7 Relative gene expression of drd2a and drd2b (encoding D2 receptors) decreased following 48 h of chronic hypoxia.** Data were normalized to the mRNA abundance of the reference gene, ef1a. Data were analyzed using a Mann-Whitney U Test and means significantly different from control are indicated by asterisks ($P < 0.01$; N = 8). Relative abundance for reference gene *ef1a* in the gill of control (normoxia) and treatment (hypoxia). Data points presented are relative to the control group. Hypoxia had no effect on the mRNA abundance of *ef1a* (Mann-Whitney U test; P>0.05; N = 7).

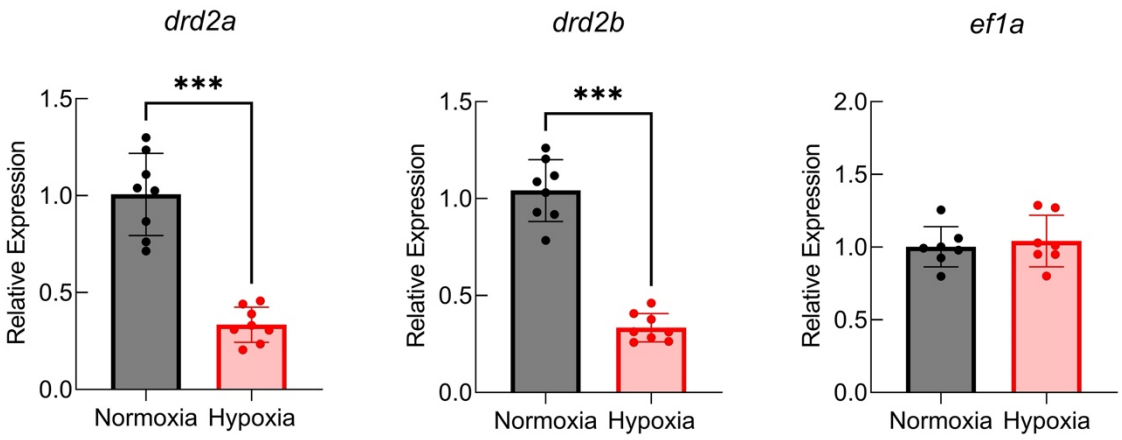
drd2a
drd2b
ef1a
***
***
Relative Expression
1.5
1.0
0.5
0.0
2.0
Normoxia
Hypoxia

Figure 2.7

**Figure 2-8 Characterization of D2-positive cells of the efferent gill epithelium.** Confocal imaging of immunohistochemical labeling of dopamine receptor 2 (D2-R) with a zebrafish-specific neuronal marker (zn-12) and neuroepithelial cells (NECs) containing synaptic (a) Labeling with anti-$D_2$-R (green) co-localized with NECs (arrows) labeled with SV2 (magenta) and nerve fibers labeled with zn-12 (magenta) in the filaments (F). (b, c) $D_2$-R and SV2/zn-12 labeling shown separately. Some zn-12-positive nerve fibers (arrowheads) of the filament and lamellae (L) were also $D_2$-R-positive. (d–f) Co-localization of NECs and $D_2$-R from a–c shown at higher magnification and titled back 45°. (g–i) Images from a–c tilted back 90°. Rotation demonstrates $D_2$-R-positive NECs in a transverse optical section oriented superficial to the efferent filament artery (eFA). Scale bar in a = 20 μm and applies to b and c. Scale bar in d = 20 μm and applies to e–i.

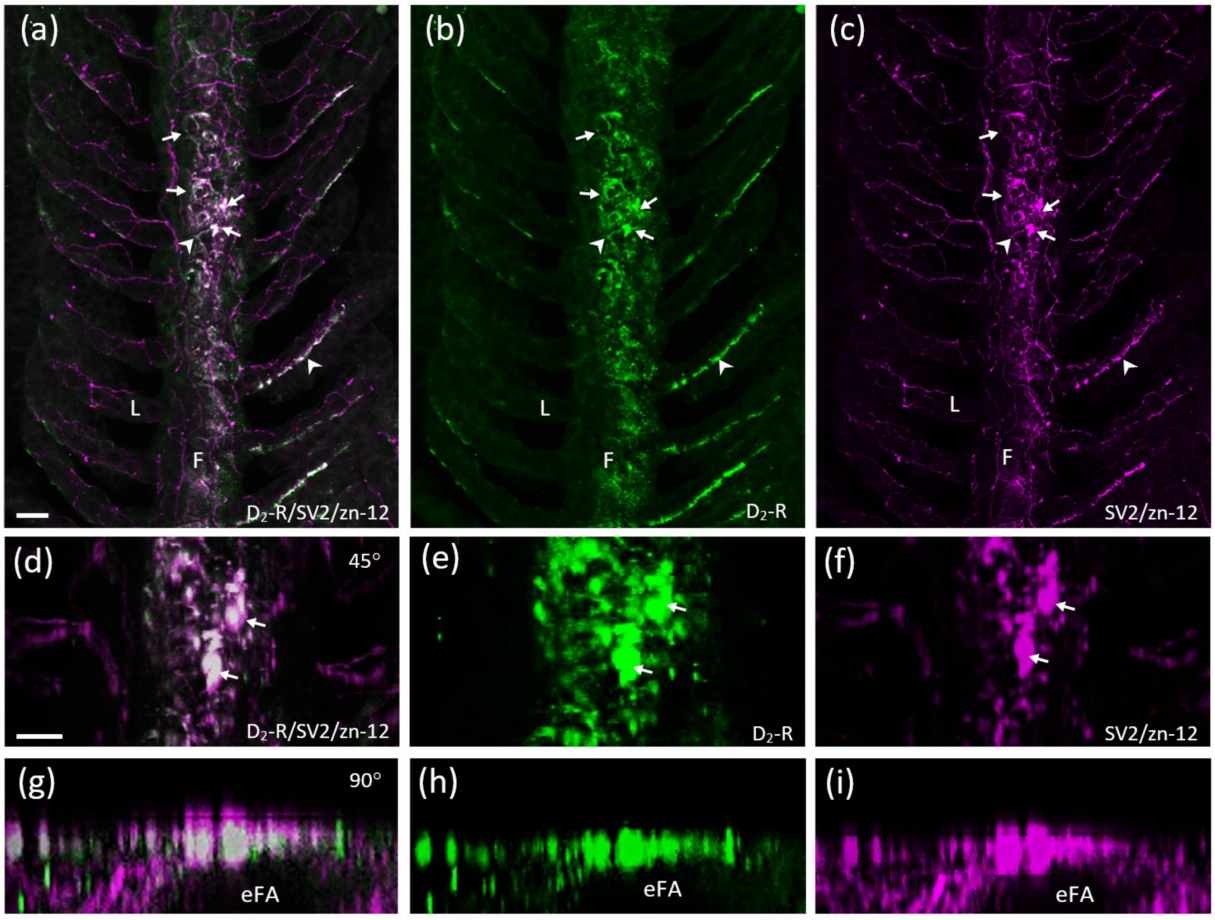


Figure 2.8

**Figure 2-9 Characterization of D2-positive cells of the afferent gill epithelium.**

(a) Confocal imaging of immunohistochemical localization of dopamine receptor 2 ($D_2$-R) on the afferent filament epithelium. (b) Co-application with DAPI labeled nuclei of $D_2$-R-positve cells. (c-d) Image from (a) was titled back 45° (c) and 90° (d). Rotation demonstrates $D_2$-R-expressing cells surround the afferent filament artery (aFA). Scale bar in a = 20 μm and applies to b-d.

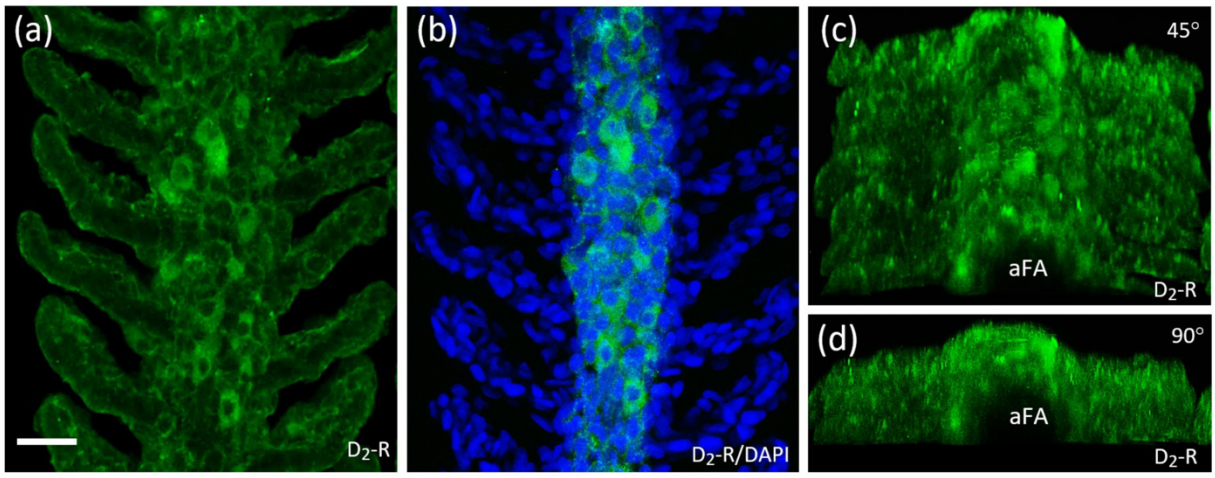


Figure 2.9

**Figure 2-10 Model of the proposed role for dopamine in modulating the hypoxic response in gill neuroepithelial cells (NECs) of the efferent epithelium.** As shown in the present study, postsynaptic nerve terminals in the gill filaments express tyrosine hydroxylase (TH) and the dopamine active transporter (DAT), involved in synthesis and uptake of dopamine (DA), respectively. When the NEC is stimulated during hypoxia: (1) Release of an unknown neurotransmitter from the NEC activates a postsynaptic receptor on the sensory nerve terminal. (2) Dopamine is then released from the nerve terminal and (3) activates pre-synaptic D2 receptors of the NEC, or is taken up postsynaptically by DAT. (4) The former leads to inhibition of the NEC response to hypoxia. The excitatory neurotransmitter released by NECs has not been confirmed but may be serotonin (5-HT). As illustrated, zebrafish NECs contain 5-HT, synaptic vesicles, and the vesicular monoamine transporter, VMAT2 (Jonz & Nurse, 2003; Pan et al., 2021). NECs also express genes encoding tryptophan hydroxylase and the serotonin transporter (SERT) for possible 5-HT synthesis and uptake (Pan et al., 2022). Created with BioRender.com.

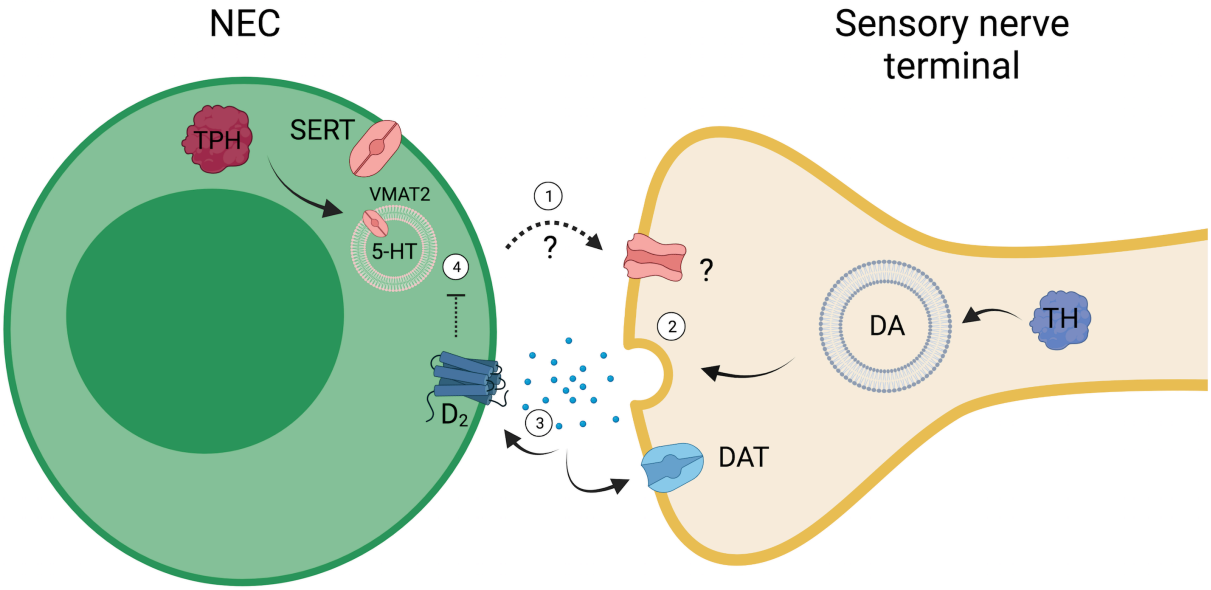
NEC
Sensory nerve terminal
TPH
SERT
VMAT2
5-HT
4
D2
1
?
?
2
DA
TH
3
DAT

Figure 2.10

## 2.5 Discussion

The present study demonstrates a role for dopamine in the gills of zebrafish as a modulator of the hyperventilatory response to hypoxia. We used immunohistochemistry, confocal microscopy and transgenic markers to localize elements of dopamine synthesis and transport to sensory nerve fibers that innervate NECs in the gill filaments. We further integrated pharmacological and molecular approaches to reveal pre-synaptic expression of $D_2$ receptors in chemoreceptive NECs and associated innervation.

### 2.5.1 Synthesis and storage of dopamine in nerve fibers of the gills

Tyrosine hydroxylase is a rate-limiting enzyme required for the synthesis of catecholamines, including dopamine. Localization of TH can therefore be used to elucidate potential sites of dopamine production in the gill. The presence of TH in gills appears to be heterogeneous across fish species. In catfish (*Ictalarus punctatus*), isolated 5-HT-positive NECs were co-labeled with antibodies against TH, suggesting that NECs may release 5-HT and dopamine in that species (Burleson et al., 2006). By contrast, a lack of TH labeling in the gills of goldfish (*Carassius auratus*), trout (*O. mykiss*) and Indian catfish (*Heteropneustes fossilis*) leave a role for dopamine in these species less clear (Porteus et al., 2013; Zaccone et al., 2003). Expression of *th2*, one of the genes encoding TH, was identified in the gill region of zebrafish embryos using *in situ* hybridization, but the cells expressing the enzyme were not identified (Chen et al., 2009).

In the present study, we detected anti-TH labeling and dopamine active transporter (*dat*) expression in nerve fibers throughout the gill filaments and respiratory lamellae. Interestingly, many TH and *dat*-positive nerve fibers were closely associated with NECs, and a previous study

described these as afferent fibers of ganglionic neurons that carry chemosensory information to the central nervous system during hypoxic stimulation of NECs (Jonz & Nurse, 2003). By comparison with the rat carotid body, Finley et al. (1992) described afferent nerve fibers of the petrosal ganglion that innervate type I cells and contained both TH and DOPA decarboxylase (DDC), a second enzyme involved in dopamine synthesis. Whereas the primary source of dopamine in the carotid body is usually regarded as the type I cell (González et al., 1994; Itturiaga et al., 2009; Nurse, 2010), Finley et al. demonstrated that 41% of all carotid body afferents were dopaminergic and suggested that postsynaptic nerve terminals may additionally synthesize and release dopamine to modulate the type I cell response to hypoxia. In addition, oxygen-sensitive NEBs of the lung epithelium in rat were shown to receive innervation by TH-positive nerve fibers (Van Genechten et al., 2004), although a similar role for dopamine in NEBs has never been shown. Our characterization indicates that, in zebrafish, TH and *dat*-positive nerve fibers that associate with gill NECs are capable of dopamine synthesis and reuptake and provide a potential mechanism for production and vesicular storage of dopamine in postsynaptic nerve fibers (Fig. 10).

We did not detect TH in NECs in the present study. Dopamine synthesis in gill NECs of zebrafish, however, remains a possibility since expression of *ddc* (the gene encoding DOPA decarboxylase) was reported in NECs and neurons in single-cell RNA-sequencing (Pan et al., 2022), and the vesicular monoamine transporter (VMAT2) is also present in NECs (Pan et al., 2021, 2022). Both are involved in the synthesis and storage of dopamine and serotonin.

### 2.5.2 Dopamine $D_2$ receptors mediate the response to hypoxia

Early evidence for a role of dopamine receptors in control of the hypoxic ventilatory response in fish was provided from isolated gills of rainbow trout, where dopamine caused a small and brief burst in chemoreceptor activity followed by a mild inhibition of receptor discharge (Burleson & Milsom, 1995). More recently, in zebrafish, exogenous application of dopamine decreased ventilation frequency as early as 7 d.p.f. (Shakarchi et al., 2013), and genes encoding members of the $D_2$-like receptor family were expressed in gill NECs and neurons (Pan et al., 2022). In the carotid body, $D_2$ is the dominant type of dopamine receptor involved in modulation of the response to hypoxia (Mir et al., 1984; Gauda et al., 2002; Carroll et al., 2005; Itturiaga et al., 2009; Nurse, 2010). We therefore used a chemical screening assay (Rahbar et al., 2016) to test whether $D_2$ in the gills might affect the hypoxic response. We report an increase in ventilation frequency in zebrafish larvae in response to the $D_2$ receptor antagonist, domperidone. Further, when the $D_2$ receptor agonist, quinpirole, was administered, larvae failed to mount a hyperventilatory response to hypoxia. These data support the hypothesis that $D_2$ receptors inhibit the hyperventilatory response to hypoxia, as it does in the carotid body. Due to potential off-target effects inherent to whole-animal experiments, we used immunohistochemical and molecular approaches for a more specific characterization of $D_2$ in the gills.

Quantitative PCR confirmed that both gene transcripts encoding $D_2$ receptors were expressed in isolated gill tissue. Further, we found co-localization of $D_2$ receptors and chemosensory NECs in the efferent gill filament epithelium. The location of these receptors is consistent with the carotid body, where inhibitory $D_2$ receptors are found on chemosensory type 1 cells, which may suggest a similar mechanism of inhibition or modulation in the zebrafish gill. However, further work is needed to explore a possible mechanism of inhibition of the hypoxic signal via $D_2$ receptors. We also found the relative gene expression of both *drd2a* and *drd2b* in

isolated gills decreased following hypoxia acclimation. Similarly, Huey & Powell (2000) showed $D_2$ receptor mRNA expression in the carotid body decreased following hypoxia acclimation and suggested this may be one mechanism by which exposure to chronic hypoxia reduces inhibition of hypoxia signaling to enhance ventilatory acclimatization to hypoxia. Our findings are consistent with the mammalian carotid body and suggest gill $D_2$ receptors may be involved in acclimatization to hypoxia.

In Figure 10, we summarize a proposed model, in which the postsynaptic release of dopamine inhibits the NEC response to hypoxia. During hypoxia, NECs depolarize, increase intracellular $Ca^{2+}$ concentration and undergo synaptic vesicle recycling, as occurs during neurotransmitter secretion (Jonz et al., 2004; Zachar et al., 2017a). The excitatory neurotransmitter responsible for relaying the initial hypoxic signal from NEC to postsynaptic nerve terminal remains unconfirmed, but may be serotonin. Evidence demonstrating that NECs in zebrafish contain 5-HT, synaptic vesicles, the vesicular monoamine transporter (VMAT2), and selectively express genes encoding tryptophan hydroxylase (TPH) and the serotonin transporter (SERT) for possible 5-HT synthesis and uptake, supports this idea (Jonz & Nurse, 2003; Pan et al., 2021, 2022). We propose that the released neurotransmitter activates postsynaptic receptors, leading to subsequent release of dopamine from sensory nerve terminals into the synaptic cleft, where it acts upon pre-synaptic $D_2$ receptors. $D_2$ receptor activation by dopamine may then provide an intracellular pathway through which NEC excitation or secretion by hypoxia is reduced. In type I cells of rabbit carotid body, dopamine was shown to inhibit voltage-gated $Ca^{2+}$ channels, thereby reducing neurosecretion (Benot & López-Barneo, 1990). Moreover, in petrosal neurons of rat carotid body, dopamine acts through $D_2$ to inhibit adenylyl cyclase and cyclic AMP, thus reducing membrane excitability (Zhang et al., 2018). Future physiological

experiments on NECs may elucidate the intracellular pathways involved in reducing NEC activity via $D_2$.

Interestingly, we found $D_2$ receptor labeling was not limited to chemosensory NECs. Immunohistochemical labeling against $D_2$ receptors also revealed some $D_2$-positive nerve fibers of the gill filaments that projected into the respiratory lamellae, and an unknown cell type in the afferent filament epithelium. A role for $D_2$ receptors at these sites in the gill is less clear. Though chemosensory NECs are primarily limited to the efferent filament epithelium (Jonz & Nurse, 2003), there are a number of cell types in the afferent filament epithelium that may be of interest in oxygen sensing and signaling. For example, acetylcholine (ACh) is a neurotransmitter thought to be involved in the facilitation of the hypoxic ventilatory response in zebrafish. In the zebrafish gill, the vesicular acetylcholine transporter (VAChT) has been localized to cells in the efferent filament epithelium as well as an abundance of cells in the afferent filament epithelium, suggesting the importance of ACh on both sides of the gill filament (Zachar et al., 2017b). Whether VAChT-positive cells in the afferent epithelium are also $D_2$-positive is currently not clear; however, given that carotid body type 1 cells contain both ACh and dopamine, it is possible that a similar organization of neurotransmitters exists in the gill.

## 2.6 Conclusion

The present study sought to evaluate a role for dopamine in hypoxia signaling within the zebrafish gill. We found evidence for postsynaptic synthesis and reuptake of dopamine in the gills and implicate pre-synaptic $D_2$ receptors in control of the hypoxic ventilatory response in zebrafish. Given the location of $D_2$ receptors, it is possible that this control takes place at the level of the chemosensory NECs within the zebrafish gill; however, further work is needed to

explore such a mechanism of inhibition. The results of our studies are consistent with carotid body mediation of hypoxia signaling via $D_2$ receptors and thus suggest that an inhibitory or modulatory role for dopamine in oxygen sensing arose early in vertebrate evolution.

# Chapter 3

# Oxygen chemoreceptor inhibition by dopamine $D_2$ receptors in isolated zebrafish gills

This chapter includes material from the following article:

Reed & Jonz (Accepted January 2025). *Oxygen chemoreceptor inhibition by dopamine $D_2$ receptors in isolated zebrafish gills.* Journal of Physiology.

## 3.1 Abstract

Dopamine is an essential modulator of oxygen sensing and control of ventilation and is the most well described and abundant neurotransmitter in the mammalian carotid body. Little is known of the evolutionary significance of dopamine in oxygen sensing, or whether it plays a similar role in anamniotes. In the model vertebrate, zebrafish (*Danio rerio*), presynaptic dopamine $D_2$ receptor ($D_2R$) expression was demonstrated in gill neuroepithelial cells (NECs)—analogues of mammalian oxygen chemoreceptors; however, a mechanism for dopamine and $D_2R$ in oxygen sensing in the gills had not been defined. The present study tested the hypothesis that presynaptic $D_2Rs$ provide a feedback mechanism that attenuates the chemoreceptor response to hypoxia. Using an isolated gill preparation from Tg(*elavl3*:GCaMP6s) zebrafish, we measured hypoxia-induced changes in intracellular $Ca^{2+}$ concentration ($[Ca^{2+}]_i$) in NECs and postsynaptic neurons. Activation of $D_2R$ with dopamine or specific $D_2R$ agonist, quinpirole, decreased hypoxic responses in NECs; whereas $D_2R$ antagonist, domperidone, had the opposite effect. Addition of SQ22536, an adenylyl cyclase (AC) inhibitor, decreased the effect of hypoxia on $[Ca^{2+}]_i$, similar to dopamine. Activation of AC by forskolin partially recovered the suppressive effect of dopamine on the $Ca^{2+}$ response to hypoxia. Further, we demonstrate that the response to hypoxia in postsynaptic sensory neurons was dependent upon innervation with NECs, and was subject to modulation by activation of presynaptic $D_2R$. Our results provide the first evidence of neurotransmission of the hypoxic signal at the NEC-nerve synapse in the gill and suggest that a presynaptic, modulatory role for dopamine in oxygen sensing arose early in vertebrate evolution.

## 3.2 Introduction

Dopamine is an important neuromodulator involved in oxygen sensing and control of reflex hyperventilation. In the mammalian carotid body, it is the most abundant neurotransmitter and has been described in numerous species (Gauda, 2002). Hypoxic activation of carotid body oxygen chemosensory type 1 (glomus) cells involves $Ca^{2+}$-dependent neurotransmitter release to act on sensory terminals of the carotid sinus nerve (González et al., 1994; Kumar & Prabhakar, 2012; López-Barneo et al., 1988; Nurse, 2010). Dopamine, released by type 1 cells, has been shown to have autocrine–paracrine actions in the carotid body via G-protein-coupled dopamine $D_2$Rs on both presynaptic type 1 cells and postsynaptic afferent terminals (Nurse, 2010; Zhang et al., 2018, Carroll et al., 2005; Gauda, 2002; Itturiaga et al., 2009; Mir et al., 1984). At the presynaptic type 1 cell, the inhibitory actions of dopamine decrease further neurotransmitter release, thereby modulating carotid body hypoxia signaling (Benot & López-Barneo, 1990). Dopamine has also been implicated in regulation of chemosensitivity during acclimatization to prolonged periods of hypoxia (Bisgard, 2000; Huey & Powell 2000; Powell, 2007), and as an important factor in development or maturation of the carotid body (Carroll et al., 2005; De Caro et al., 2013; Gauda, 1996, 2002).

In fish, oxygen sensing occurs in the gills via chemoreceptive neuroepithelial cells (NECs) in a manner similar to carotid body type I cells. NECs are found in the gill filament epithelium and respond to a decrease in $P_{O_2}$ by inhibition of background $K^+$ channels, membrane depolarization, and $Ca^{2+}$-dependent vesicular recycling (Jonz et al., 2004; Zachar et al., 2017a). The latter is consistent with neurotransmitter release into the synaptic cleft, which may lead to activation of sensory nerve fibres to control ventilation. NECs are polymodal, such that they are sensitive to changes in $O_2$, $CO_2$, $H^+$ and lactate (Abdallah et al., 2015; Jonz, 2018; Qin

et al., 2010; Leonard et al., 2022) and are characterized by immunoreactivity to serotonin (5-hydroxytryptamine [5-HT]) and synaptic vesicle protein, SV2 (Jonz & Nurse, 2003). Teleost gill arches are innervated by branches of the glossopharyngeal (IX) and vagus (X) cranial nerves, which carry parasympathetic efferent fibres to the gill vasculature and sensory (afferent) fibres from chemoreceptors of the gill filaments (Nilsson, 1984; de Graaf, 1990; Sundin and Nilsson, 2002). Beneath the efferent filament artery lies a series of 4-6 neuronal somata found along a nerve bundle that travels the length of the filament. These are referred to as chain neurons (ChNs) and may provide an additional source of sensory innervation to NECs (Jonz & Nurse, 2003).

The gill arches in fish are homologues of the sites of $O_2$-sensing organs in mammals, such as the carotid body and pulmonary neuroepithelial bodies; however, whether gill NECs are functionally similar (i.e. homologous) with carotid body type I cells or neuroepithelial bodies, is controversial (Milsom & Burleson, 2007; Zachar & Jonz, 2012, Hockman et al., 2017; Jonz, 2024). Despite the similarities between NECs and type I cells, and in contrast to the well-described neurochemistry of the carotid body (Nurse, 2010), a mechanism for control of ventilation during hypoxia via neurotransmission in the gills of fish has never been defined.

Early evidence of a role for dopamine in the gills was shown in isolated gills of rainbow trout (*Oncorhynchus mykiss*), where dopamine caused a small, brief burst in afferent nerve activity followed by mild inhibition (Burleson & Milsom, 1995). In live, whole-animal experiments using zebrafish larvae, application of dopamine or the dopamine $D_2R$ agonist, quinpirole, both decreased ventilation frequency, suggesting inhibitory effects of dopamine on ventilation (Shakarchi et al., 2013, Reed et al., 2024). In isolated gill tissue from adult zebrafish, quantitative polymerase chain reaction analysis confirmed expression of *drd2a* and *drd2b* (genes

encoding $D_2$Rs) in the gills, and their relative abundance decreased following acclimation to hypoxia for 48 h (Reed et al., 2024). Further, immunohistochemical labelling in the gill localized $D_2$R to presynaptic NECs, as well as provided evidence for the synthesis and storage of dopamine by nerve terminals of postsynaptic sensory neurons that innervate NECs (Reed et al., 2024). While these findings point to an inhibitory role for dopamine via $D_2$R in the gill, a direct mechanism for how dopamine may participate in oxygen sensing has not been elucidated.

The goal of the present study was to delineate a mechanism by which presynaptic $D_2$Rs provide a feedback mechanism that attenuates the chemoreceptor response to hypoxia. Using a genetically-encoded $Ca^{2+}$ indicator in gills isolated from transgenic zebrafish, we found that activation of presynaptic $D_2$R decreased the NEC $Ca^{2+}$ response to hypoxia via intracellular adenylyl cyclase (AC) activation. Further, we provide evidence for postsynaptic modulation of the hypoxic signal in sensory neurons originating via activation of presynaptic $D_2$R.

## 3.3 Methods

### 3.3.1 Ethical approval

All wild-type and transgenic zebrafish were bred and maintained at the Laboratory for the Physiology and Genetics of Aquatic Organisms, University of Ottawa. Zebrafish were kept at 28°C on a 14:10-h light:dark cycle (Westerfield, 2007). Embryos and larvae were reared on a diet of rotifers and Gemma 75 (Skretting Canada, St. Andrews, NB), juveniles were fed Artemia and Gemma 150-300 (Skretting), and adults were fed Adult Zebrafish Diet (Ziegler Feeds, Gardners, PA, USA). Adult zebrafish were euthanized by concussion and terminated by decapitation. All procedures for animal use and euthanasia were carried out in accordance with institutional guidelines according to protocol BL-3666, and guidelines provided by the Canadian

Council on Animal Care. The present work complies with the ethical guidelines set out by the journal and with those according to Animals in Research: Reporting In Vivo Experiments (ARRIVE).

In this study we used transgenic zebrafish Tg(*elavl3*:GCaMP6s) expressing the genetically encoded $Ca^{2+}$ indicator GCaMP6s under the pan-neuronal promotor *elavl3* (Dunn et al. 2016). GCaMP6s contains the green fluorescent protein (GFP) as part of its structure. The Tg(*dat:tom20 MLS-mCherry*) line has previously been used to visualize dopaminergic neurons (Reed et al., 2024). In this line, the regulatory elements of the dopamine transporter gene (*dat*) were targeted to a reporter, mCherry, after fusion with the mitochondrial localizing signal (MLS) of Tom20 (Noble et al., 2015). To determine the distribution of dopaminergic nerve terminals relative to GFP-positive NECs, adult Tg(*elavl3*:GCaMP6s) fish were crossed with adult Tg(*dat:tom20 MLS-mCherry*) to generate double transgenic offspring containing both mCherry and GFP.

### 3.3.2 Immunohistochemistry

Techniques for tissue extraction and immunolabeling were carried out as previously described (Jonz & Nurse, 2003). Following termination by concussion and decapitation, whole gill baskets were removed and immersed in phosphate buffered solution (PBS) containing (mM): NaCl 137, $Na_2HPO_4$ 15.2, KCl 2.7, and $KH_2PO_4$ 1.5 at pH 7.8 (Bradford et al., 1994). Gill baskets were fixed by immersion in 4% paraformaldehyde in PBS overnight at 4°C. Tissues were removed and rinsed in PBS three times at 3 min before permeabilization for 24 h at 4°C. Permeabilizing solution (PBS-TX) contained 0.5-2% Triton X-100 in PBS (pH 7.8). After 3 rinses in PBS, gill baskets were then separated into individual arches. Gill arches were incubated

in primary antibodies for 24 h at 4°C, rinsed with PBS three times at 3 min, and immersed in secondary antibodies for 1 h at room temperature in darkness.

NECs were identified using antibodies against serotonin (5-HT) or synaptic vesicle protein SV2. Polyclonal anti-5-HT was raised in rabbit against a 5-HT creatinine sulfate complex conjugated with bovine serum albumin (manufacturer specifications; cat. no. S5545, Sigma-Aldrich, Oakville, ON, Canada; Antibody Registry ID: AB_477522). Anti-5HT was used at 1:250 and localized with goat anti-rabbit secondary antibodies conjugated with fluorescein isothiocyanate (FITC, 1:50, cat. no. 111-095-003, Cedarlane, Burlington, ON, Canada). Monoclonal SV2 raised in mouse (AB_2315387 and AB_531908; Developmental Studies Hybridoma Bank, University of Iowa, IA, USA) was used at 1:100 and targeted by goat anti-mouse secondary antibodies conjugated with Alexa 594 at 1:100 (cat. no. A11005, Invitrogen, Burlington, ON, Canada). Neurons and nerve fibres were identified using antibodies against a zebrafish-specific neuronal marker (zn-12). Monoclonal anti-zn-12 raised in mouse (RRID: AB_2315387; Developmental Studies Hybridoma Bank, University of Iowa) was used at 1:100 and visualized using goat anti-mouse secondary antibodies conjugated with Alexa 594 at 1:100 (cat. no. A11005, Invitrogen, Burlington, ON, Canada). Labelling by these antibodies in the zebrafish gill has been previously characterized (Jonz & Nurse, 2003).

### 3.3.3 Relative $[Ca^{2+}]_i$ measurements

Following termination by concussion and decapitation, whole gill baskets were removed and separated into individual gill arches and immersed in extracellular solution containing (mM): 120 NaCl, 5 KCl, 2.5 $CaCl_2$, 2 $MgCl_2$, 10 HEPES, 10 glucose at pH 7.8. Isolated intact gill arches from Tg(*elavl3*:GCaMP6s) zebrafish were secured in a Petri dish using a metal tissue

anchor (cat. no. 640251, Warner Instruments). The Petri fish was continuously perfused with extracellular solution (ECS) at pH 7.8. GFP-fluorescing cells were observed using a Nikon 40× water-immersion objective. NECs were identified by their size, presence of GFP, position along the centre of the filament epithelium, and location at the distal end of the filament. Using a Lambda DG-5 wavelength changer (Sutter Instruments, Novato, CA, USA), the preparation was exposed to 490 nm excitation light for 600 ms at a sampling frequency of 1 $s^{-1}$. Images were captured with a CCD camera (QImaging, Surrey, BC, Canada), and fluorescence intensity was recorded with NIS Elements software (Nikon).

Dual recordings of NECs and chain neurons (ChNs) were carried out as above, with a modified depth of focus. Since these two cell types are located in different layers of the gill filament, the recording plane was set at an intermediate depth between the NEC and ChN, where both cell types were slightly out of focus, but still within the field of view, and therefore could be recorded simultaneously (see Fig. 9C).

### 3.3.4 Solutions and drug treatments

High $K^+$ extracellular solution was prepared with 90 mM NaCl, 35 mM KCl, 2.5 mM $CaCl_2$, 2 mM $MgCl_2$, 10 mM HEPES, 10 mM glucose. Zero $Ca^{2+}$ extracellular solution was prepared with 120 mM NaCl, 5 mM KCl, 4.5 mM $MgCl_2$, 10 mM HEPES, 10 mM glucose, and 1 mM EGTA. pH of all solutions was kept at 7.8. 100% $N_2$ was bubbled through an air stone into solution reservoirs to create hypoxic solutions with a $PO_2$ of approximately 25 mmHg. All control solutions were bubbled with compressed air for the same duration of time.

Drugs were introduced into the recording chamber by perfusion in extracellular solution. Nifedipine (cat. no. N7643, Sigma-Aldrich) and dantrolene (cat. no. 0507, Tocris) were used to

block entry of extracellular $Ca^{2+}$ and release of stored $Ca^{2+}$, respectively. To target dopamine receptors, the D2R antagonist, domperidone (cat. no. D122; Sigma-Aldrich), and the D2R agonist, quinpirole (cat. no. Q102, Sigma-Aldrich), were tested. To identify an intracellular mechanism for $D_2R$, the AC inhibitor SQ22536 (cat. no. 1435, Tocris) and AC activator forskolin (cat. no. 11018, Cayman Chemical) were tested. All drugs were first dissolved in dimethyl sulfoxide (DMSO) to produce a final DMSO concentration of <0.1%. At this concentration, DMSO had no effect on $Ca^{2+}$ baseline and did not produce changes in fluorescence intensity (relative $[Ca^{2+}]_i$).

### 3.3.5 Statistical Analysis

For all reported data, sample size (n) refers to individual cells. While multiple gill arches were assessed per animal, only one cell from each arch was included in the analysis to avoid repeated exposures or treatments in the same tissue. Throughout this study, hypoxic responses from a total of 73 cells were recorded from 41 adult zebrafish. For each recording, the baseline fluorescence was calculated as the average fluorescence intensity of a cell for the first 30 s in normoxia. All fluorescence values were divided by the baseline to evaluate changes in fluorescence intensity over time throughout a single recording. Statistical analysis for comparison of two groups was carried out using the Kruskal-Wallis test with Prism software (GraphPad Software Inc., La Jolla, CA, USA). All data were expressed as means ± standard deviation (SD).

## 3.4 Results

### 3.4.1 NECs contain GCaMP6s and display a $Ca^{2+}$ response to hypoxia *in situ*

The transgenic Tg(*elavl3*:GCaMP6s) zebrafish used in this study expresses a genetically-encoded $Ca^{2+}$ reporter, GCaMP, under the control of the pan-neuronal promotor, *elavl3* (Dunn et al. 2016). To confirm expression of GCaMP in chemoreceptors, we used immunohistochemistry to identify GFP (part of the GCaMP complex) with known markers of gill NECs. Labelling of GFP-positive GCaMP-containing cells colocalized with anti-SV2 (Fig. 1A-C) and anti-5-HT (Fig. 1D-F), demonstrating that GCaMP is contained within NECs. We developed a procedure to record brief elevations in $[Ca^{2+}]_i$ that were associated with a hypoxic stimulus in single chemoreceptors *in situ* using isolated gills (Fig. 2). GCaMP-positive NECs were first identified using brightfield and 490 nm illumination (Fig. 2B), and then confirmed after successful $Ca^{2+}$-imaging experiments by fixation and immunohistochemistry (Fig. 2C). These GCaMP-positive NECs displayed a $Ca^{2+}$ response to hypoxia (Fig. 2D) and the magnitude of these responses did not change over time, or after multiple exposures (Fig. 2E, Kruskal-Wallis test, $P>0.999$, $n=7$ cells).

### 3.4.2 Extracellular and stored $Ca^{2+}$ contribute to the NEC response to hypoxia

A combination of intracellular and extracellular blockers were used to evaluate the source of $Ca^{2+}$ in the NEC response to hypoxia. In experiments where NECs were exposed to successive bouts of hypoxia, the $Ca^{2+}$ response was significantly reduced by 50.4% with the addition of 100 μM nifedipine, an L-type $Ca^{2+}$ channel blocker (Fig. 3A). The $Ca^{2+}$ response fully recovered after 15 min washout of nifedipine (Fig. 3A,B; Kruskal-Wallis test, $P=0.006$, $n=6$ cells). Similarly, the response to hypoxia was partially reduced by 41.9% when $Ca^{2+}$ was removed from the extracellular solution (Fig. 3C,D; Kruskal-Wallis test, $P<0.0059$, $n=6$ cells).

The NEC $Ca^{2+}$ response to hypoxia was partially reduced by 30.4% with the addition of dantrolene, an inhibitor of intracellular $Ca^{2+}$ release (Fig. 4A,C; Kruskal-Wallis test, P=0.007, n=6 cells). To confirm that the $Ca^{2+}$ response to hypoxia was a reflection of the sum of $Ca^{2+}$ arising from both intracellular and extracellular sources, we exposed NECs to hypoxia in the presence of dantrolene and $Ca^{2+}$-free solution (Fig. 4B,D; Kruskal-Wallis test, P<0.0079, n=5 cells). When compared to all other treatments, blocking both intracellular and extracellular $Ca^{2+}$ resulted in the largest reduction in the $Ca^{2+}$ response to hypoxia (Fig. 4E).

### 3.4.3 The NEC $Ca^{2+}$ response to hypoxia is reduced by $D_2$ receptor activity

Previous studies reported a decrease in ventilation frequency of larval zebrafish with dopamine or the specific dopamine $D_2R$ agonist, quinpirole (Shakarchi et al., 2013; Reed et al., 2024). Additionally, immunohistochemical labelling has shown co-localization of dopamine $D_2R$ with NECs and has provided evidence for the postsynaptic synthesis and reuptake of dopamine in the gill (Reed et al., 2024). In this study, we sought to determine an inhibitory role for $D_2R$ within the gill at the level of the presynaptic NEC. We found the NEC $Ca^{2+}$ response to hypoxia was reversibly reduced by 44.1% with the addition of dopamine (Fig. 5A,B; Kruskal-Wallis test, P=0.0116, n=5 cells), as well as reduced by 57.9% with the addition of quinpirole (Figure 5C,D; Kruskal-Wallis test, P=0.007, n=6 cells). Domperidone, a $D_2R$ antagonist, had the opposite effect and enhanced the NEC $Ca^{2+}$ response to hypoxia by 26.7% compared to hypoxia alone (Fig. 5E,F; Kruskal-Wallis test, P=0.0347, n=6 cells).

To evaluate an intracellular pathway for the inhibition of the NEC $Ca^{2+}$ response to hypoxia via dopamine $D_2Rs$, we used drugs to target AC. Activation of $D_2R$ reduces AC activity (Usiello et al., 2000). We found a decrease in the response to hypoxia with the addition of

SQ22536, an inhibitor of AC (Fig. 6A,B; Kruskal-Wallis test, P=0.0099, n=6 cells). Further, when the $Ca^{2+}$ response to hypoxia was reduced in the presence of dopamine, activation of AC with forskolin partially restored the normal $Ca^{2+}$ response to hypoxia (Fig. 6C,D; Kruskal-Wallis test, P=0.0019, n=6 cells).

### 3.4.4 Postsynaptic responses to hypoxia are modulated by presynaptic $D_2$ activity

In addition to NECs, immunohistochemical labelling confirmed that SV2/zn-12-positive ChNs in the gill of Tg(*elavl3*:GCaMP6s) zebrafish are GCaMP-positive (Fig. 7). ChNs extend the complete length of gill filaments and were previously shown to innervate NECs in zebrafish (Jonz and Nurse, 2003). Rotation of confocal images by 90° shows zn-12-positive nerve fibres in close association with GCaMP-positive NECs and ChNs (Fig. 7D-I).

In our whole-gill recording preparation, multiple ChNs of a single gill filament showed nearly simultaneous $Ca^{2+}$ responses to hypoxia (Fig. 8A,B). Since NECs are confined to the distal end of the gill filament, the filament was transected at a proximal region where ChNs were present but no NECs were observable (Fig. 8C). This technique was used to mechanically remove synaptic contact between NECs and ChNs to determine whether ChNs can respond to hypoxia independently of NECs. After the filament was cut, the ChN response to hypoxia was completely abolished, though ChNs were still able to show a response to high extracellular $K^+$, indicating that ChNs were not adversely affected by the cut (Fig. 8D). In these experiments, we observed a mean $F/F_0$ response of 4.84±0.67 (n=5) to hypoxia before nerve transection, compared to 5.46±1.03 (n=5) produced by high $K^+$.

To further confirm NECs were innervated by ChNs, fish were treated with 50 uM 6-OHDA, a neurotoxin used to destroy the nerve terminals of dopaminergic neurons, for 24-h prior

to euthanization and gill tissue extraction. Since NECs are innervated by nerve fibres containing the dopamine active transporter (DAT) (Reed et al., 2024, this technique was used to chemically remove the ability of postsynaptic ChNs to receive inputs from NECs. In transgenic animals produced by crossing the Tg(*dat:tom20 MLS-mCherry*) and Tg(*elavl3*:GCaMP6s) lines, labelling of DAT-positive ChN terminals around NECs was partially reduced in fish treated with 6-OHDA (Fig. 8E). Importantly, after treatment with 6-OHDA, ChNs showed no response to hypoxia while still maintaining the ability to respond to high $K^+$ (Fig. 8F, overlayed traces, n=6 cells).

Finally, we aimed to link our characterization of $D_2R$ activity in NECs with the $Ca^{2+}$ response in postsynaptic ChNs. High $K^+$ was used to depolarize the membranes of ChNs with and without the addition of quinpirole. In agreement with the reported absence of $D_2R$ on ChNs (Reed et al., 2024), both 50 μM and 100 μM quinpirole failed to reduce the $[Ca^{2+}]_i$ response during a high $K^+$ stimulus, confirming that dopamine and quinpirole do not affect ChNs directly and must be acting presynaptically (Fig. 9A,B). In dual recording of NECs and ChNs, in which synaptic contact between cells was left intact, $[Ca^{2+}]_i$ was simultaneously recorded in both cell types during exposure to hypoxia (Fig. 9C). Under these conditions, NECs responded first with an increase in $[Ca^{2+}]_i$, followed by a $[Ca^{2+}]_i$ response in ChNs after a latency of 25.6 ± 4.7 s (Fig. 9D, n=5). There was a reduction in both the NEC and ChN $Ca^{2+}$ response to hypoxia with the $D_2R$ agonist, quinpirole (Fig. 9D,E; NEC: Kruskal-Wallis test, P=0.003, n=5 cells, and ChN: Kruskal-Wallis test, P=0.013, n=5 cells).

**Figure 3-1 Characterization of GCaMP-positive neuroepithelial cells (NECs) in the gill epithelium of transgenic *elavl3*:GCaMP6s zebrafish.** Confocal imaging of immunohistochemical localization of GCaMP with NECs containing synaptic vesicle protein-2 (SV2) and 5-hydroxytryptamine (5-HT). (A) Labelling with GFP (green) co-localized with NECs containing SV2 (magenta). (B, C) GCaMP and SV2 labelling shown separately. Scale bar in A=20 μm and applies to B and C. (D) Labelling with GCaMP (green) co-localized with NECs containing 5-HT (magenta, arrows). (E, F) GCaMP and 5-HT labelling shown separately. Scale bar in D=20 μm and applies to E and F.

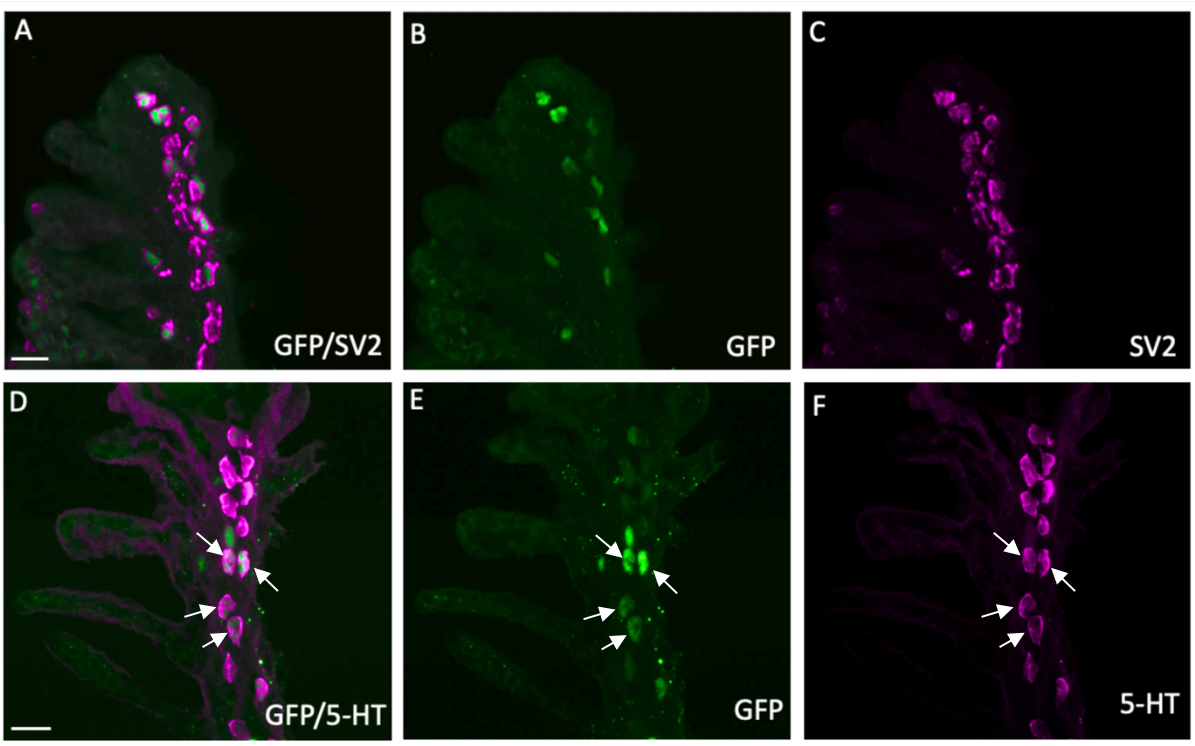


Figure 3.1

**Figure 3-2 Hypoxia induced intracellular $Ca^{2+}$ responses in gill neuroepithelial cells from Tg(*elavl3*:GCaMP6s) zebrafish.** (A) Schematic of the GCaMP recording preparation illustrating (left) a fluorescence microscope, (centre) an isolated gill in a recording chamber fitted with in- and out-flow for superfusion, and (right) fluorescence excitation in a cell during a hypoxic stimulus. (B) Overlay of brightfield and green fluorescence (488 nm) images of a GCaMP-positive neuroepithelial cell (NEC, arrowhead) *in situ* containing GCaMP from a Tg(*elavl3:*GCaMP6s) zebrafish. (C) Post hoc confocal imaging confirming immunohistochemical co-localization of GCaMP (green) with synaptic vesicle protein-2 (SV2, magenta) in the NEC (arrowheads) identified in (B). The panels show (from left) GCaMP and SV2 separately, and GCaMP and SV2 labelling together. (D) $Ca^{2+}$ imaging trace from the GCaMP-containing cell in (A) during three bouts of hypoxia. Scale indicates time (min) and relative changes in fluorescence ($F/F_0$) corresponding to changes in intracellular $Ca^{2+}$ concentration ($[Ca^{2+}]_i$). Time-series micrographs above show fluorescence changes over time. (E) Mean (± SD) $F/F_0$ in NECs in response to three consecutive bouts of hypoxia. There was no significant change in the magnitude of the $Ca^{2+}$ response to hypoxia over time (Kruskal-Wallis test, $P>0.999$, $n=7$ cells). Panel A created with BioRender.com.

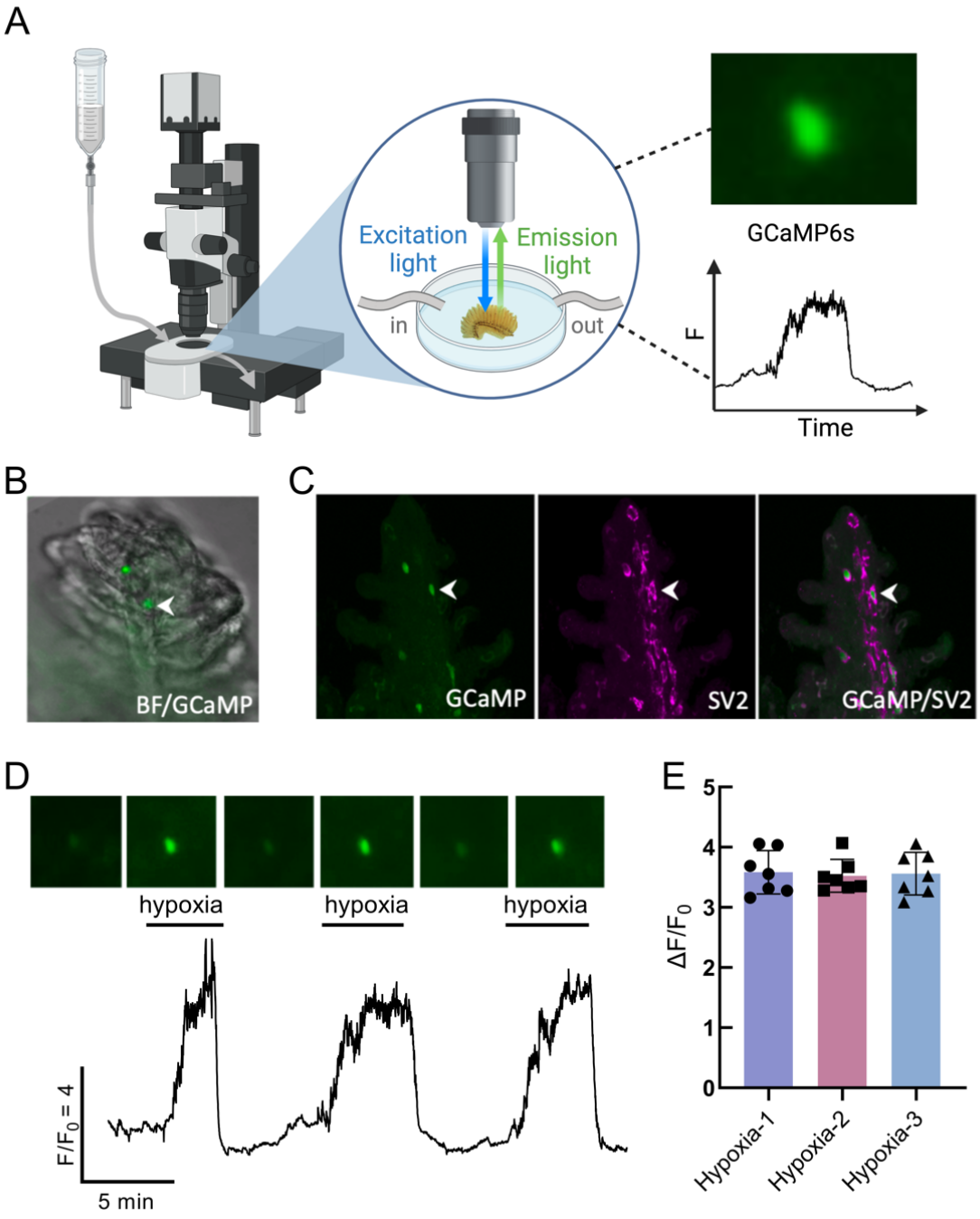
A
Excitation light
Emission light
in
out
GCaMP6s
F
Time
B
BF/GCaMP
C
GCaMP
SV2
GCaMP/SV2
D
hypoxia
hypoxia
hypoxia
F/F0 = 4
5 min
E
ΔF/F0
Hypoxia-1
Hypoxia-2
Hypoxia-3

Figure 3.2

**Figure 3-3 Extracellular $Ca^{2+}$ contributes to the response to hypoxia in neuroepithelial cells (NECs).** (A) $Ca^{2+}$ imaging trace from a GCaMP-containing NEC, where the response to hypoxia was reduced with the addition of 100 μM nifedipine, an L-type $Ca^{2+}$ channel blocker. The response to hypoxia was fully recovered after 15 min washout (break in trace). (B) Summary data from NECs as treated in (A) illustrating a reduction in the mean (± SD) $F/F_0$ (Kruskal-Wallis test, P=0.006, n=6 cells). 3 cells were evaluated for recovery after a 15-min washout period (Kruskal-Wallis test, P>0.999, n=3 cells). (C) $Ca^{2+}$ imaging trace from a GCaMP-containing NEC, where the response to hypoxia was reversibly reduced when $Ca^{2+}$ was removed from the extracellular solution. (D) Summary data from NECs as treated in (C) showing a reduction in the mean (± SD) $F/F_0$ (Kruskal-Wallis test, P<0.006, n=6 cells). The response to hypoxia fully recovered after zero $Ca^{2+}$ treatment (Kruskal-Wallis test, P>0.999).

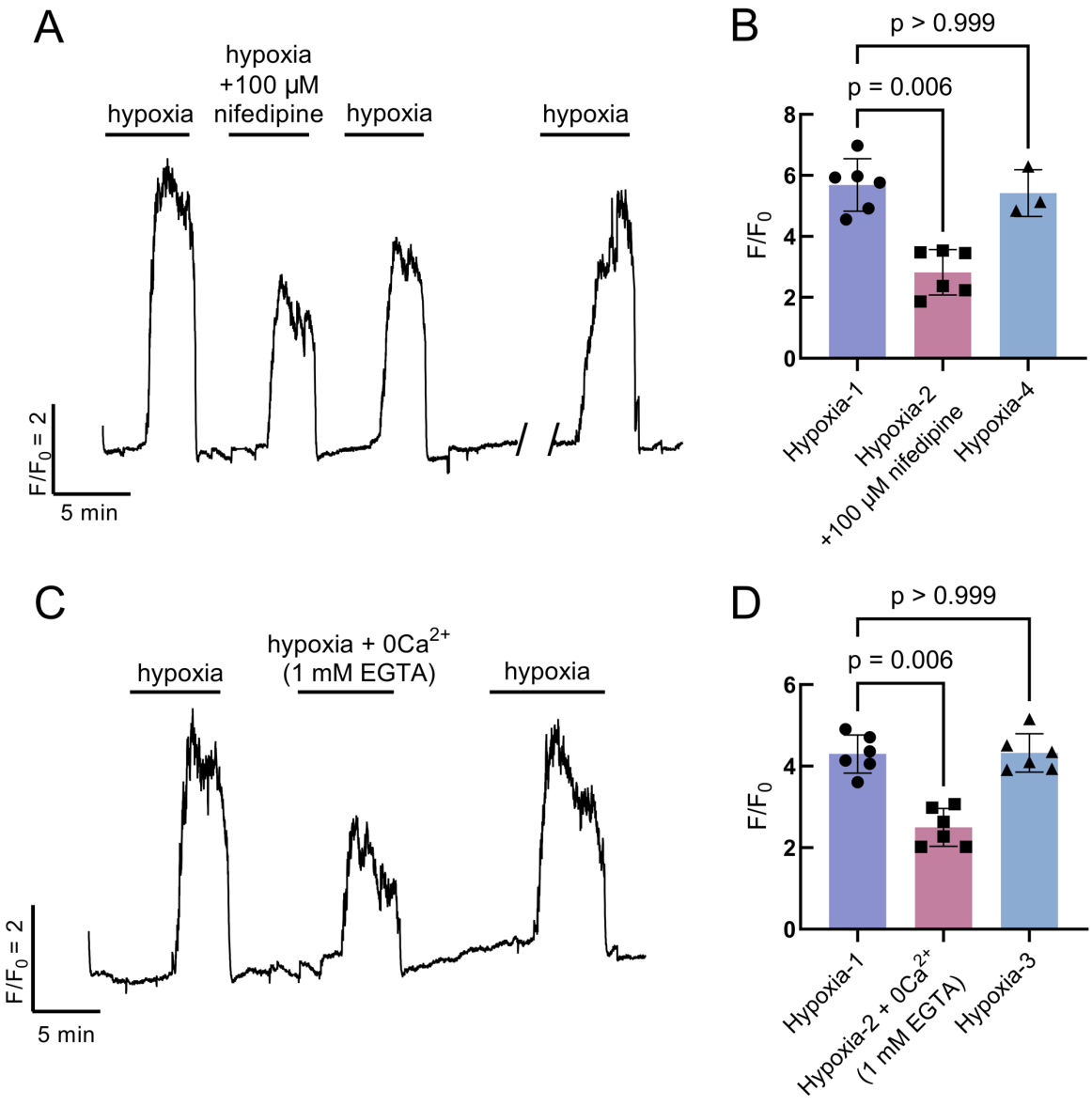
A
hypoxia
hypoxia
+100 µM
nifedipine
hypoxia
hypoxia
F/F0 = 2
5 min
B
p > 0.999
p = 0.006
F/F0
Hypoxia-1
Hypoxia-2
+100 µM nifedipine
Hypoxia-4
C
hypoxia
hypoxia + 0Ca2+
(1 mM EGTA)
hypoxia
F/F0 = 2
5 min
D
p > 0.999
p = 0.006
F/F0
Hypoxia-1
Hypoxia-2 + 0Ca2+
(1 mM EGTA)
Hypoxia-3

Figure 3.3

**Figure 3-4 Intracellular $Ca^{2+}$ contributes to the response to hypoxia in neuroepithelial cells (NECs).** (A) $Ca^{2+}$ imaging trace from a GCaMP-containing NEC, where the response to hypoxia was reversibly reduced with the addition of 50 μM dantrolene, an inhibitor of intracellular $Ca^{2+}$ release. (B) $Ca^{2+}$ imaging trace from a GCaMP-containing NEC demonstrating the combined contributions of intracellular and extracellular $Ca^{2+}$. The response to hypoxia was further reduced with the addition of 50 μM dantrolene in $Ca^{2+}$-free extracellular solution. (C) Summary data as treated in (A) showing reduction in mean (± SD) $F/F_0$ (Kruskal-Wallis test, P=0.007, n=6 cells). The response to hypoxia fully recovered (Kruskal-Wallis test, P>0.999, n=6 cells). (D) Summary data as treated in (B) showing a reduction in mean (± SD) $F/F_0$ (Kruskal-Wallis test, P<0.008, n=5 cells). The response to hypoxia fully recovered (Kruskal-Wallis test, P>0.999, n=5 cells). (E) Summary comparing all $Ca^{2+}$ blocking treatments. The combination of dantrolene with $Ca^{2+}$-free extracellular solution resulted in an additive effect compared to dantrolene alone.

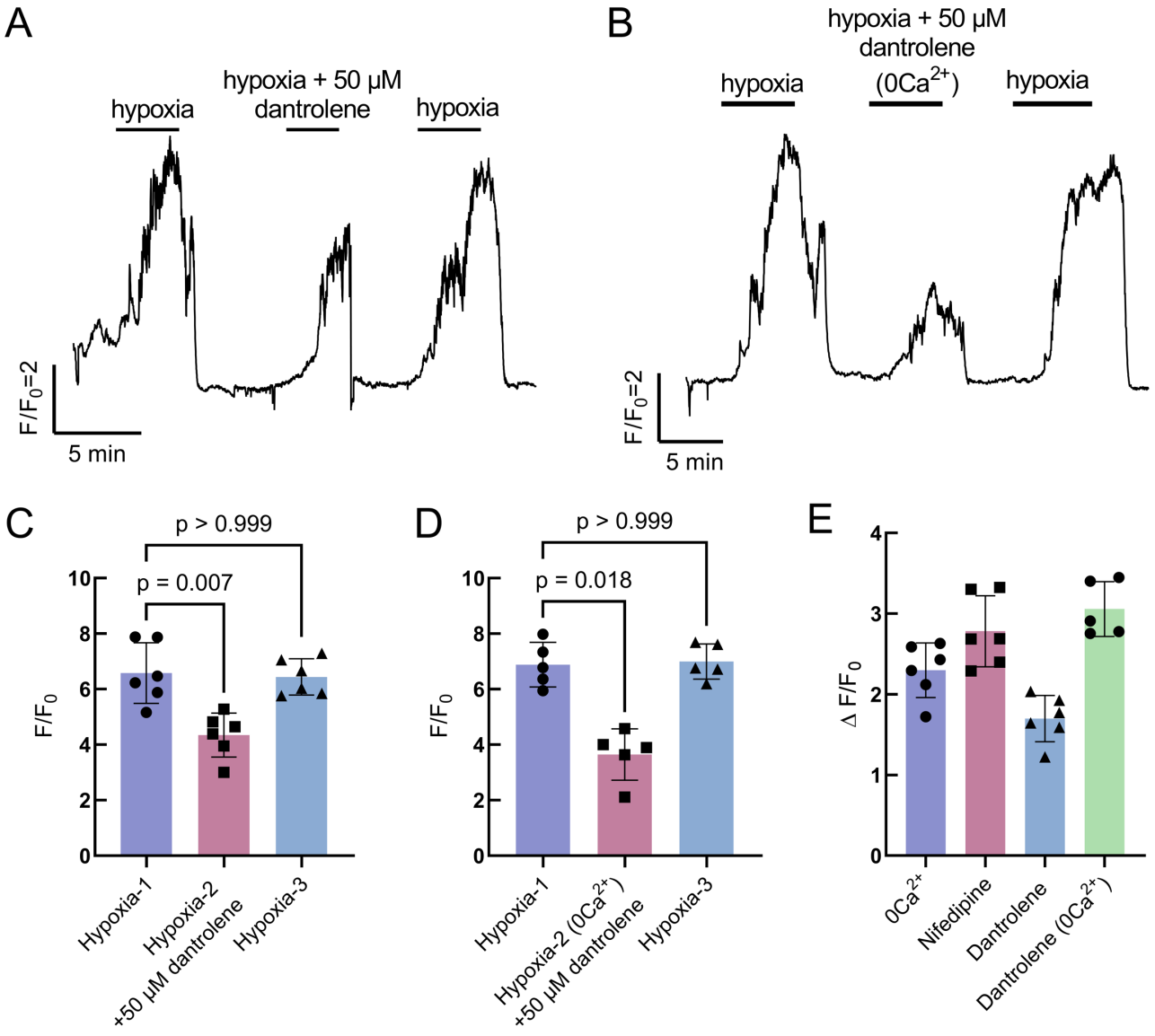
A
hypoxia
hypoxia + 50 μM dantrolene
hypoxia
F/F0=2
5 min
B
hypoxia + 50 μM dantrolene
hypoxia
(0Ca2+)
hypoxia
F/F0=2
5 min
C
p > 0.999
p = 0.007
F/F0
Hypoxia-1
Hypoxia-2 +50 μM dantrolene
Hypoxia-3
D
p > 0.999
p = 0.018
F/F0
Hypoxia-1
Hypoxia-2 (0Ca2+) +50 μM dantrolene
Hypoxia-3
E
Δ F/F0
0Ca2+
Nifedipine
Dantrolene
Dantrolene (0Ca2+)

Figure 3.4

**Figure 3-5 The effects of dopamine and $D_2R$ activity on the neuroepithelial cell (NEC) response to hypoxia**. Shown are the effects of dopamine (A,B), quinpirole (C,D) and domperidone (E,F). (A) $Ca^{2+}$ imaging trace from a GCaMP-containing NEC where the response to hypoxia was reversibly reduced with the addition of 50 μM dopamine (DA). (C) $Ca^{2+}$ imaging trace from a GCaMP-containing NEC where the response to hypoxia was reversibly reduced with the addition of 50 μM quinpirole, a specific dopamine $D_2R$ agonist. (E) $Ca^{2+}$ imaging trace from a GCaMP-containing NEC where the response to hypoxia was enhanced with the addition of 100 μM domperidone, a specific dopamine $D_2R$ antagonist. (B,D,F) Summary data showing mean (± SD.) $F/F_0$ corresponding to experiments in (A,C,E). Addition of 50 μM dopamine significantly reduced the $Ca^{2+}$ response to hypoxia (B, Kruskal-Wallis test, P=0.012, n=5 cells), as well as 50 μM quinpirole (D, Kruskal-Wallis test, P=0.007, n=6 cells), while domperidone increased mean (± SD) $F/F_0$ (F, Kruskal-Wallis test, P=0.035, n=6 cells). The response to hypoxia fully recovered following all treatments (Kruskal-Wallis test, P>0.999, n=5-6 cells).

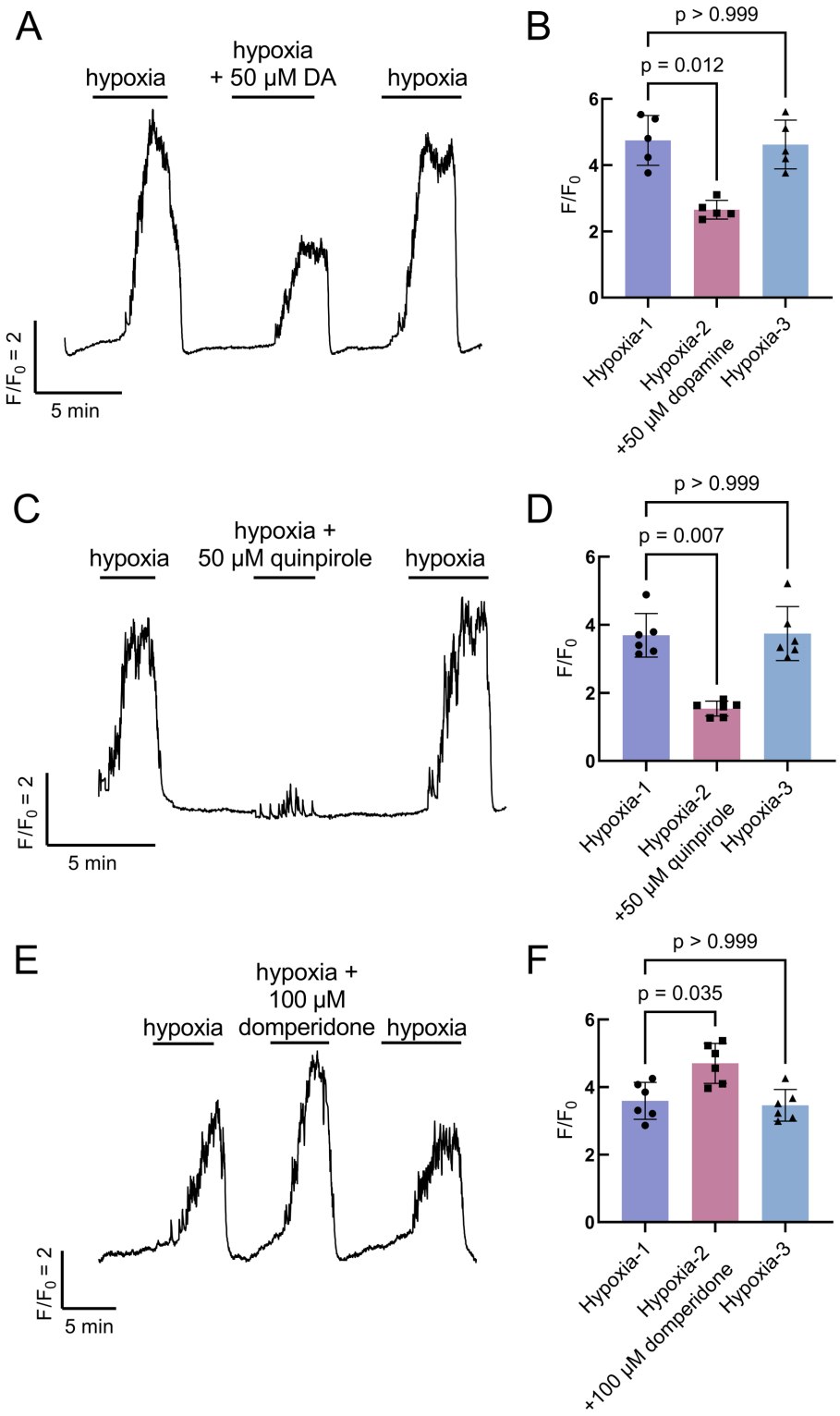
A
hypoxia
hypoxia
+ 50 µM DA
hypoxia
F/F0 = 2
5 min
B
p > 0.999
p = 0.012
F/F0
Hypoxia-1
Hypoxia-2
+50 µM dopamine
Hypoxia-3
C
hypoxia
hypoxia +
50 µM quinpirole
hypoxia
F/F0 = 2
5 min
D
p > 0.999
p = 0.007
F/F0
Hypoxia-1
Hypoxia-2
+50 µM quinpirole
Hypoxia-3
E
hypoxia
hypoxia +
100 µM
domperidone
hypoxia
F/F0 = 2
5 min
F
p > 0.999
p = 0.035
F/F0
Hypoxia-1
Hypoxia-2
+100 µM domperidone
Hypoxia-3

Figure 3.5

**Figure 3-6 Dopamine acts through intracellular secondary messenger cyclic adenosine 3′,5′-monophosphate (cAMP) in neuroepithelial cells (NECs).** (A) Addition of SQ22536, an adenylyl cyclase (AC) inhibitor, decreased the effect of hypoxia on intracellular $Ca^{2+}$. (B) Summary data as treated in (A) showing mean (± SD) $F/F_0$ during the first two minutes of hypoxia exposure (Hypoxia-1), the reduction in mean (± SD) $F/F_0$ during the entire duration of SQ22536 exposure (Hypoxia-2 + SQ22536; Kruskal-Wallis test, P=0.010, n=6 cells), and the mean (± SD) $F/F_0$ during the last two minutes of hypoxia exposure (Hypoxia-3). (C) Forskolin, an AC activator, partially recovered the suppressive effect of dopamine on the $Ca^{2+}$ response to hypoxia. (D) Summary data as treated in (C) showing recovery in mean (± SD) $F/F_0$ of the hypoxic response from dopamine with forskolin (Kruskal-Wallis test, P=0.002, n=6 cells). The response to hypoxia fully recovered following both treatments (Kruskal-Wallis test, P>0.999, n=6 cells).

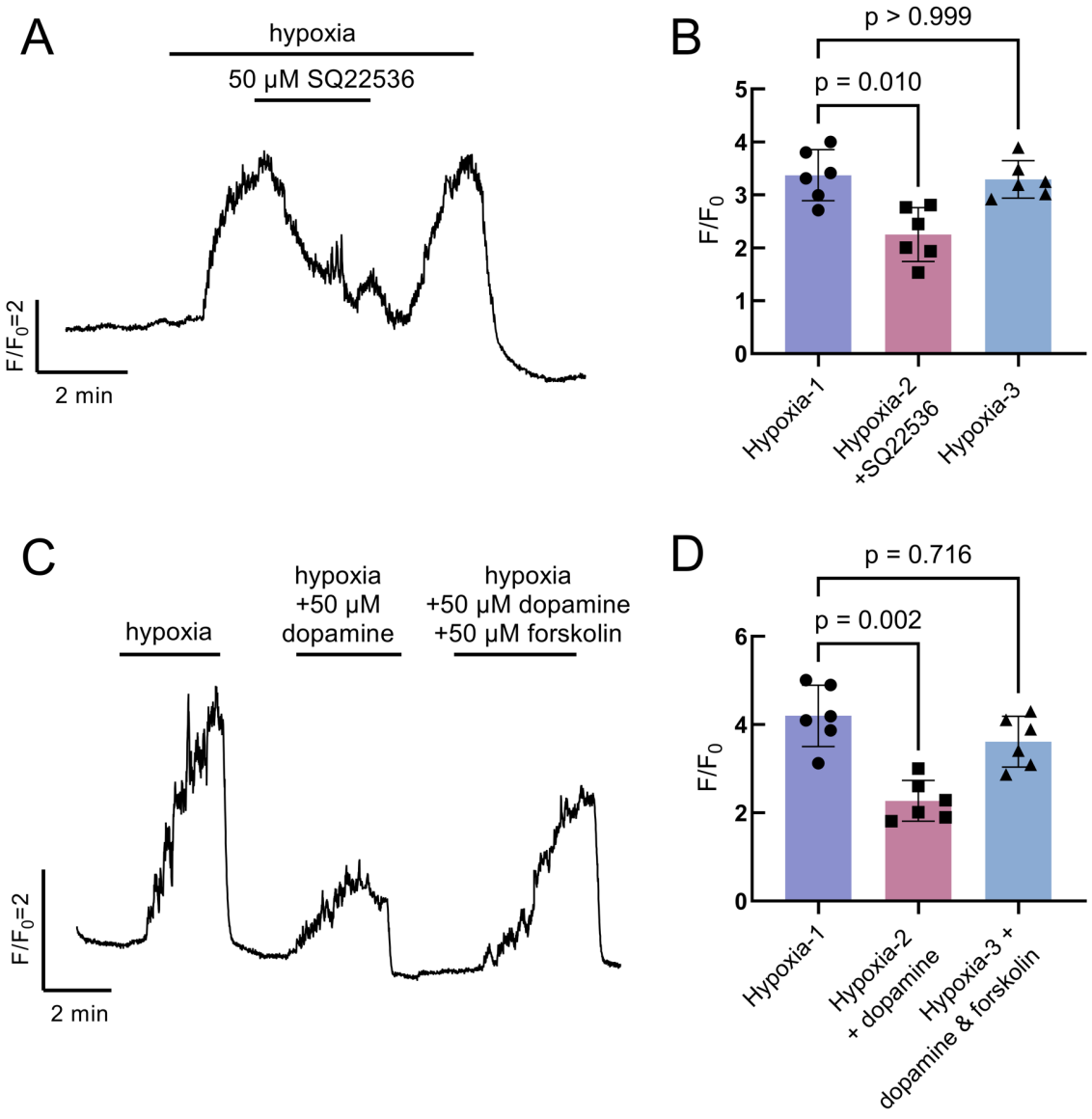
A
hypoxia
50 μM SQ22536
F/F0=2
2 min
B
p > 0.999
p = 0.010
F/F0
Hypoxia-1
Hypoxia-2 +SQ22536
Hypoxia-3
C
hypoxia
hypoxia +50 μM dopamine
hypoxia +50 μM dopamine +50 μM forskolin
F/F0=2
2 min
D
p = 0.716
p = 0.002
F/F0
Hypoxia-1
Hypoxia-2 + dopamine
Hypoxia-3 + dopamine & forskolin

Figure 3.6

**Figure 3-7 Characterization of GCaMP-positive postsynaptic chain neurons (ChNs) in Tg(*elavl3*:GCaMP6s) zebrafish gills.** (A-C) confocal imaging of immunohistochemical localization of GCaMP in a ChN containing synaptic vesicle protein-2 (SV2, magenta). (B,C) GCaMP and SV2 labelling shown separately. Scale bar in A=50 μm and applies to B and C. (D-F) co-labelling of GCaMP-positive ChNs and NECs (green, arrows) with nerve fibres labelled with zn-12 (magenta). (E, F) GCaMP and zn-12 labelling shown separately. Scale bar in D=50 μm and applies to E and F. (G-I) Images from panels (D-F) cropped and titled back 90°. Rotation demonstrates neural connection (arrowhead) between nerve fibres located below the efferent filament artery (eFA) where ChNs are located, projecting to GCaMP-positive NECs.

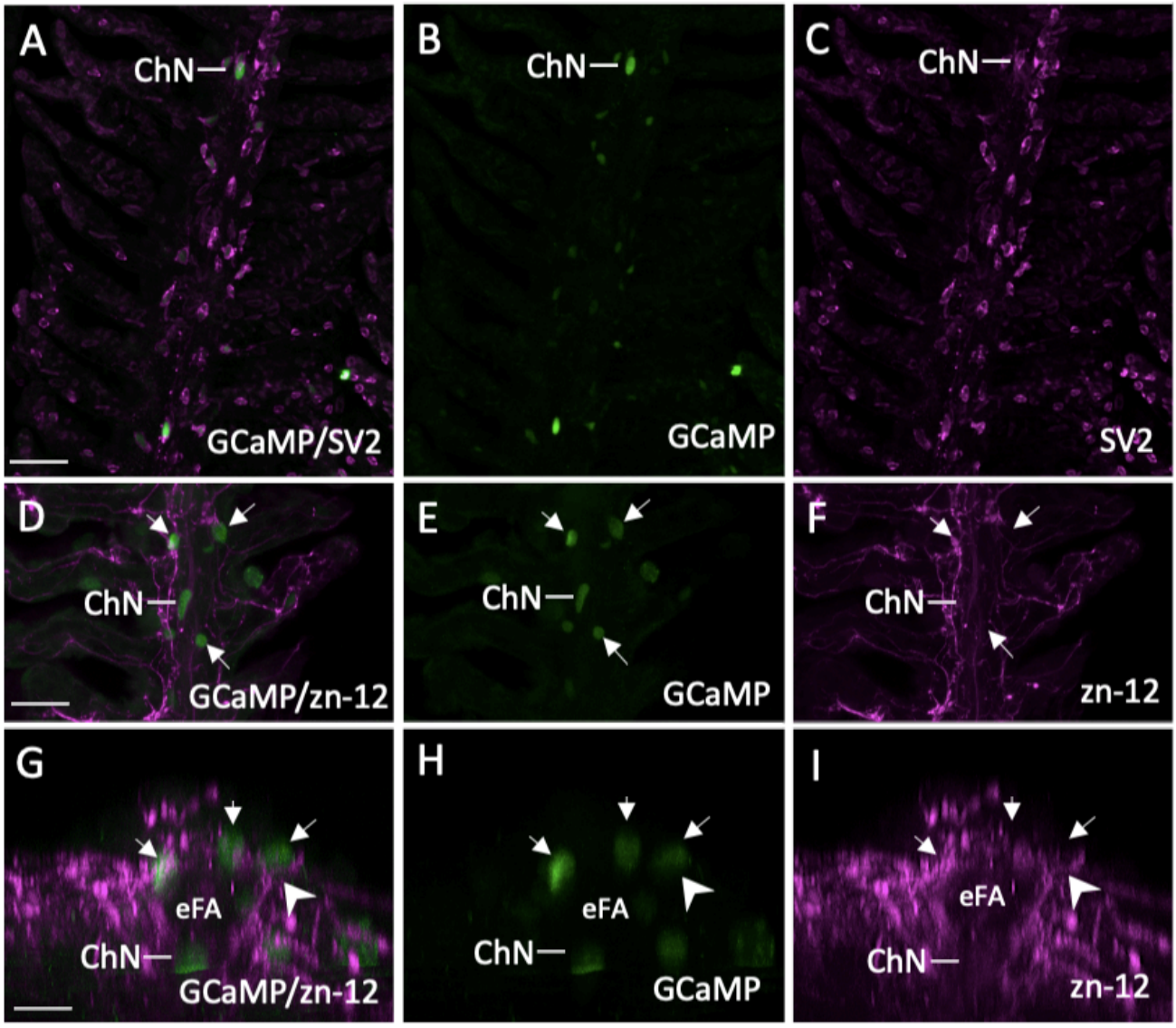
A
ChN
GCaMP/SV2
B
ChN
GCaMP
C
ChN
SV2
D
ChN
GCaMP/zn-12
E
ChN
GCaMP
F
ChN
zn-12
G
eFA
ChN
GCaMP/zn-12
H
eFA
ChN
GCaMP
I
eFA
ChN
zn-12

Figure 3.7

**Figure 3-8 The chain neuron (ChN) calcium response to hypoxia requires synaptic contact with neuroepithelial cells (NECs). ).** (A) Examples from live fluorescence imaging at 488 nm of four ChNs along a single filament in normoxia (left micrograph) and hypoxia (right micrograph). (B) Calcium traces from the four ChNs shown in (A) responding to hypoxia. Different colours represent corresponding cells (ChN 1-4) in (A). (C) Schematic of a gill filament (left) and rotation by 90° on the y-axis (right) illustrate filament transection. Filaments were cut along the red dashed line at the proximal end where a ChN was present, but no NECs were observable. (D) Calcium imaging trace of a single ChN before and after filament transection. After the filament was cut (break in trace), the neuron no longer responded to hypoxia (n=5 cells). As a positive control, viability of the neuron was demonstrated by stimulation with a solution of high extracellular $K^+$. (E) Confocal imaging of gills from a double transgenic animal produced by crossing Tg(*elavl3*:GCaMP6s) and Tg(*dat:tom20 MLS-mCherry*) fish showing the relationship between the dopamine active transporter (DAT) nerve endings (magenta) and GCaMP-positive NECs (green) in control (left micrograph) and 6-OHDA-treated gills (right micrograph). DAT labelling was found in close proximity to NECs but was reduced after 6-OHDA treatment. (F) Overlayed $Ca^{2+}$ imaging traces from 6-OHDA treated animals. After 6-OHDA treatment the ChNs did not respond to hypoxia (n=6 cells). Response to high extracellular $K^+$ confirmed cell viability. Panel C created with BioRender.com.

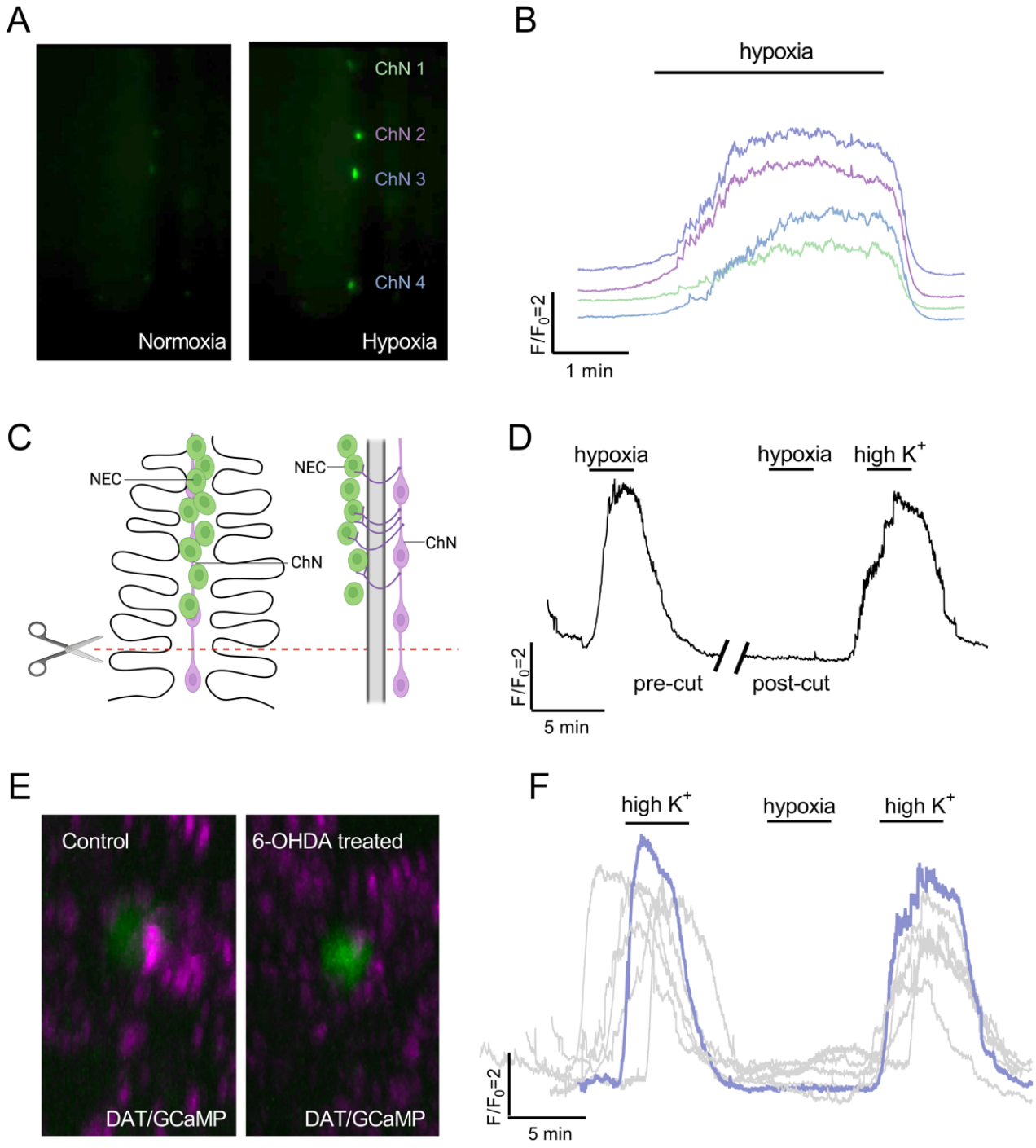
A
ChN 1
ChN 2
ChN 3
ChN 4
Normoxia
Hypoxia
B
hypoxia
F/F0=2
1 min
C
NEC
NEC
ChN
ChN
D
hypoxia
hypoxia
high K+
F/F0=2
pre-cut
post-cut
5 min
E
Control
6-OHDA treated
DAT/GCaMP
DAT/GCaMP
F
high K+
hypoxia
high K+
F/F0=2
5 min

Figure 3.8

**Figure 3-9 Postsynaptic modulation of the hypoxic response by presynaptic $D_2R$ activation.** (A) Calcium imaging trace from a single chain neuron with summary data showing no change in the response to high $K^+$ with the addition of 50 μM quinpirole. (B) Calcium imaging trace from a single chain neuron (ChN) with summary data showing no change in the response to high $K^+$ with the addition of 100 μM quinpirole. (C) Schematic illustration of preparation for dual recording of neuroepithelial cell (NEC) and ChN. Focus plane for recording was set at a tissue depth between both cells (green line) where both cells were still in view (blue box). (D) Dual-recording $Ca^{2+}$ imaging trace of a NEC (grey) and ChN (blue) recorded simultaneously. (E) Summary data as treated in D showing a decrease in the hypoxic signal produced by NECs (Kruskal-Wallis test, $p=0.003$, $n=5$ cells) and ChNs (Kruskal-Wallis test, $p=0.013$, $n=5$ cells) with quinpirole. In both NECs and ChNs, the hypoxic response was fully recovered after quinpirole treatment (Kruskal-Wallis test, $p>0.999$, $n=4$ cells). Panel C created with BioRender.com.

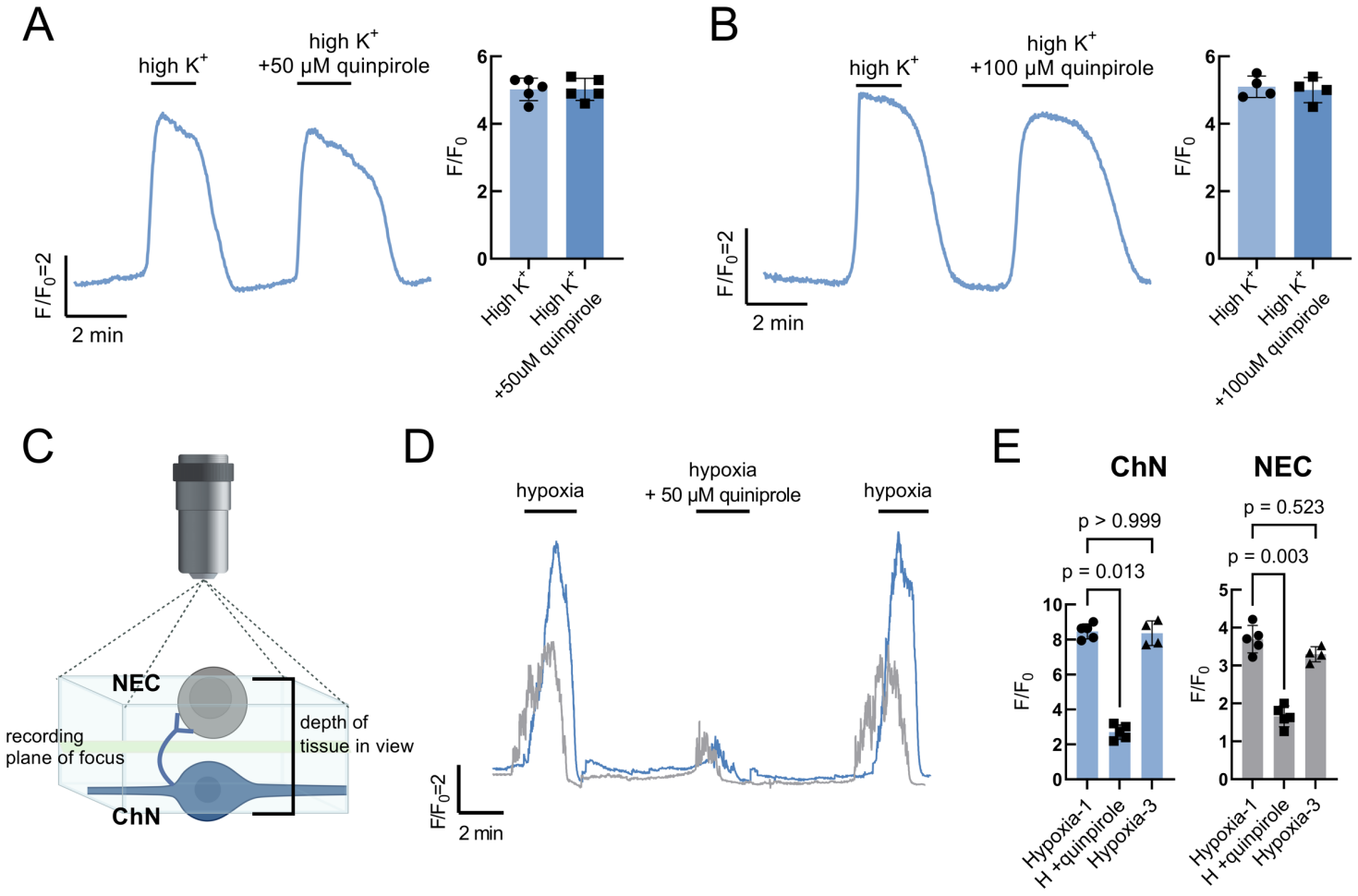
A
high K+
high K+
+50 µM quinpirole
F/F0=2
2 min
F/F0
High K+
High K+
+50uM quinpirole
B
high K+
high K+
+100 µM quinpirole
F/F0=2
2 min
F/F0
High K+
High K+
+100uM quinpirole
C
NEC
recording
plane of focus
depth of
tissue in view
ChN
D
hypoxia
hypoxia
+ 50 µM quiniprole
hypoxia
F/F0=2
2 min
E
ChN
NEC
p > 0.999
p = 0.013
p = 0.523
p = 0.003
F/F0
Hypoxia-1
H +quinpirole
Hypoxia-3

Figure 3.9

## 3.5 Discussion

The present study demonstrates neuromodulation of the chemoreceptor response to hypoxia produced by activation of $D_2R$ in NECs in the gills of zebrafish. We used a transgenic zebrafish line in which the $Ca^{2+}$ reporter, GCaMP, was genetically encoded to reveal dopaminergic inhibition of the NEC $Ca^{2+}$ response to hypoxia, acting through $D_2R$ and inhibition of AC. We further demonstrated a link between the inhibitory effect of activation of presynaptic $D_2R$ and modulation of the hypoxic signal in postsynaptic neurons that innervate NECs.

### 3.5.1 The gill as a model for the chemoreceptor response to hypoxia

Evaluating responses of chemoreceptors to hypoxia in previous work has typically relied on the techniques of classical $Ca^{2+}$ imaging, where the loading of $Ca^{2+}$ reporting dyes into isolated cells was required in the carotid body (Montoro et al. 1996), neuroepithelial bodies (Livermore et al., 2015) and gill NECs (Zhang et al., 2011; Porteus et al., 2014; Abdallah et al., 2015; Leonard et al., 2022). Here, we developed an intact, whole-gill preparation using the endogenous $Ca^{2+}$ indicator, GCaMP. This preparation allows us to observe chemoreceptor responses to hypoxia without the added complication of dye loading, while maintaining functional connectivity throughout the organ. Gill GCaMP-positive chemoreceptors showed a reliable response to hypoxia that was consistent over time and multiple hypoxic stimuli, serving as a useful model to evaluate chemoreceptor responses to hypoxia.

Though several studies have used $Ca^{2+}$ imaging to evaluate chemoreceptor activity in gill NECs (Zhang et al., 2011; Porteus et al., 2014; Abdallah et al., 2015; Leonard et al., 2022), the source of $Ca^{2+}$ contributing to the response to hypoxia in NECs had not clearly been determined. In the present study, we determine the NEC $Ca^{2+}$ response to hypoxia involves both extracellular

$Ca^{2+}$ influx through L-type $Ca^{2+}$ channels, as well as release from intracellular stores. Similarly in the carotid body, a combination of $Ca^{2+}$ entry through voltage-gated $Ca^{2+}$ channels and intracellular $Ca^{2+}$ release may be important in chemoreceptor responses to hypoxia (Kim et al., 2020).

### 3.5.2 Dopaminergic modulation of chemoreceptor activity during hypoxia

In the present study, we demonstrated a reduction in the NEC $Ca^{2+}$ response to hypoxia produced by application of dopamine or the specific $D_2R$ agonist, quinpirole. $D_2Rs$ were previously localized to gill NECs in zebrafish by immunohistochemistry, whereas $D_2R$ was not found on postsynaptic ChNs (Reed et al., 2024). In addition, $D_2R$ expression in NECs was demonstrated using single-cell RNA-sequencing (Pan et al., 2022). Accordingly, the present results confirm that ChNs showed no direct response to quinpirole. We therefore attribute the suppressive effects of dopamine and quinpirole to activation of presynaptic $D_2Rs$. Dopamine receptors are a type of G-protein-coupled receptor (GPCR) that play a crucial role in mediating the effects of the neurotransmitter, dopamine. There are five known subtypes of dopamine receptors classified into two main families based on their signaling mechanisms: $D_1$-like ($D_1$ and $D_5$), and $D_2$-like ($D_2$, $D_3$, and $D_4$). Upon dopamine binding, dopamine receptors undergo conformational changes that activate intracellular signaling pathways through interactions with G-proteins. Activation of $D_2$-like receptors inhibit AC activity through Gαi/o proteins, leading to decreased cAMP levels within the cell (reviewed by Beaulieu & Gainetdinov, 2011). We showed that inhibition of AC with SQ22536 mimicked the modulation of the NEC hypoxic response by dopamine. Further, the modulatory effects of dopamine were reversed by addition of forskolin, an AC activator. Together, these results provide evidence for the dopaminergic inhibition of AC,

and suggest subsequent decreases in cAMP activity, leading to modulation of the NEC $Ca^{2+}$ response to hypoxia. This mechanism of inhibition by $D_2R$ is similar to carotid body type 1 cells, where dopamine causes a dose-dependent decrease in the type 1 cell cAMP content induced by forskolin (Batuca et al., 2003). Downstream effectors of AC-cAMP on chemoreceptor activity may involve the modulation of $Ca^{2+}$ influx. In many preparations $D_2R$ activation has been associated with activation of $K^+$ channel currents, causing hyperpolarization, and the reduction of voltage gated $Ca^{2+}$ currents (Vargas and Lucero, 1999).

### 3.5.3 Dopaminergic modulation of gill hypoxia signalling

The present study demonstrates modulation of the ChN response to hypoxia via presynaptic $D_2R$ activation, which suggests $D_2R$ at the NEC-ChN synapse may act on ventilation. ChNs are part of a nerve bundle in the gill located beneath the efferent filament artery that sends projections to innervate NECs. Using gill transection experiments we identified a pathway for the transmission of the hypoxic signal in the gill through a functional unit containing two parts: the postsynaptic ChN, and any number of NECs innervated by that ChN. We further showed that within this functional unit, the inhibitory actions of dopamine on the presynaptic NEC can be observed in the postsynaptic ChN, suggesting a mechanism of modulation at the NEC-ChN synapse. Moreover, in dual recordings, the $Ca^{2+}$ response to hypoxia in NECs always preceded the response in ChNs, suggesting that the hypoxic signal is carried from NECs to sensory ChNs. This mechanism may be similar to the carotid body, where dopamine released by type 1 cells has an autocrine-paracrine action on dopaminergic $D_2Rs$ located on type 1 cells to inhibit $Ca^{2+}$-channels, leading to negative feedback regulation of further neurotransmitter release during hypoxia (Benot & López-Barneo, 1990). The excitatory

neurotransmitter at the NEC-ChN synapse has yet to be elucidated. Candidates include acetylcholine, which is excitatory in the carotid body and is found in the zebrafish gill (Zachar et al., 2017b) and 5-HT, which is present in most NECs in zebrafish (Jonz & Nurse 2003).

ChNs were previously shown to innervate NECs in gills of zebrafish (Jonz & Nurse, 2003), but their physiological role has been elusive. We propose that ChNs may act as interneurons that carry a hypoxic signal from NECs to afferent fibres of the glossopharyngeal or vagus nerves—the cranial nerves that carry chemoreceptor activity to the CNS in fish (Burleson & Milsom, 1995; Sundin & Nilsson, 2002). ChNs contain varicose processes that indicate multiple locations of synaptic contact, possibly with the adjacent sensory fibres of the extrinsic nerve bundle (Jonz & Nurse, 2003). Furthermore, in zebrafish larvae exogenous application of dopamine reduces ventilation frequency, whereas the $D_2R$ agonist, quinpirole, attenuates the hyperventilatory response to hypoxia (Shakarhi et al., 2013; Reed et al., 2024). These results, combined with the present findings, suggest the observed decrease in hyperventilation is the result of presynaptic $D_2R$ activation and a reduction in NEC activity.

Intriguingly, in the present study we report that the $D_2R$ antagonist, domperidone, enhanced the NEC $Ca^{2+}$ response to hypoxia. This observation points to endogenous dopamine release during hypoxia acting upon presynaptic $D_2Rs$ to limit the cellular response to hypoxia. Previous work has identified postsynaptic neurons, including ChNs, as a source of dopamine production and storage in the gill (Reed et al., 2024). Presynaptic type 1 cells are largely responsible for synthesizing and releasing dopamine in the mammalian carotid body. However, many carotid body afferents are also dopaminergic (Finley et al., 1992), and carotid sinus nerve fibres innervating type 1 cells release dopamine (Almaraz et al., 1993), suggesting an additional

postsynaptic source of dopamine to further modulate the type 1 cell response to hypoxia, similar to that observed in the gill.

### 3.5.4 Implications

The results of this study have implications for the field of oxygen sensing, and may contribute to our understanding of acclimatization, development, and evolution in vertebrates. For example, modulation of presynaptic chemoreceptor inhibition by $D_2R$ may contribute to hypoxia acclimatization. In zebrafish, total gill $D_2R$ mRNA expression decreases after 48 h of hypoxia exposure, a timepoint in acclimation where there is a shift away from aquatic surface respiration behaviour, allowing the animal to rely more heavily on hyperventilation (Reed et al., 2024). Acclimation may lower the number of inhibitory $D_2Rs$ expressed by NECs and lead to a change in chemoreceptor sensitivity of the cell to dopamine. A similar involvement of $D_2Rs$ in hypoxia acclimation has been proposed in the carotid body by Huey and Powell (2000), who showed decreased carotid body $D_2R$ mRNA expression following hypoxia acclimation and suggested this may be one mechanism by which exposure to chronic hypoxia reduces inhibition of hypoxia signaling to enhance ventilatory acclimatization to hypoxia.

The zebrafish model used in this study may be particularly useful in characterizing the mechanisms involved in age-related changes in chemosensitivity. In the mammalian carotid body, expression of genes encoding important components of the dopaminergic system are altered during development. These changes coincide with changes in chemoreceptor activity and output observed in early postnatal development in rats (Gauda et al., 1996, Gauda 2002, Bairam & Carroll 2005). Zebrafish have already shown an adaptable dopaminergic system under

hypoxia (Reed et al., 2024), and thus may serve as a great model for exploring changes in chemoreceptor sensitivity during development.

$D_2R$ is the predominant dopamine receptor in the carotid body, which is consistent with what we have found here in the zebrafish gill; however, that does not rule out contributions of other dopamine receptors such as $D_1$. mRNA expression of $D_1$ receptors has been found in the carotid body of rats, cats, and rabbits (Bairam et al., 1998). Further, RNA sequencing showed expression of other dopamine receptors in the gill, specifically $D_1$-like receptors in NECs (Pan et al., 2022). Zebrafish have served as an excellent model to explore the evolutionary origins of dopamine, and $D_2$Rs, and may be particularly useful in clarifying a role for other dopamine receptors in hypoxia signalling.

### 3.6 Conclusion

The present study delineated a mechanism by which presynaptic dopamine $D_2$Rs provide a feedback mechanism that attenuates the chemoreceptor response to hypoxia. We found activation of presynaptic $D_2$Rs decreases the NEC $Ca^{2+}$ response to hypoxia via intracellular AC inhibition. We provide evidence for postsynaptic modulation of the $Ca^{2+}$ response to hypoxia via presynaptic $D_2$Rs and suggest a link between chemoreceptor inhibition by dopamine and modulation of the hypoxic ventilatory response. Our results provide the first evidence of neuromodulation of the hypoxic signal produced by NECs in the gill and suggests that a modulatory role for dopamine in oxygen sensing arose early in vertebrate evolution.

# Chapter 4

# Cholinergic transmission of hypoxia signalling in the zebrafish gill

## 4.1 Abstract

The present study investigated a role for cholinergic and serotonergic transmission of the hypoxia signal in the gill by chain neurons (ChNs). Utilizing the genetically-encoded calcium reporter, GCaMP, we demonstrated that acetylcholine (ACh) and nicotine induced a dose-dependent increase in intracellular calcium concentration ($[Ca^{2+}]_i$) in ChNs. Blockade of nicotinic acetylcholine receptors with hexamethonium completely abolished the hypoxia-induced increase in $[Ca^{2+}]_i$ in chain neurons, indicating the critical involvement of these receptors in the excitatory ChN signaling pathway. Immunohistochemical labelling identified a novel population of ACh containing neurosecretory cells in the efferent gill filament. Additionally, qPCR revealed upregulation of several nicotinic receptor subunits following hypoxia exposure, suggesting a compensatory enhancement of cholinergic transmission. The cholinergic activation of hypoxia signalling was also observed in vagal and epibranchial ganglia, two populations of neurons which innervate the gills and play a critical role in controlling hyperventilation, emphasizing the broader implications of acetylcholine on respiratory regulation. Similarly, 5-HT and the 5-$HT_3$ receptor agonist, phenylbiguanide, produced an increase in ganglion $[Ca^{2+}]_i$, while blockade of 5-$HT_3$ receptors reduced the hypoxia-induced increase in $[Ca^{2+}]_i$. qPCR analysis confirmed relative expression of *htr3a* and *htr3b* (the genes encoding $5HT_3$ receptors) in isolated gill tissue; however, all concentrations of 5-HT tested failed to elicit a change in ChN $[Ca^{2+}]_i$ activity indicating the serotonergic signalling pathway in the gill acts independently from ChNs. Our investigation into cholinergic and serotonergic signaling in the gill and its potential involvement in reflex hyperventilation provides critical insights into the evolutionary conservation and adaptation of respiratory control mechanisms.

## 4.2 Introduction

Oxygen sensing and the physiological responses to hypoxia are critical processes for survival in aquatic environments. In teleost fish, the gills serve as the primary site for oxygen detection and initiation of compensatory responses (Perry et al., 2009). Gill neuroepithelial cells (NECs) have been identified as the major peripheral oxygen sensing cells in aquatic vertebrates and share morphological similarities with mammalian oxygen chemoreceptors such as those found in the carotid body (Jonz et al., 2004). NECs respond to hypoxia through a mechanism involving the inhibition of background $K^+$ channels, leading to membrane depolarization and subsequent neurotransmitter release (Jonz et al., 2004; Zachar et al., 2017). This process activates sensory pathways in the gill, ultimately resulting in physiological responses such as hyperventilation. Multiple populations of NECs have been identified in zebrafish gill epithelia, including both serotonergic (characterized by serotonin (5-HT) and synaptic vesicle protein-2 (SV2) immunoreactivity) and nonserotonergic NECs (characterized by SV2 immunoreactivity) (Jonz & Nurse, 2003; Jonz et al., 2004).

The development of oxygen sensing in zebrafish occurs early in their life cycle. NECs are first expressed in gill filament primordia of larvae at 5 days post-fertilization (dpf) and become fully innervated by 7 dpf (Jonz & Nurse, 2005). Interestingly, a behavioral response to hypoxia has been observed in embryos as early as 2 dpf, suggesting the presence of alternative oxygen-sensing mechanisms before the complete development of gill NECs (Jonz & Nurse, 2005). Adult-like responses to hypoxia are observed as early as 15 dpf, indicating a rapid maturation of the oxygen-sensing system (Pan et al., 2019).

Fish gills are innervated by branches of cranial nerves, primarily the glossopharyngeal (IX) and vagus (X) nerves, and NECs receive innervation from both extrinsic and intrinsic

sources (Sundin & Nilsson, 2002; Jonz & Nurse, 2003). One source of intrinsic innervation arises from sensory "chain neurons" (ChNs), whose cell bodies are distributed along the gill filament artery and send projections to innervate NECs (Jonz et al., 2004). Recent studies using transgenic Tg(*elavl3*:GCaMP6s) zebrafish, which express a genetically-encoded $Ca^{2+}$ reporter, GCaMP, under the control of a pan-neuronal promoter, have provided insights into the functional aspects of the NEC-ChN synapse (Reed et al. 2024; Reed & Jonz, 2025). In these animals, both NECs and ChNs display a hypoxia-induced increase in intracellular calcium ($[Ca^{2+}]_i$). Further, it was found that functional NEC-ChN synapse is necessary for the hypoxia-induced increase in $[Ca^{2+}]_i$ of ChNs, and post-synaptic responses are modulated by pre-synaptic dopamine via $D_2$ receptors (Reed & Jonz, 2025).

The neurotransmitter(s) driving the excitatory transmission of hypoxia signalling at the NEC-ChN synapse are currently unclear. Serotonin (5-HT), the most abundant neurotransmitter in gill NECs, and acetylcholine (ACh) have both been suggested as excitatory neurotransmitters in the gills (Jonz & Nurse, 2003; Porteus et al., 2012; Zachar et al., 2017). Single-cell RNA sequencing has provided deeper insights into the cellular composition and gene expression profiles of zebrafish gill cells, including NECs and neurons. These studies have revealed that NECs and gill neurons express genes associated with chemosensory transduction of hypoxic signals, many of which are shared with mammalian chemoreceptor cells (Pan et al., 2022). Notably of these, genes encoding 5-HT receptors and nicotinic ACh receptors are expressed in the gill and specifically show high expression in gill neurons (Pan et al., 2023).

As our understanding of the cellular and molecular mechanisms underlying oxygen sensing and signaling in fish gills continues to evolve, it becomes increasingly clear that this system involves a sophisticated network of neurotransmitters and receptors. The goal of the

present study was to elucidate the role of ChNs in ventilatory responses to hypoxia and to uncover the neurochemical basis of excitatory NEC-ChN signalling.Using a combination of Ca2+ imaging and immunohistochemistry we provide evidence for ACh as a key excitatory neurotransmitter in the hypoxia signaling pathway in zebrafish at the NEC-ChN synapse, and implicate activation of this synapse in the higher order centers responsible for control of ventilation. We further show that 5-HT also appears to be involved in the hypoxic response, potentially through gill 5-$HT_3$ receptors, but in a manner independent of the ChN pathway.

## 4.3 Methods

### 4.3.1 Animal ethics statement

All wild-type and transgenic zebrafish were bred and maintained at the Laboratory for the Physiology and Genetics of Aquatic Organisms, University of Ottawa. Zebrafish were kept at 28°C on a 14:10-h light:dark cycle (Westerfield, 2007). Embryos and larvae were reared on a diet of rotifers and Gemma 75 (Skretting Canada, St. Andrews, NB), juveniles were fed Artemia and Gemma 150-300 (Skretting), and adults were fed Adult Zebrafish Diet (Ziegler Feeds, Gardners, PA, USA). Adult zebrafish were euthanized by concussion and terminated by decapitation. Larval zebrafish were euthanized by hypothermic shock by immersion in an ice bath for 20 min.

All procedures for animal use and euthanasia were carried out in accordance with institutional guidelines according to protocol BL-3666, and guidelines provided by the Canadian Council on Animal Care. The present work complies with the ethical guidelines set out by the journal and with those according to Animals in Research: Reporting In Vivo Experiments (ARRIVE).

### 4.3.2 Relative $[Ca^{2+}]_i$ measurements

In this study we used transgenic zebrafish Tg(*elavl3*:GCaMP6s) expressing the genetically encoded $Ca^{2+}$ indicator GCaMP6s under the pan-neuronal promotor *elavl3* (Dunn et al. 2016). GCaMP6s contains the green fluorescent protein (GFP) as part of its structure. Whole gill baskets were removed and separated into individual gill arches and immersed in extracellular solution containing (mM): 120 NaCl, 5 KCl, 2.5 $CaCl_2$, 2 $MgCl_2$, 10 HEPES, 10 glucose at pH 7.8. Isolated intact gill arches from Tg(*elavl3*:GCaMP6s) zebrafish were secured in a Petri dish using a metal tissue anchor (cat. no. 640251, Warner Instruments). The Petri dish was continuously perfused with extracellular solution (ECS) at pH 7.8. GFP-fluorescing cells were observed using a Nikon 40× water-immersion objective. GCaMP-containing ChNs were identified by their distinct morphology and presence of GFP, as previously described (Reed & Jonz, 2025). Using a Lambda DG-5 wavelength changer (Sutter Instruments, Novato, CA, USA), the preparation was exposed to 490 nm excitation light for 600 ms at a sampling frequency of 1 $s^{-1}$. Images were captured with a CCD camera (QImaging, Surrey, BC, Canada), and fluorescence intensity was recorded with NIS Elements software (Nikon). For each recording, the baseline fluorescence was calculated as the average fluorescence intensity of a cell for the first 30 s in normoxia. All fluorescence values were divided by the baseline to evaluate changes in fluorescence intensity over time throughout a single recording.

Larval nerve recordings were carried out with whole, anesthetized animals from the Tg(*elavl3*:GCaMP6s) line aged 14-21 days post fertilization. Animals were anesthetized with 0.01 mg/ml tricaine and held in place under a metal tissue anchor. Nodose and epibranchial ganglia were identified by position relative to the eye, otolith, gills and hindbrain. Recording regions were set to encompass the entire visible cluster of neurons associated with these ganglia,

rather than individual neurons (see Fig. 7AB, D). For simultaneous recordings of epibranchial and nodose ganglia, sampling frequency was increased to 4 $s^{-1}$ to more accurately observe the delay in activation time between these structures. Latency was defined as the difference between nodose activation time and epibranchial activation time ($Time_{nodose} - Time_{epibranchial}$). Onset of the $[Ca^{2+}]_i$ response was characterized as the time where relative fluorescence ($F/F_0$) first doubled ($F/F_0=2$). Larval recording experiments were otherwise performed as described for whole gill recording, including ECS, equipment setup and calculation of fluorescence intensity. All drugs were introduced into the recording chamber by perfusion in ECS.

### 4.3.3 Immunohistochemistry

Techniques for tissue extraction and immunolabeling were carried out as previously described (Jonz & Nurse, 2003). Whole gill baskets were removed and immersed in phosphate buffered solution (PBS) containing (mM): NaCl 137, $Na_2HPO_4$ 15.2, KCl 2.7, and $KH_2PO_4$ 1.5 at pH 7.8 (Bradford et al., 1994). Gill baskets were fixed by immersion in 4% paraformaldehyde in PBS overnight at 4°C. Tissues were removed and rinsed in PBS three times at 3 min before permeabilization for 24 h at 4°C. Permeabilizing solution (PBS-TX) contained 0.5-2% Triton X-100 in PBS (pH 7.8). After 3 rinses in PBS, gill baskets were then separated into individual arches. Gill arches were incubated in primary antibodies for 24 h at 4°C, rinsed with PBS three times at 3 min, and immersed in secondary antibodies for 1 h at room temperature in darkness.

ACh-positive cells were identified using polyclonal anti-acetylcholine raised in rabbit (NB100-64656; Bio-Techne Canada). The nAChR subunit α2 was identified using monoclonal anti-CHRNA2 raised in mouse (AB_2787307). Both antibodies were used at 1:100 and visualized with goat anti-rabbit secondary antibodies conjugated with fluorescein isothiocyanate

(FITC, 1:50, cat. no. 111-095-003, Cedarlane, Burlington, ON, Canada). To control for the specificity of α2 in our preparation we used the specific control peptide corresponding to the immunogen sequence (DLEQMERTVDLKD, Alomone, BLP-NC002). Pre-adsorption of the control peptide with the α2 antibodies blocked all immunolabeling in gill tissue. NECs were identified using monoclonal SV2 raised in mouse (AB_2315387; Developmental Studies Hybridoma Bank, University of Iowa, IA, USA) at 1:100 and visualized by goat anti-mouse secondary antibodies conjugated with Alexa 594 at 1:100 (cat. no. A11005, Invitrogen, Burlington, ON, Canada). Monoclonal zn-12 raised in mouse (RRID: AB_531908; Developmental Studies Hybridoma Bank, University of Iowa) was used to visualize gill neurons. zn-12 targets membrane fractions from adult zebrafish CNS and recognizes an HNK-1-like epitope (manufacturer specifications). zn-12 was used at 1:100 and targeted by goat anti-mouse secondary antibodies conjugated with Alexa 594 at 1:100 (cat. no. A11005; Invitrogen).

5HT-positive NECs were identified using the transgenic ET(*vmat2:GFP*) zebrafish previously described by Wen et al. (2008) and obtained from the Becker Laboratory at the University of Edinburgh. VMAT2 is an integral membrane protein that mediates storage of monoamines, such as 5-HT, into synaptic vesicles. ET(*vmat2:GFP*) zebrafish contained a reporter gene for green fluorescent protein (GFP) under the expression of the vesicular monoamine transporter (*vmat2* also known as *slc18a2*) and were used to visualize 5-HT-containing NECs (Pan et al., 2021).

Whole-mount preparations were examined using an upright microscope platform (H101A ProScan, Olympus, Canada) with motorized XYZ control and a confocal scanning system (FV100 BX61 LSM, Olympus) equipped with continuous laser lines at 405 nm, 488 nm and 561 nm.

### 4.3.4 Acclimation to chronic hypoxia

Adult zebrafish were placed in 2.5-L tanks and acclimated to hypoxia (35 mmHg) for 48 h. A group of control zebrafish were simultaneously maintained in an identical tank at normoxia (~160 mmHg) for the same period of time. For acclimated fish, water $P_{O_2}$ was gradually lowered over 8 h at a rate of ~16 mmHg $h^{-1}$ by introducing a mixture of compressed air and 100% $N_2$ from a gas mixer (Pegas 4000 MF; Columbus Instruments) and delivered through a porous air stone. Water temperature was kept at 28°C by placing tanks in a temperature-controlled water bath, and 50% water changes were performed in both tanks every day.

### 4.3.5 Quantitative polymerase chain reaction

Whole gill baskets were removed from zebrafish acclimated to hypoxia or normoxic controls after 48 h, as described in Section 2.3 and immediately frozen on dry ice. Total RNA from gill baskets was extracted using Trizol reagent (Life Technologies) and quantified using a NanoDrop 2000c UV–Vis Spectrophotometer (Thermo Fisher Scientific). cDNA was generated using 1000 ng of RNA from whole gill baskets using QuantiTect Reverse Transcription Kit (Qiagen) following manufacturers protocol. To check for genomic DNA contamination, a no-template negative control and a no reverse transcriptase negative control were included. mRNA gene expression of nicotinic receptor subunits α2, α3, α4, α6, α7, β2, β3, and β4 (*chrna2a, chrna3, chrna4, chrna6, chrna7, chrnb2a, chrnb3, and chrnb4*) and serotonin receptor 5HT3 (*htr3a* and *htr3b*) in the gill was assessed by real-time reverse transcription quantitative polymerase chain reaction (RT-qPCR) using SsoAdvanced Universal SYBR Green Supermix (Bio-Rad). Expression of reference gene, elongation factor 1a (*ef1a*), was stable between gill

baskets of normoxia and hypoxia groups and was therefore used to normalize mRNA expression of all genes (Reed et al., 2024). Standard curves were generated using a serial dilution of pooled cDNA to optimize primer reaction conditions. Quantitative polymerase chain reaction (qPCR) included 1 µL cDNA, 1 µL specific forward primer, 1 µL specific reverse primer, 7 µL nuclease-free water, and 10 µL Universal SYBR Green Supermix for a total reaction volume of 20 µL. Each reaction included an initial step at 98°C to activate the enzymes in the mix, followed by 40 repeats of a denaturation step at 95°C and an annealing/extension step at the optimized temperature for each primer pair (Table 1). A melt step from 66 to 95°C in 0.5°C increments was included at the end of the reaction to check the specificity of the amplicon produced. Each biological sample was run in triplicate, and the relative abundance of mRNA was calculated using the $\Delta\Delta C_t$ method (Livak & Schmittgen, 2001). All primers were designed using Primer3 software. Statistical analysis was carried out using the Mann–Whitney *U* test with Prism software.

**Table 4.1.** Nicotinic receptor subunit primer pair conditions used for mRNA quantification by real-time reverse transcription polymerase chain reaction.

| Gene | Primer sequence (5'-3') | Annealing temperature | Efficiency %, $R^2$ |
|---|---|---|---|
| *chrna2a* | F: CCCTTTATCCCACTGCTCAA<br>R: TAATTGCACGACCTCCACAA | 58°C | 97.4%, 0.991 |
| *chrna3* | F: CATCACAGAAACCATCCCATC<br>R: GAACATAACCCGAGGAAGCA | 58°C | 96.6%, 0.990 |
| *chrna4b* | F: TCCAGCACAACTTCCTTTCC | 60°C | 100.7%, 0.996 |

| | | | |
|---|---|---|---|
| | R: CCTGCTCCCAGAACACTCTC | | |
| *chrna6* | F: CCGCAACAAAGCTAAAGAGG | 57°C | 97.2%, 0.980 |
| | R: GGCCCAAAGTTCCTAACACA | | |
| *chrna7* | F: TCAGTATTTTGCCACCACCA | 54°C | 98.7%, 0.988 |
| | R: CTTTGTCTTCGCCAGGTCTC | | |
| *chrnb2a* | F: GACCTACGACCGCACAGAAC | 58°C | 96.2%, 0.991 |
| | R: AAAACCAGGGCAAGAGA | | |
| *chrnb3a* | F: TGGTGGATGTGGATGAAAAA | 60°C | 94.8%, 0.994 |
| | R: TGTCAAAGGGGAAAAAGGTG | | |
| *chrnb4* | F:GCCACCAGTCAGAAACAACA | 60°C | 101.9%, 0.990 |
| | R:TCCCCCAGTGTAAAGACGAA | | |

Primer sequences for all genes were designed using Primer3 software.

Abbreviations: F, forward primer; R, reverse primer.

**Table 4.2.** Serotonin receptor primer pair conditions used for mRNA quantification by real-time reverse transcription polymerase chain reaction.

| Gene | Primer sequence (5'-3') | Annealing temperature | Efficiency %, $R^2$ | Reference |
|---|---|---|---|---|
| *hrt3a* | F: TGTTGATCGTGAGGCTGGT | 54°C | 95.6%, 0.992 | designed |
| | R: TTGCAGTGAATGGCAGTGTT | | | |
| *htr3b* | F: TCGCATCACTTTCAAGACCA | 53°C | 97.9%, 0.997 | designed |
| | R: ATGCAACAGCTTCACCACAA | | | |

Primer sequences for all genes were designed using Primer3 software.

Abbreviations: F, forward primer; R, reverse primer.

### 4.3.6 Statistical analysis

For all reported data, sample size (n) refers to individual cells. While multiple gill arches were assessed per animal, only one cell from each arch was included in the analysis to avoid repeated exposures or treatments in the same tissue. For each recording, the baseline fluorescence was calculated as the average fluorescence intensity of a cell for the first 30 s in normoxia. All fluorescence values were divided by the baseline to evaluate changes in fluorescence intensity over time throughout a single recording. Statistical analysis for gill and whole animal $Ca^{2+}$-imaging recordings were carried out using the Wilcoxon matched-pairs signed rank test for paired comparisons or the Mann-Whitney U test for unpaired comparisons with Prism (GraphPad Software Inc., La Jolla, CA, USA). For comparison of paired samples exposed to three or more treatments a Friedman test with Dunn's multiple comparison test was used. Dose-responses were normalized to the maximum concentration of each drug. For estimation of $EC_{50}$, a line constrained from the origin at zero was fit to the data using a nonlinear [agonist/antagonist] vs. normalized response model with least squares following the equation: $y=100*(X^{HillSlope})/(EC50^{HillSlope} + X^{HillSlope})$ (Prism v9.5.1; GraphPad Software). All data were expressed as means ± standard deviation (SD).

## 4.4 Results

### 4.4.1 Cholinergic activation of increased intracellular $Ca^{2+}$ concentration ($[Ca^{2+}]_i$) in chain neurons (ChN)

To evaluate a role for ACh as an excitatory neurotransmitter in the ChN response to hypoxia, we first examined changes in ChN $[Ca^{2+}]_i$ in response to drugs that target cholinergic receptors. Exogenous addition of ACh, at concentrations between 50 and 500 μM, caused a dose-dependent increase in $[Ca^{2+}]_i$ (Fig. 1A, B) with an $EC_{50}$ of 168.30 μM (Fig. 1C). In a similar

manner, the ACh receptor agonist, nicotine, caused a dose-dependent increase in $[Ca^{2+}]_i$ (Fig 1D,E) with an $EC_{50}$ of 37.68 μM (Fig. 1F). Further, blockade of nicotinic ACh receptors using hexamethonium reduced the ChN response to hypoxia in a dose-dependent manner (Fig. 2A, B). In experiments where the ChN was first exposed to hypoxia alone, during a second bout of hypoxia the $[Ca^{2+}]_i$ response was reduced by 31.25% with 25 μM (Wilcoxon matched-pairs signed rank test, p=0.0623, n=5), by 46.91% with 50 μM (Wilcoxon matched-pairs signed rank test, p=0.0313, n=6), by 51.16% with 100 μM (Wilcoxon matched-pairs signed rank test, p=0.0156, n=6), by 68.89% with 200 μM (Wilcoxon matched-pairs signed rank test, p=0.0156, n=6), and by 74.66% with 300 μM hexamethonium (Wilcoxon matched-pairs signed rank test, p=0.0313, n=5). The hypoxic response, with the addition of 200 μM and 300 μM hexamethonium, was not significantly different from baseline fluorescence in normoxia (Wilcoxon matched-pairs signed rank test, P>0.9999, n=5-6), indicating the hypoxia-induced increase in $[Ca^{2+}]_i$ was completely abolished by hexamethonium at these concentrations. The $EC_{50}$ of hexamethonium was 79.74 μM (Fig. 2C).

### 4.4.2 Acetylcholine (ACh) and nicotinic ACh receptors (nAChRs) were localized in the gills.

The experiments presented in Figure 2 suggested that ACh was endogenously released from chemoreceptors during hypoxia. Using immunohistochemistry and confocal imaging, we localized ACh immunoreactivity (IR) to the gill filament. ACh-IR colocalized with SV2 (Fig. 3A-C), a common marker for neurosecretory cells in the gills including NECs, that do not contain 5-HT (Jonz and Nurse, 2003). Moreover, ACh-IR was found in a number of GCaMP-positive NECs (Fig. 3D-F), though ACh-IR did not co-localize with VMAT2 expression (Fig. 3G-I)—a marker of serotonergic NECs—suggesting that ACh-IR cells were an independent

population of NEC that do not contain 5-HT. This observation raises the idea of two distinct populations of NECs, which we shall refer to as: SV2-positive serotonin (5-HT)-containing S-NECs, and SV2-positive ACh-containing A-NECs.

Using $Ca^{2+}$ imaging in isolated gills, we demonstrated that hypoxia enhanced the ChN response to low concentrations of nicotine at 25 μM (Wilcoxon matched-pairs signed rank test, p=0.0313, n=5) and 50 μM (Wilcoxon matched-pairs signed rank test, p=0.313, n=5), but at higher concentrations of nicotine (100-300 μM) the ChN response was not significantly enhanced by hypoxia (Wilcoxon matched-pairs signed rank test, n=4-5) (Fig. 4A, B). The amount of fluorescence signal added by hypoxia drastically declined at concentrations of nicotine above 100 μM (Fig. 4C). This occlusion of the enhancing effect of hypoxia on higher nicotine concentrations suggests the endogenous excitatory neurotransmitter acting on ChNs was acting through nicotinic ACh receptors.

In qPCR experiments using isolated gill tissue, we confirmed expression of genes *chrna2a, chrna3, chrna4, chrna6, chrna7, chrb2a*, *chrnb3* and *chrnb4*, encoding nicotinic receptor subunits α2, α3, α4, α6, α7, β2, β3 and β4 respectively. 48 h of hypoxia exposure upregulated expression of many of these genes, including *chrna2a* (Mann-Whitney test, p=0.0006, n=7), *chrna3* (Mann-Whitney test, p=0.0012, n=7), *chrnb2a* (Mann-Whitney test, p=0.0262, n=7) and *chrnb4* (Mann-Whitney test, p=0.0006, n=7). Importantly, these data showed that the gene encoding the α2 subunit displayed the greatest relative increase in expression following hypoxia, suggesting a possible role in hypoxia signalling.

Using confocal microscopy, we localized nicotinic ACh receptor α2 subunit-IR to nerve fibres travelling along the midline of the gill filament (Fig. 6A-C). α2 subunit labelling was punctuated with regions of increased fluorescence intensity and colocalized with anti-zn-12 (Fig.

6A-C, arrows), a zebrafish neuronal marker that also labels other nerve fibres and ChNs. Rotation by 90° showed that nerve fibres projecting from ChNs coursed around the filament artery to the superficial layer, where α2 subunit-IR was found (Fig. 6D-F, arrow). When ACh-R α2 subunit immunoreactivity was combined with anti-SV2, it was evident that α2 subunit-IR puncta occurred along the nerve fibre in close proximity with SV2-positive NECs (Fig. 6G-I).

### 4.4.3 Cholinergic effects on extrabranchial vagus nerve (cranial nerve X)ganglia.

To determine whether the hypoxic signal generated in the gill was transmitted towards the central nervous system, we developed a preparation to investigate ganglionic activity in the head of intact Tg(*elavl3*:GCaMP6s) larvae (Fig. 7A, B). Each gill arch receives sensory autonomic innervation from an epibranchial ganglion, which projects to the larger nodose ganglion of the vagus nerve (cranial nerve X). Gill denervation of cranial nerve X decreases the magnitude of the hypoxic ventilatory response in many fish species (Milsom, 2012). Exposure of intact larvae to hypoxia corresponded with a significant rise in $[Ca^{2+}]_i$ from the nodose ganglion (Fig. 7C, Wilcoxon matched-pairs signed rank test, p=0.156, n=7). Next, we simultaneously evaluated $[Ca^{2+}]_i$ responses from the posterior epibranchial ganglion above the fourth gill arch and the nodose ganglion.When whole larvae were exposed to hypoxia, both ganglia displayed an increase in $[Ca^{2+}]_i$ (Fig. 7D, E). Notably, when recorded simultaneously, we observed that the epibranchial ganglion, closest to the gill, was always first to respond to hypoxia followed by the nodose ganglion. When measuring the onset of the $[Ca^{2+}]_i$ response as the time where $F/F_0$ doubled, the response in the nodose ganglion occurred after a delay of 6.3 ± 0.6 s (n=7) compared to the epibranchial ganglion (Fig. 7E). In contrast, both populations of ganglionic neurons were activated within 1.2 ± 0.4 s (n=7) of each other, and in no specific order, in

response to ECS containing high $K^+$. This served as a control experiment to demonstrate that when both ganglia responded directly to the same stimulus, a sequence of responses could not be determined. A significant time delay between activation of the epibranchial and nodose ganglia during hypoxia was found when compared to high $K^+$ (Mann-Whitney test, p=0.0006, n=7), suggesting that hypoxia signaling involves directional transmission of the signal towards the nodose, as opposed to the immediate and more direct response caused by high $K^+$.

Exogenous addition of ACh or nicotine, which activated ChNs in the gill in a manner similar to that of hypoxia (Fig. 1, 4), evoked an increase in $[Ca^{2+}]_i$ from the nodose ganglion in recordings from intact larvae (Fig. 8A, B). Further, a significant difference in the time delay between ACh activation of the epibranchial and nodose ganglia was found compared to activation by high $K^+$ (Fig. 8C; 8.1 ± 0.7 s, Mann-Whitney test, p=0.0006 n=7), as well as between nicotine and high $K^+$ (Fig. 8D; 8.8 ± 0.9 s, Mann-Whitney test, p=0.0006, n=7), suggesting that, like hypoxia, ACh and nicotine activated ChNs in the gill.

### 4.4.4 Serotonergic hypoxia signalling occurs independently from the gill chain neuron (ChN) pathway.

Given the prevalence of 5-HT in the gill, and that gill neurons in zebrafish display strong expression of 5-$HT_3$ receptors (Pan et al., 2022), we investigated the potential effects of 5-HT on ChN signalling in both our whole-animal larval preparation and isolated gill preparation. Both 5-HT and the 5-$HT_3$ receptor agonist, phenylbiguanide, produced an increase in nodose ganglion $[Ca^{2+}]_i$ (Fig. 9A,B). Blockade of 5-$HT_3$ receptors with MDL7222 reduced the hypoxia-induced increase in $[Ca^{2+}]_i$ in the epibranchial ganglion (Fig. 9C, Wilcoxon matched-pairs signed rank test, p=0.0313, n=5). qPCR analysis confirmed relative expression of *htr3a* and *htr3b* (the genes encoding 5$HT_3$ receptors) in isolated gill tissue, though expression remained unchanged

following acclimation to hypoxia (Fig. 9D). Together, these results suggest the involvement of 5-HT excitatory neurotransmission in the gill acting via 5-$HT_3$ receptors in hypoxia signalling. However, in our isolated gill preparation, all concentrations of 5-HT tested failed to elicit a change in ChN $[Ca^{2+}]_i$ activity (Fig. 9E; Friedman test, $p>0.9999$, $n=5$), and application of the 5-$HT_3$ receptor antagonist, MDL 7222, had no effect on the ChN response to hypoxia (Fig. 9F, Wilcoxon matched-pairs signed rank test, $p=0.8125$, $n=5$).

**Figure 4-1 Chain neurons (ChNs) displayed a dose-dependent increase in intracellular $Ca^{2+}$ concentration ($[Ca^{2+}]_i$) in response to exogenous acetylcholine and nicotine.** (A) Overlayed $Ca^{2+}$ imaging traces from 6 ChNs exposed to 50 μM-300 μM acetylcholine (ACh). Scale indicates time (min) and relative changes in fluorescence ($F/F_0$) corresponding to changes in $[Ca^{2+}]_i$. (B) Summary data from ChNs as treated in (A) (n=4-6). (C) Dose response from summary data in (B) showing concentration versus percent maximum response. Data points were fit using a nonlinear [agonist] vs. normalized response model with least squares following the equation: $y=100*(X^{HillSlope})/(EC50^{HillSlope} + X^{HillSlope})$. The effective half maximal concentration ($EC_{50}$) for ACh was 168.30 uM. (D) Overlayed $Ca^{2+}$ imaging traces from 5 ChNs exposed to 25 μM-300 μM nicotine. Scale indicates time (min) and relative changes in fluorescence ($F/F_0$) corresponding to changes in $[Ca^{2+}]_i$. (E) Summary data from ChNs as treated in (D) (n=4=6). (F) Dose response from summary data in (E) showing concentration versus percent maximum response. $EC_{50}$ for nicotine was 37.68 μM.

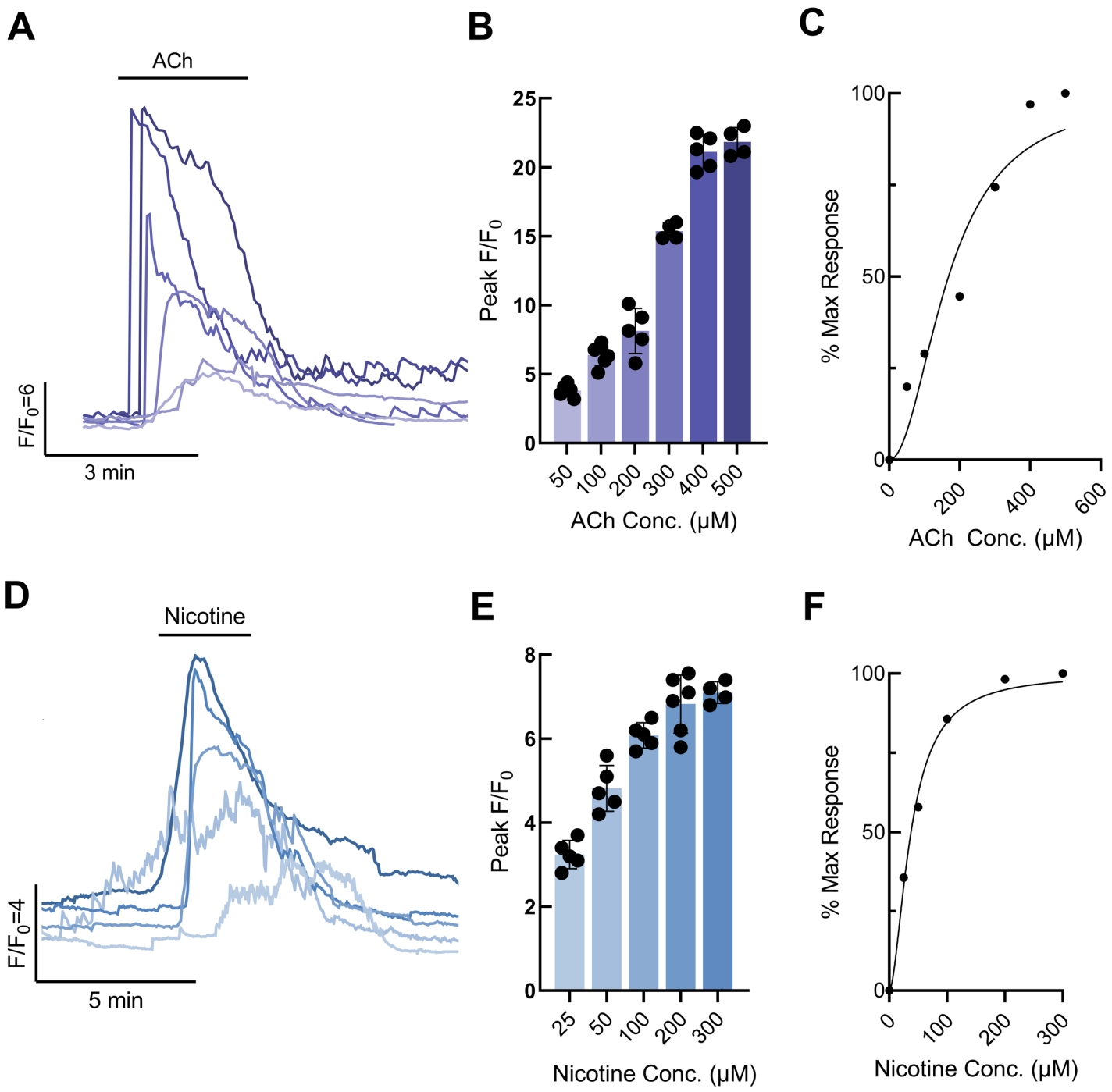
A
ACh
F/F0=6
3 min
B
Peak F/F0
25
20
15
10
5
0
50
100
200
300
400
500
ACh Conc. (μM)
C
% Max Response
100
50
0
0
200
400
600
ACh Conc. (μM)
D
Nicotine
F/F0=4
5 min
E
Peak F/F0
8
6
4
2
0
25
50
100
200
300
Nicotine Conc. (μM)
F
% Max Response
100
50
0
0
100
200
300
Nicotine Conc. (μM)

Figure 4.1

**Figure 4-2 The chain neuron (ChN) hypoxia-induced increase in intracellular calcium concentration ($[Ca^{2+}]_i$) was abolished by the nicotinic acetylcholine receptor antagonist, hexamethonium**. (A) $Ca^{2+}$ imaging traces from 5 ChNs each exposed to a 2-min bout of hypoxia followed by recovery in normoxia and a second bout of hypoxia in the presence of increasing concentrations of hexamethonium (25 μM-300 μM). (B) Summary data from ChNs as treated in (A) comparing average relative changes in fluorescence ($F/F_0$) during the following conditions: baseline fluorescence in normoxia (B), first hypoxia exposure (H), and second hypoxia exposure with hexamethonium (H+HEX). The hypoxic response (increase in $[Ca^{2+}]_i$) was reduced by 31.25% with 25 μM hexamethonium (Wilcoxon matched-pairs signed rank test, p=0.0623, n=5), by 46.91% with 50 μM hexamethonium (Wilcoxon matched-pairs signed rank test, p=0.0313, n=6) by 51.16% with 100 uM hexamethonium (Wilcoxon matched-pairs signed rank test, p=0.0156, n=6), by 68.89% with 200 μM hexamethonium (Wilcoxon matched-pairs signed rank test, p=0.0156, n=6), and by 74.66% with 300 μM hexamethonium (Wilcoxon matched-pairs signed rank test, p=0.0313, n=5). The hypoxic response with the addition of 200 μM and 300 μM hexamethonium was not significantly different than baseline activity in normoxia (Wilcoxon matched-pairs signed rank test, P>0.9999, n=6). (E) Dose response generated from summary data in (D) showing concentration versus percent maximum response. Data points were fit using a nonlinear [antagonist] vs. normalized response model with least squares following the equation: $y=100*(X^{HillSlope})/(EC50^{HillSlope} + X^{HillSlope})$. The $EC_{50}$ for hexamethonium was 79.74 μM.

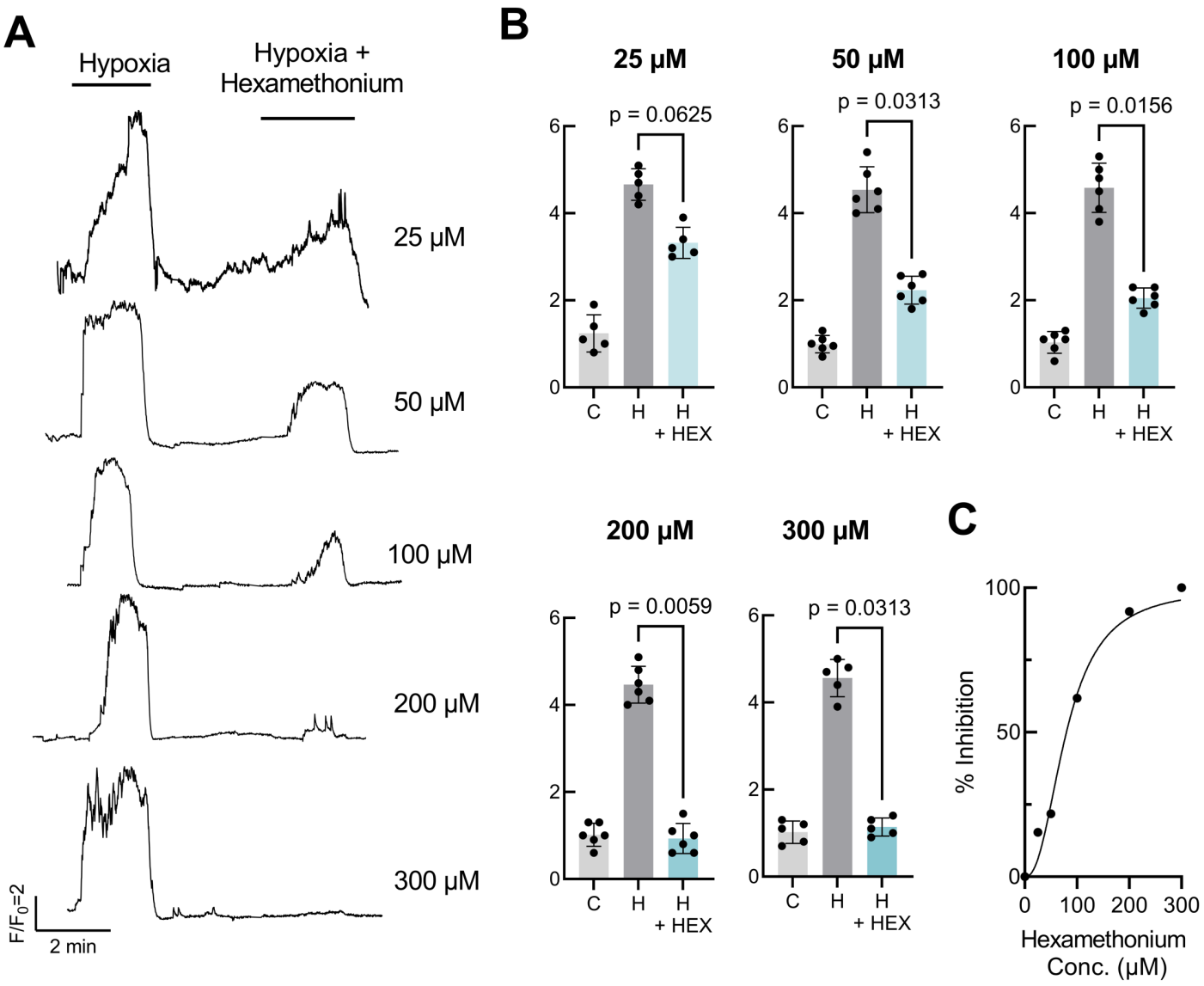
A
Hypoxia
Hypoxia +
Hexamethonium
25 µM
50 µM
100 µM
200 µM
300 µM
F/F0=2
2 min
B
25 µM
p = 0.0625
50 µM
p = 0.0313
100 µM
p = 0.0156
200 µM
p = 0.0059
300 µM
p = 0.0313
C
H
H
+ HEX
C
% Inhibition
Hexamethonium
Conc. (µM)

Figure 4.2

**Figure 4-3 Confocal imaging of immunohistochemical localization of acetylcholine (ACh)-positive neurosecretory cells in the efferent gill filament epithelium.** (A-C) Co-labelling of ACh (green) in neurosecretory cells containing synaptic vesicle protein-2 (SV2, magenta, arrows). (B,C) ACh and SV2 labelling shown separately. Scale bar in A=50 μM and applies to B and C. (D-F) Confocal imaging of immunohistochemical localization of ACh (magenta) in GCaMP-positive NECs (green, arrows) in gill filaments of Tg(*elavl3*:GCaMP6s) zebrafish. (E, F) ACh and GCaMP labelling shown separately. Scale bar in D=50 μM and applies to E and F. (G-I) Co-labeling of ACh (magenta) and the vesicular monoamine transporter-2 (*vmat2*, green). Scale bar in G=50 μM and applies to H and I. ACh-positive neurosecretory cells (arrow) do not co-localize with *vmat2*-positive NECs (arrowhead). (H,I) ACh and *vmat2* labelling shown separately.

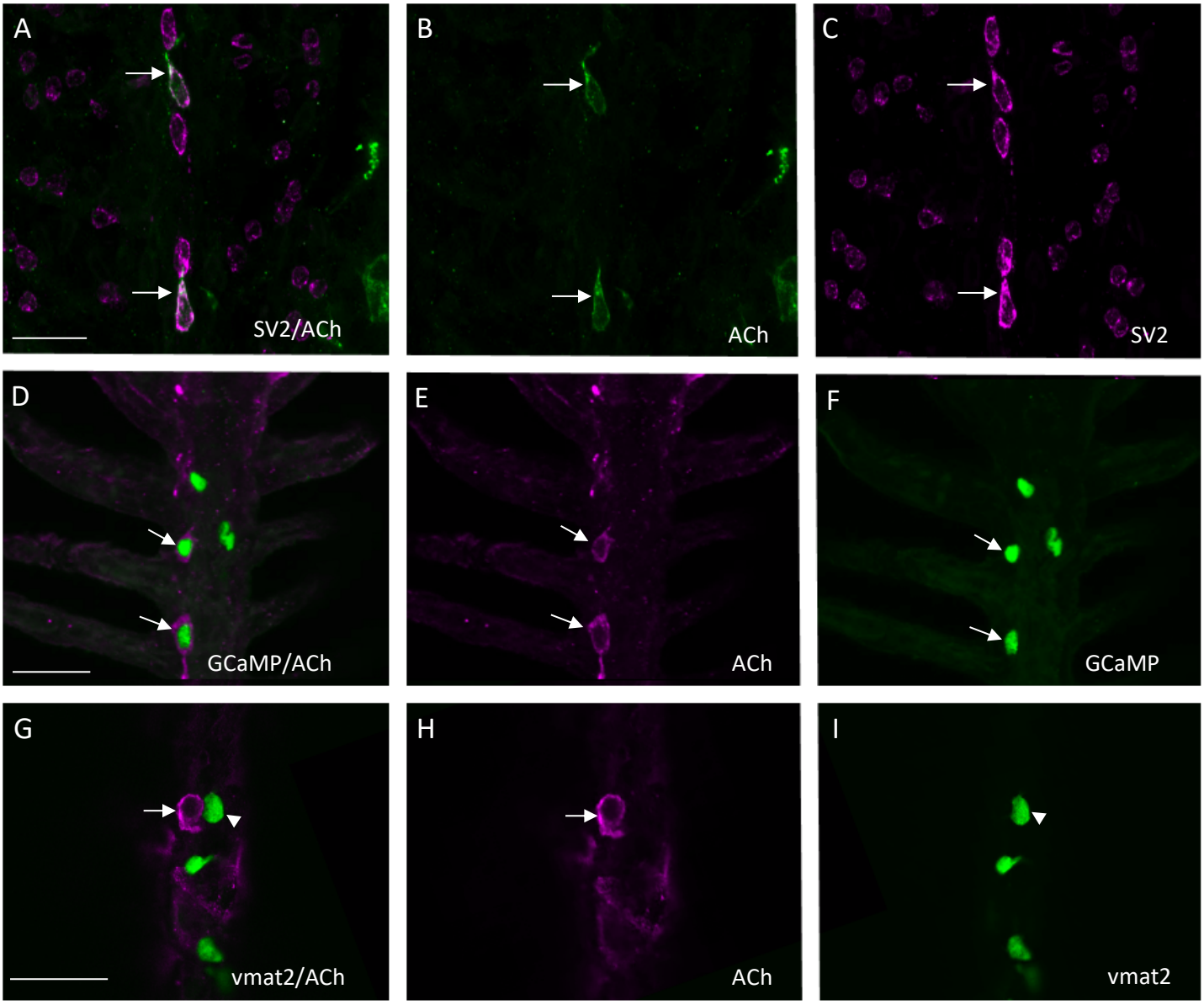
A
SV2/ACh
B
ACh
C
SV2
D
GCaMP/ACh
E
ACh
F
GCaMP
G
vmat2/ACh
H
ACh
I
vmat2

Figure 4.3

**Figure 4-4 The additive effect of hypoxia on the chain neuron (ChNs) increase in intracellular calcium concentration ($[Ca^{2+}]_i$) in response to nicotine is abolished at high nicotine concentrations**. (A) $Ca^{2+}$imaging trace from 5 GCaMP-containing ChNs comparing the $[Ca^{2+}]_i$ response to increasing concentrations of nicotine with and without the addition of hypoxia. The same concentration of nicotine was applied twice in each trace. (B) Summary data from ChNs as treated in (A) comparing the effect of hypoxia on each concentration of nicotine. Hypoxia had a significant enhancing effect on the ChN response to 25 μM (Wilcoxon matched-pairs signed rank test, p=0.0313, n=5) and 50 μM nicotine (Wilcoxon matched-pairs signed rank test, p=0.313, n=5) but did not significantly enhance 100-300 uM nicotine (Wilcoxon matched-pairs signed rank test, n=4-5). (C) Summary data from (B) showing the $F/F_0$ corresponding to changes in $[Ca^{2+}]_i$ added by hypoxia at each concentration of nicotine. The additive effect of hypoxia is occluded at high nicotine concentrations.

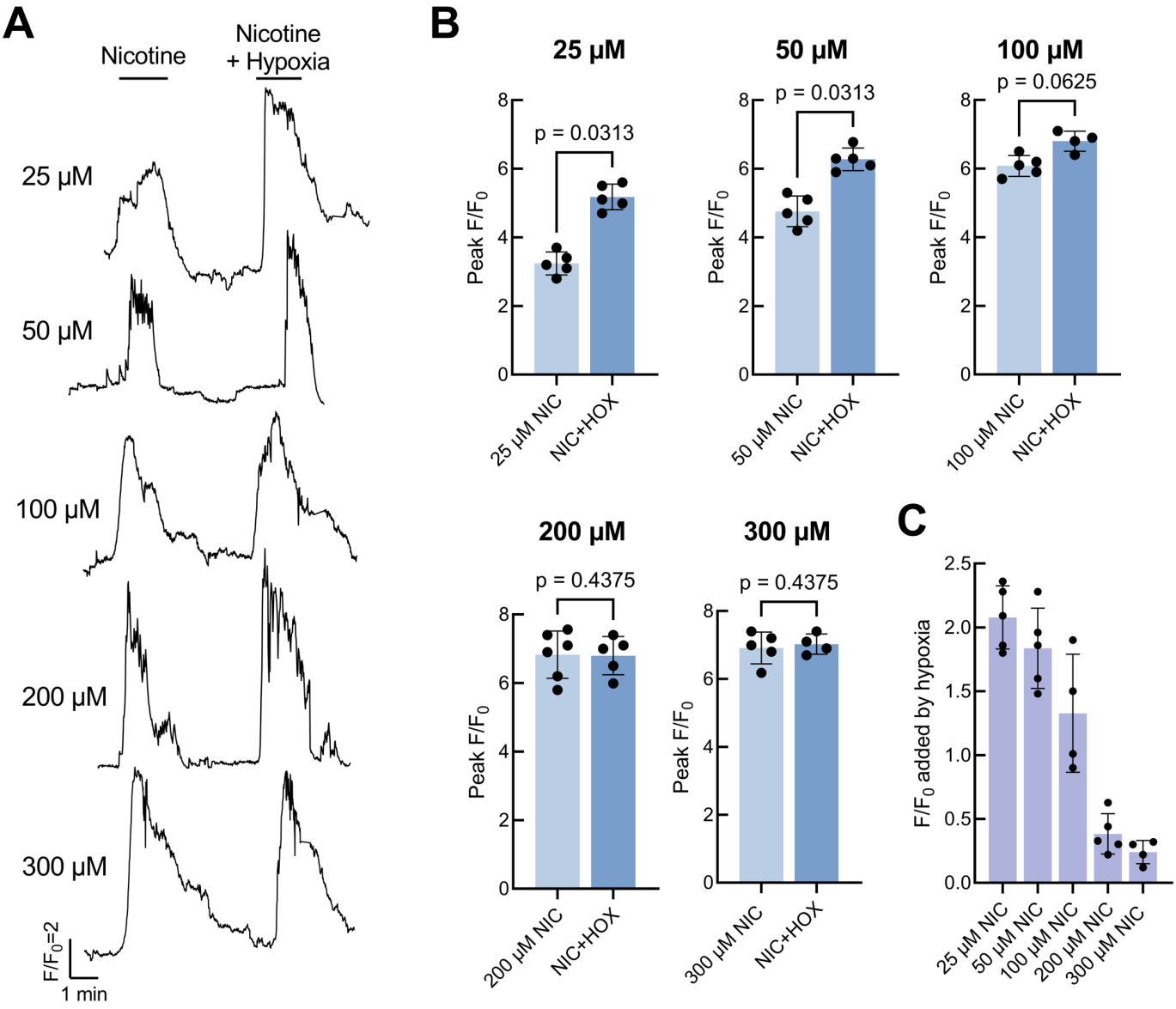
A
Nicotine
Nicotine
+ Hypoxia
25 µM
50 µM
100 µM
200 µM
300 µM
F/F0=2
1 min
B
25 µM
p = 0.0313
Peak F/F0
25 µM NIC
NIC+HOX
50 µM
p = 0.0313
50 µM NIC
NIC+HOX
100 µM
p = 0.0625
100 µM NIC
NIC+HOX
200 µM
p = 0.4375
200 µM NIC
NIC+HOX
300 µM
p = 0.4375
300 µM NIC
NIC+HOX
C
F/F0 added by hypoxia
25 µM NIC
50 µM NIC
100 µM NIC
200 µM NIC
300 µM NIC

Figure 4.4

**Figure 4-5 Relative mRNA expression of genes encoding nicotinic acetylcholine receptor (nAChR) subunits in isolated gill tissue.** Expression of *chrna2a, chrna3, chrb2a*, and *chrnb4* (encoding nAChR subunits α2, α3, β2, and β4) increased following 48 h of chronic hypoxia exposure. Data were normalized to the mRNA abundance of the reference gene, *ef1a*. Data were analyzed using a Mann–Whitney *U* test (n = 7).

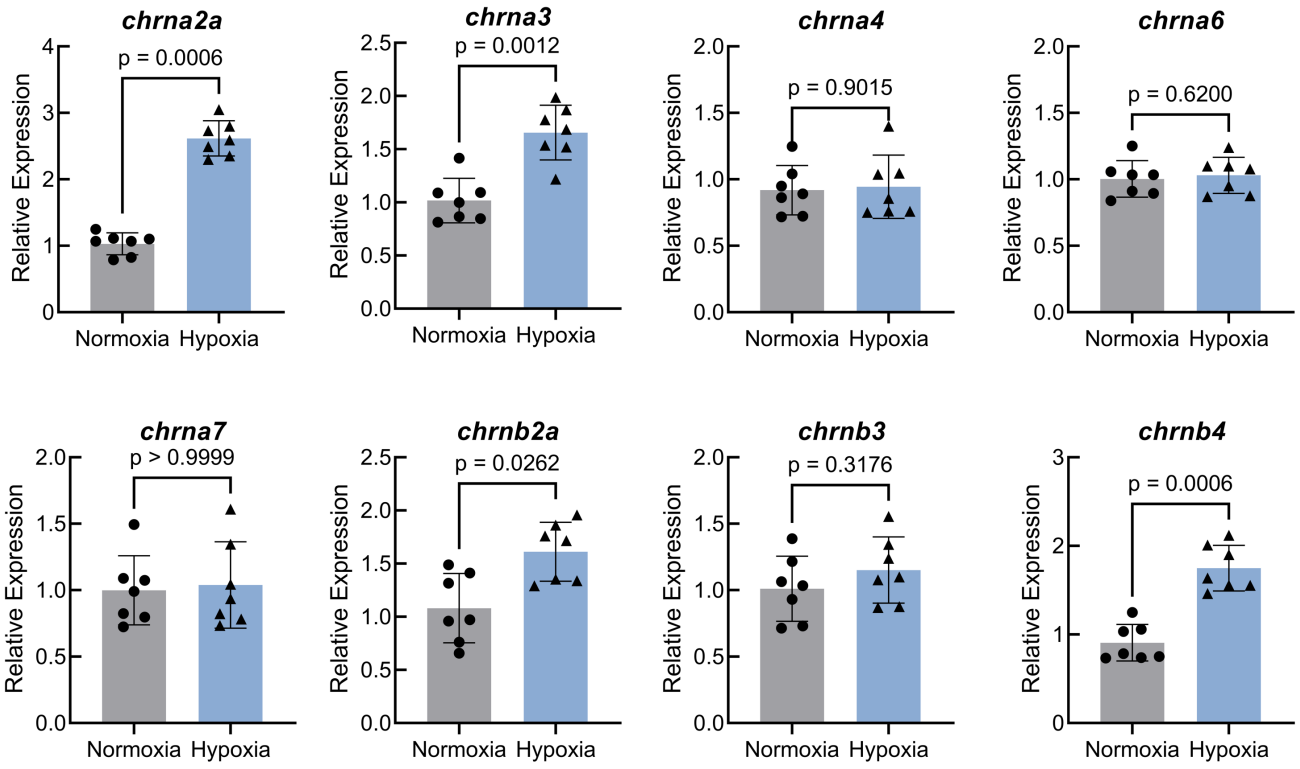
chrna2a
p = 0.0006
Relative Expression
Normoxia Hypoxia
chrna3
p = 0.0012
chrna4
p = 0.9015
chrna6
p = 0.6200
chrna7
p > 0.9999
chrnb2a
p = 0.0262
chrnb3
p = 0.3176
chrnb4
p = 0.0006

Figure 4.5

**Figure 4-6 Nerve fibres containing acetylcholine receptor (AChR) subunit α2 arise from chain neurons and contact neuroepithelial cells (NECs).** (A) Immunolabelling of AChR α2 subunit (green, arrows) was punctuated with regions of increased fluorescence intensity and colocalized with anti zn-12 labelled nerve fibres (magenta). Scale bar = 50 μm . (B, C) AChR α2 subunit (green) and zn-12 (magenta) labelling shown separately. (D-F) Images from A-C tilted 90° to show spatial separation between the α2-positive nerves, which lie superficial to the efferent filament artery (efA), and the deeper chain neurons (ChNs). (G) SV2 labelled NEC (magenta) in the efferent gill epithelium in close association with AChR subunit α2-positive nerve fibre (green, arrowhead). Scale bar = 50 μm. (H,I) α2 subunit (green) and SV2 (magenta) labelling shown separately.

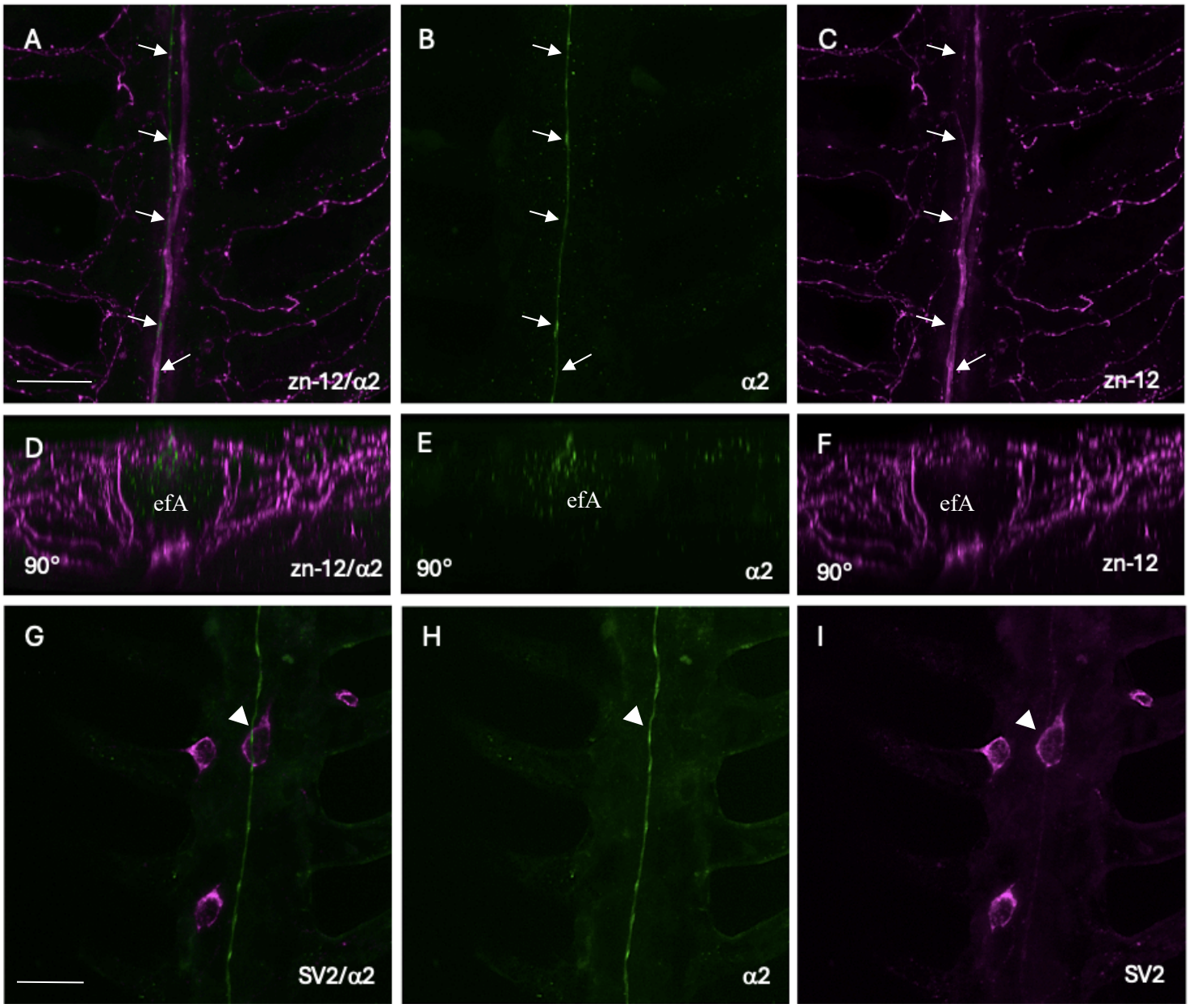
A
zn-12/α2
B
α2
C
zn-12
D
efA
90°
zn-12/α2
E
efA
90°
α2
F
efA
90°
zn-12
G
SV2/α2
H
α2
I
SV2

Figure 4.6

**Figure 4-7 Larval preparation for evaluating extrabranchial vagus nerve associated ganglionic changes in intracellular calcium concentration ($[Ca^{2+}]_i$) in response to hypoxia.** (A) Biorender schematic of cranial nerve X innervation of the gills including the large vagal nerve nodose ganglion as well as the 4 epibranchial ganglion above each gill arch in a larval zebrafish. (B) Confocal image from a 15 days post-ferilization larval Tg(elavl3:GCaMP6s) zebrafish expressing GFP (green) associated with GCaMP in the nodose ganglion (dashed box) and epibranchial ganglion (1-4). (C) $Ca^{2+}$ imaging trace from the nodose ganglion during whole animal exposure to hypoxia (left). Summary data (mean ± SD) for hypoxia-induced $[Ca^{2+}]_i$ increases in larval nodose ganglion (right, Wilcoxon matched-pairs signed rank test, p=0.156, n=7). (D) Overlay of brightfield and green fluorescence (488 nm) image of the vagal nerve ganglion *in situ* containing GCaMP from a larval Tg(*elavl3:*GCaMP6s) zebrafish. Dashed box indicates modified area of focus to include the nodose and epibranchial ganglia to be recorded simultaneously. Ganglia were identified by position relative to the eye, otolith (OT), gill arches (1-4), and hindbrain. (E,left) Simultaneous $Ca^{2+}$ imaging trace from an epibranchial ganglion (blue) and nodose (grey) corresponding to the dashed white box in (D) in response to hypoxia. (E, right) Summary (mean ± SD) of the time delay between the onset of epibranchial and nodose $[Ca^{2+}]_i$ responses to hypoxia and high $K^+$ in 7 fish. Onset of the $[Ca^{2+}]_i$ response was characterized as the time where relative fluorescence ($F/F_0$) first doubled ($F/F_0=2$). Hypoxia exposure resulted in a larger time delay between activation of the epibranchial and nodose ganglia compared to high $K^+$ (Mann-Whitney test, p=0.0006, n=7). (F) $Ca^{2+}$ imaging trace of all 4 epibranchial ganglion from a single animal responding to hypoxia simultaneously.

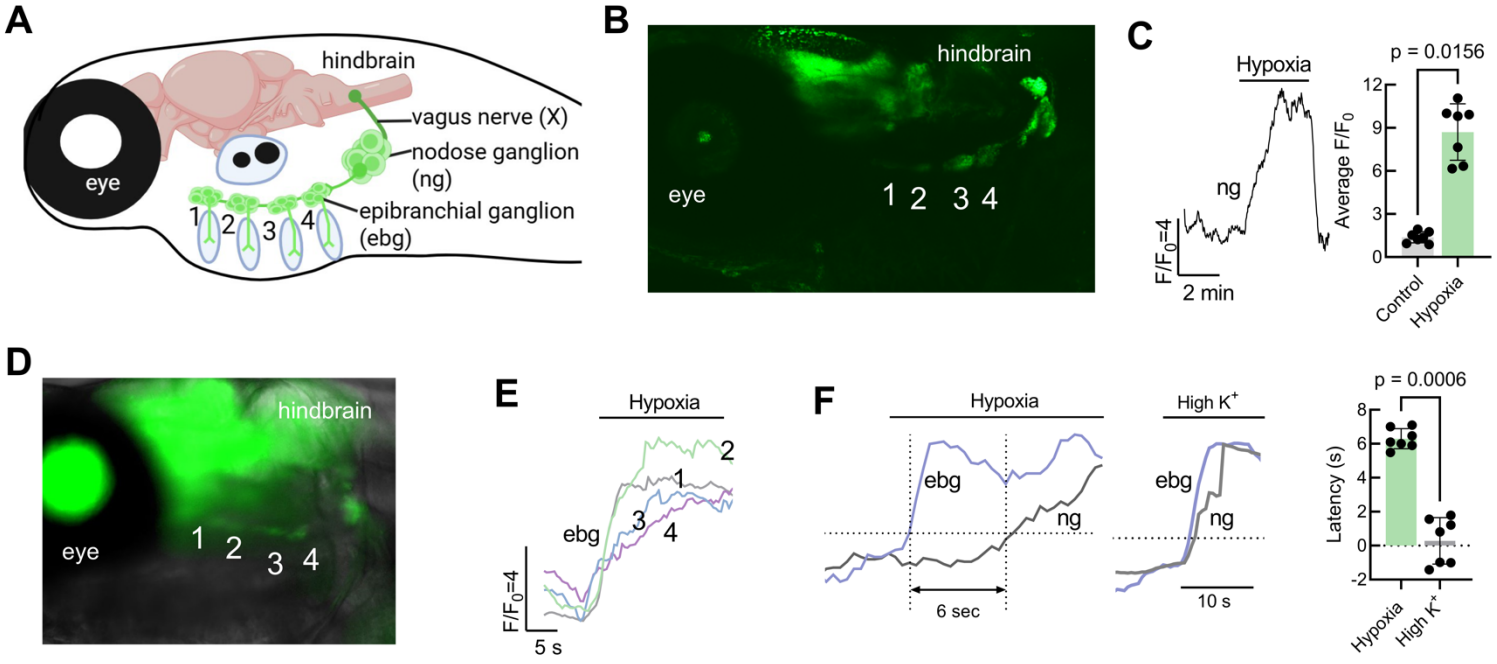
A
hindbrain
vagus nerve (X)
nodose ganglion
(ng)
epibranchial ganglion
(ebg)
eye
1
2
3
4
B
hindbrain
eye
1 2 3 4
C
Hypoxia
ng
F/F0=4
2 min
Average F/F0
p = 0.0156
Control
Hypoxia
D
hindbrain
eye
1 2 3 4
E
Hypoxia
ebg
1
2
3
4
F/F0=4
5 s
F
Hypoxia
ebg
ng
6 sec
High K+
ebg
ng
10 s
p = 0.0006
Latency (s)
Hypoxia
High K+

Figure 4.7

**Figure 4-8 Extrabranchial ganglia increased intracellular calcium concentration ($[Ca^{2+}]_i$) in response to ACh and nicotine in whole-animal larval $Ca^{2+}$ imaging recordings.** (A) $Ca^{2+}$ imaging trace from a larval GCaMP-containing nodose ganglion (ng) during exposure to 50 μM ACh (left). Scale indicates time (min) and relative changes in fluorescence ($F/F_0$) corresponding to changes in $[Ca^{2+}]_i$. Average (mean ± SD) $F/F_0$ nodose ganglion responses to ACh (Wilcoxon matched-pairs signed rank test, p=0.0156, n=7). (B) $Ca^{2+}$ imaging trace from a larval GCaMP-containing nodose ganglion during exposure to 50 μM nicotine (left). Scale indicates time (min) and relative changes in fluorescence ($F/F_0$) corresponding to changes in $[Ca^{2+}]_i$. Average (mean ± SD) $F/F_0$ nodose responses to nicotine (right, Wilcoxon matched-pairs signed rank test, p=0.0313, n=7). (C) Simultaneous $Ca^{2+}$ imaging recording showing response onset time for the epibranchial and nodose ganglia in response to ACh (left). Onset of the $[Ca^{2+}]_i$ response was characterized as the time where relative fluorescence first doubled ($F/F_0$=2). Summary data showing average (mean ± SD) time between onset of epibranchial (ebg) and nodose ganglia $[Ca^{2+}]_i$ responses to ACh compared to high $K^+$ control (right, Mann-Whitney test, p=0.0006 n=7). (D) Simultaneous $Ca^{2+}$ imaging recording showing response onset time for the epibranchial and nodose ganglia in response to nicotine (left). Onset of the $[Ca^{2+}]_i$ response was characterized as the time where relative fluorescence ($F/F_0$) first doubled. Summary data showing average (mean ± SD) time between epibranchial and nodose ganglia $[Ca^{2+}]_i$ responses to nicotine compared to high $K^+$ control (right, Mann-Whitney test, p=0.0006, n=7). Both ACh and nicotine showed a larger delay in activation between activation of epibranchial and nodose ganglia compared to the high $K^+$ control.

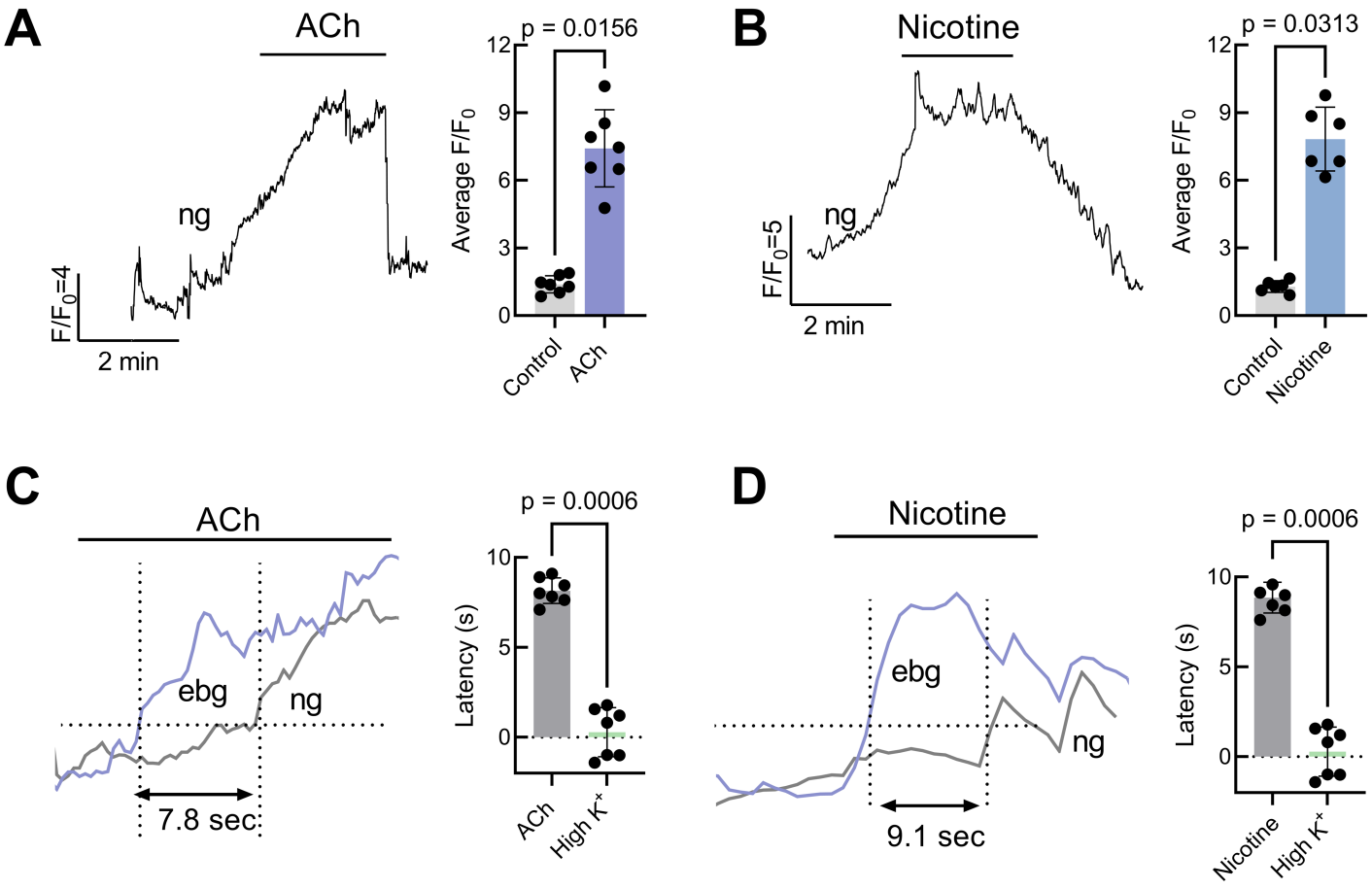
A
ACh
ng
F/F0=4
2 min
p = 0.0156
Average F/F0
Control
ACh
B
Nicotine
ng
F/F0=5
2 min
p = 0.0313
Average F/F0
Control
Nicotine
C
ACh
ebg
ng
7.8 sec
p = 0.0006
Latency (s)
ACh
High K+
D
Nicotine
ebg
ng
9.1 sec
p = 0.0006
Latency (s)
Nicotine
High K+

Figure 4.8

**Figure 4-9 Serotonergic hypoxia signalling occurs independently from the chain neuron (ChN) pathway.** (A) $Ca^{2+}$ imaging trace (left) and summary data (right) from larval nodose (ng) ganglion responses to 5-HT. 5-HT induced an increase in intracellular calcium concentration ($[Ca^{2+}]_i$) in this cluster of neurons (Wilcoxon matched-pairs signed rank test, p=0.0156, n=6). (B) $Ca^{2+}$ imaging trace (left) and summary data (right) from larval nodose ganglion responses to the $5HT_3$ receptor agonist, phenylbiguanide. 5-$HT_3$ receptor activation induced an increase in $[Ca^{2+}]_i$ in these neurons (Wilcoxon matched-pairs signed rank test, p=0.0313, n=5). (C) $Ca^{2+}$ imaging trace and summary data from epibranchial ganglia (ebg) in animals exposed to a bout of hypoxia followed by a second bout of hypoxia in the presence of the 5-$HT_3$ receptor antagonist, MDL72222 (left). A third bout of hypoxia was applied to control for changes in fluorescence over time. MDL7222 reduced the increase in epibranchial ganglion $[Ca^{2+}]_i$ associated with hypoxia (Wilcoxon matched-pairs signed rank test, p=0.0313, n=5). (D) qPCR relative expression of *htr3a* and *htr3b* (genes encoding 5-$HT_3$ receptors) in isolated gill tissue. Both genes were expressed in the gills with no changes in expression between 48 h normoxia and hypoxia-exposed animals (Mann Whitney test, p=0.4557, n=7). (E, right) $Ca^{2+}$ imaging trace from a chain neuron (ChN) in an adult isolated gill exposed to hypoxia, followed by increasing concentrations of 5-HT (100 μM and 200 μM). A second bout of hypoxia was applied at the end of the recording to ensure viability of the preparation over time and multiple drug exposures. (E, left) Summary data from ChNs as treated in A. Both concentrations of 5-HT tested failed to produce a signal significantly higher from the baseline fluorescence in normoxia (Friedman test, p>0.9999, n=5). (F, left) $Ca^{2+}$ imaging trace from a ChN in an adult isolated gill exposed to hypoxia followed by a second bout of hypoxia in the presence of the 5-$HT_3$ receptor antagonist,

MDL72222. (F, right) Summary data from ChNs as treated in A. 5-$HT_3$ blockade did not effect the ChN response to hypoxia (Wilcoxon matched-pairs signed rank test, p=0.8125, n=5).

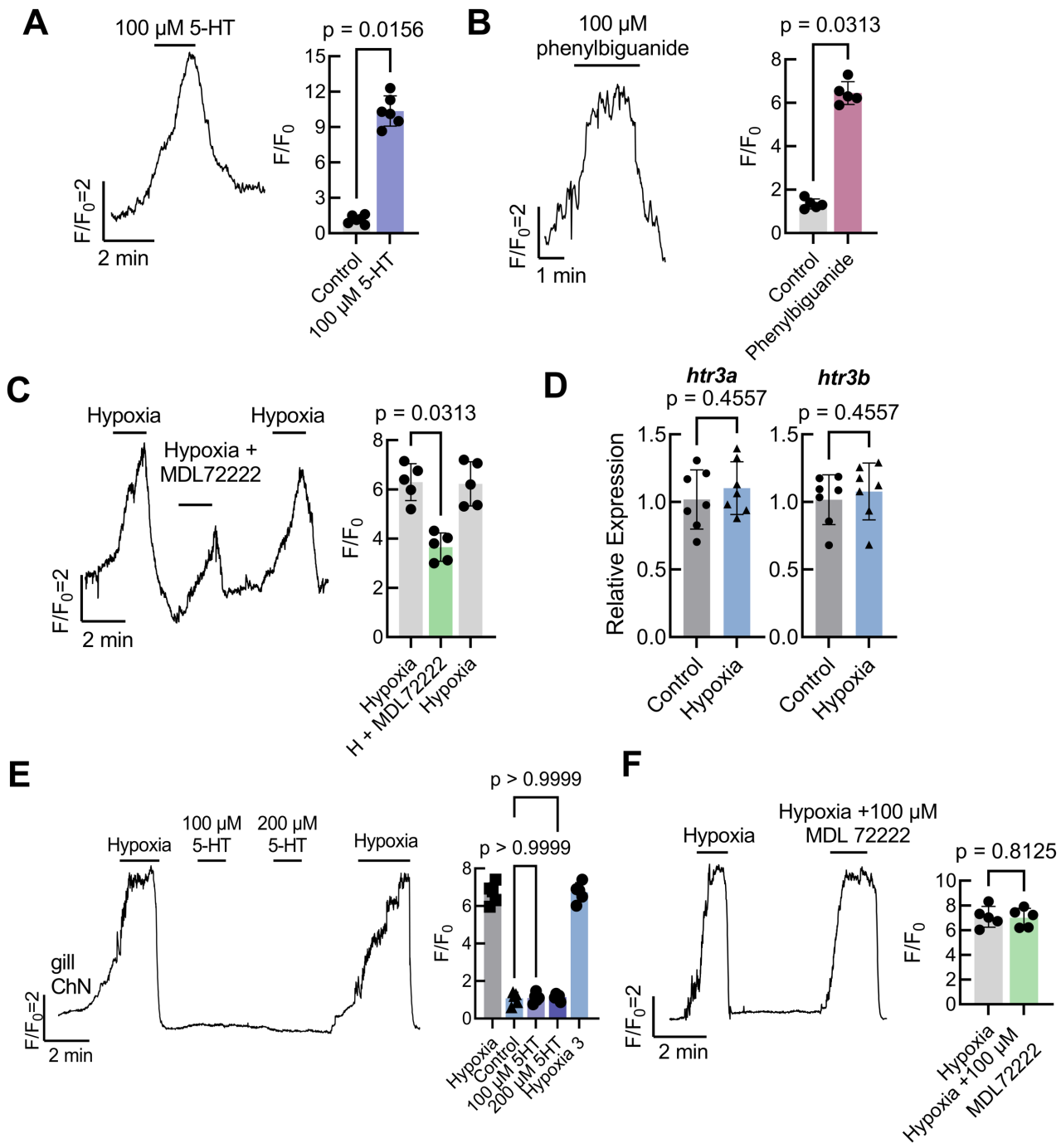
A
100 µM 5-HT
p = 0.0156
F/F0=2
2 min
F/F0
Control
100 µM 5-HT
B
100 µM
phenylbiguanide
p = 0.0313
F/F0=2
1 min
F/F0
Control
Phenylbiguanide
C
Hypoxia
Hypoxia
Hypoxia +
MDL72222
p = 0.0313
F/F0=2
2 min
F/F0
Hypoxia
H + MDL72222
Hypoxia
D
htr3a
p = 0.4557
htr3b
p = 0.4557
Relative Expression
Control
Hypoxia
Control
Hypoxia
E
Hypoxia
100 µM
5-HT
200 µM
5-HT
Hypoxia
p > 0.9999
p > 0.9999
gill
ChN
F/F0=2
2 min
F/F0
Hypoxia
Control
100 µM 5HT
200 µM 5HT
Hypoxia 3
F
Hypoxia
Hypoxia +100 µM
MDL 72222
p = 0.8125
F/F0=2
2 min
F/F0
Hypoxia
Hypoxia +100 µM
MDL72222

Figure 4.9

**Figure 4-10 Biorender schematic of a proposed mechanism of cholinergic hypoxia signalling via acetylcholine-type (A-type) NECs and chain neurons (ChN), and separate transmission of a hypoxia signal via serotonin-type (S-type) NECs.** (A) Biorender schematic of cranial nerve X innervation of the gills including the large vagal nerve (nodose) ganglion as well as the 4 epibranchial ganglia above each gill arch in a larval zebrafish. (B, left) highlighted view of a single gill filament showing distribution of A-type NECs, S-type NECs, and chain neurons (ChN). (B, right) Rotation of gill filament by 90° to show innervation of A-type and S-type NECs by ChN projections and nerve terminals from the extrabranchial nerve bundle. Our model suggests convergence of these two pathways before the nerve bundle exits the gill. (C) Close up view of A-type and S-type NEC signalling. A-type NECs (blue) contain ACh and transmit the hypoxia stimulus via nAChRs on postsynaptic ChNs. S-type NECs (green) contain 5-HT and transmit the hypoxia stimulus via $5HT_3$ receptors via a separate neural pathway from ChNs. Our model assumes both NEC populations of NECs are modulated by post-synaptic dopamine via $D_2$ receptors.

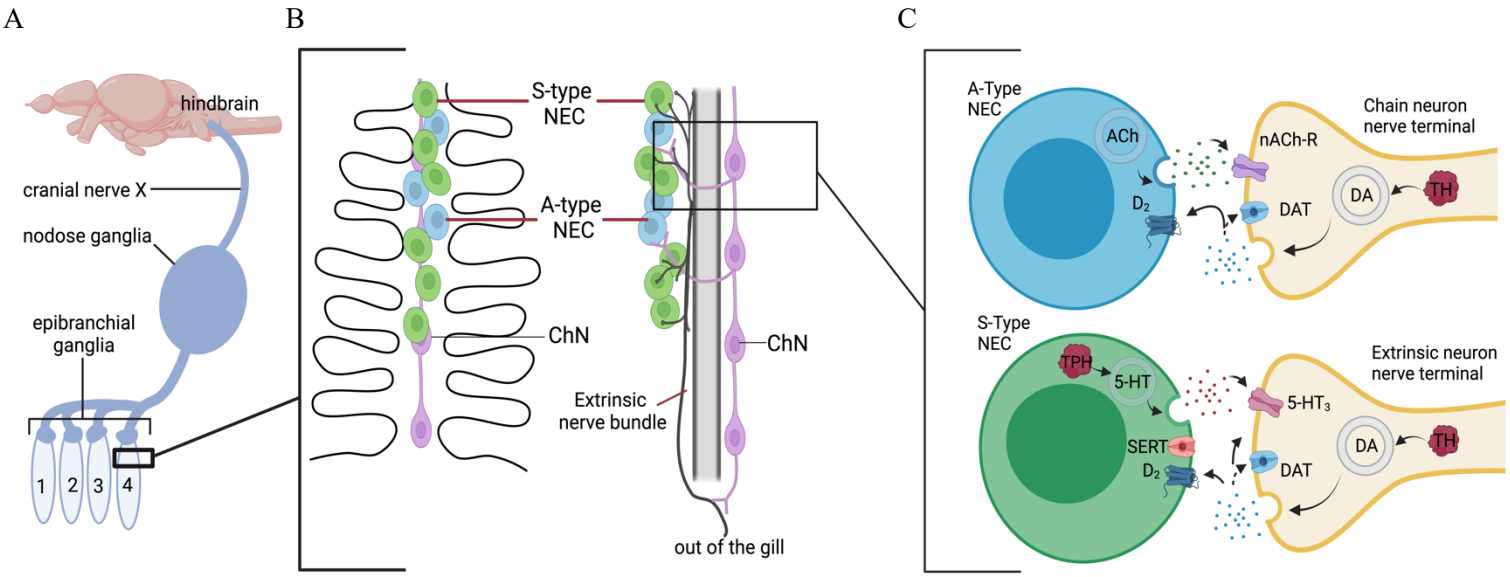
A
B
C
hindbrain
cranial nerve X
nodose ganglia
epibranchial ganglia
1
2
3
4
S-type NEC
A-type NEC
ChN
ChN
Extrinsic nerve bundle
out of the gill
A-Type NEC
ACh
D2
nACh-R
Chain neuron nerve terminal
DAT
DA
TH
S-Type NEC
TPH
5-HT
SERT
D2
5-HT3
DAT
DA
TH
Extrinsic neuron nerve terminal

Figure 4.10

## 4.5 Discussion

This study provides evidence for ACh as a key excitatory neurotransmitter in the hypoxia signaling pathway in zebrafish at the NEC-ChN synapse. Our findings demonstrate that exogenous ACh and nicotine significantly increase $[Ca^{2+}]_i$ in ChNs, indicating that the nicotinic acetylcholine receptors (nAChRs) mediate this excitatory response. We further provide evidence of endogenous hypoxia-induced ACh release and nAChR excitation and present the idea of two distinct populations of gill NECs: the ACh-containing A-type NECs, and the serotonin (5-HT) containing S-type NECs. This study not only sheds light on the functional organization of chemosensory cells in zebrafish but also addresses intriguing questions about the evolutionary conservation of cholinergic mechanisms in hypoxia responses across vertebrates.

### 4.5.1 Cholinergic Signaling in Chain Neurons (ChNs) and acetylcholine (ACh) containing neurosecretory cells in the gill.

While the role of ACh in hypoxia sensing is well-characterized in mammals, its function in fish gills remains less clear. Electrophysiological recordings from trout gills have shown that ACh and nicotine stimulate hypoxia-sensitive nerve fibers (Burleson and Milsom, 1995). Further, ACh, nicotine and hexamethonium have been used in zebrafish ventilation assays to show a cholinergic element of the hypoxic ventilatory response (Shakarchi et al. 2013; Jonz et al. 2015). In our investigations of the gill, we observed that the exogenous application of both ACh and nicotine effectively activates postsynaptic ChNs, indicating a shared mechanism for excitatory signaling through the targeting of nAChRs. This was further supported by the dose-dependent inhibition of the hypoxia-induced $[Ca^{2+}]_i$ increase by hexamethonium, a nAChR antagonist. The complete abolishment of the hypoxic response at higher concentrations of

hexamethonium indicates that cholinergic signaling is critical for the ChNs response to hypoxia. These results emphasize the role of cholinergic signaling in the ChNs response to hypoxia and suggest that similar mechanisms may underlie hypoxia responses across vertebrates.

In addition to its role in ChN activation, ACh appears to be released from specific neurosecretory cells in the gill epithelium. Chemosensory NECs in the gill filament epithelium can be identified by immunoreactivity to synaptic vesicle protein-2 (SV2), retention of the neurotransmitter 5-hydroxytryptophan (5-HT, serotonin) and/or expression of the vesicular monoamine transporter (*vmat2*) in zebrafish (Jonz & Nurse, 2003; Pan et al. 2021). Non-serotonergic, NEC-like cells containing the vesicular ACh transporter, VAChT, have also been previously described in zebrafish (Shakarchi et al., 2013; Zachar et al., 2017) and mangrove rivulus (*Kryptolebias marmoratus*; Regan et al., 2011).

The localization of ACh immunoreactivity in the present study to GCaMP-positive and SV2-positive NECs, but not to *vmat2*-expressing (serotonergic) NECs, suggests the existence of at least two distinct subpopulations of neurosecretory cells that differ by their stored neurotransmitters: the serotonin-containing S-type NEC, and the ACh-containing A-type NEC (Fig. 10A, B). A key observation in our study is the enhancement of ChN responses to nicotine during hypoxia, even though ChNs do not directly respond to hypoxia (Reed & Jonz, 2025). This suggests that hypoxia triggers the release of endogenous ACh, presumably from A-type NECs, which then activates ChNs via nAChRs. The fact that the response to nicotine is occluded at higher concentrations further supports the idea that hypoxia-induced ACh release and nicotine share the same receptor targets, and that there is a maximal level to the excitatory activation of ChNs, possibly reflecting receptor saturation.

### 4.5.2 Nicotinic acetylcholine receptor (nAChR) subunits in the gill.

While our physiological data suggest that hypoxia stimulates the release of endogenous ACh, which in turn activates cholinergic ChNs via nAChRs, evidence confirming the presence of nAChRs on ChNs, particularly in the gill, was lacking. To address this, it was essential to identify and localize the specific nAChR subunits expressed in the gill. Given the diversity of nAChR subtypes, we began by narrowing down the subunits expressed in this tissue. Our results demonstrate the expression of several nAChR subunits in the gill, including α2, α3, α4, α6, α7, β2, β3, and β4. Notably, exposure to hypoxia for 48 h upregulated the expression of α2, α3, β2, and β4 subunits, suggesting their involvement in the adaptive response to low-oxygen environments. The upregulation of nAChR subunits in response to hypoxia bears some similarities to mechanisms observed in the mammalian carotid body, where chronic hypoxia induces up-regulation of nicotinic receptor subunits (α3 and α7) on petrosal neurons that provide afferent innervation to the carotid body (Dinger et al., 2003). He et al. (2005) extended these findings by showing increased nicotinic receptor-mediated responses in afferent fibres that innervate type 1 cells (He et al., 2005). Previous research (Pan et al., 2022) has also implicated some of these subunits, such as α2 and β4, specifically in gill-associated neurons in zebrafish.

The α2 subunit can form heteromeric receptors with either β2 or β4 subunits, conformations that are known to mediate excitatory neurotransmission (Whiteaker et al., 2009). Interestingly, we observed that both β2 and β4 subunits were expressed in isolated gill tissue, with β4 showing a predominant neuronal localization in RNA sequencing studies (Pan et al., 2022), which aligns with our findings of α2 subunit expression in nerve fibers. Moreover, the upregulation of β2 and β4 expression following hypoxic exposure in the present study further suggests a functional role for these subunits in the hypoxia-induced adaptive mechanisms of

ChNs. Together, these results point to the potential formation of functional nAChRs in gill neurons, likely involving combinations of α2, β2, and/or β4 subunits that contribute to ChN activation during hypoxia.

Supporting this hypothesis, our immunohistochemical data show that α2 subunit immunoreactivity was closely associated with nerve fibers near NECs. ChN cell bodies are located beneath the filament artery, but their projections extend around the artery to form synapses with NECs (Jonz & Nurse, 2003). It is possible the α2-positive nerve fibers we observed near NECs are terminals of ChNs (see summary Fig. 10), further pointing to the idea that nAChRs, particularly those involving α2, β2, and β4 subunits, are involved in the hypoxia-induced activation of ChNs and the subsequent signaling in the gill. Future investigation of these beta subunits will be particularly interesting.

### 4.5.3 Cholinergic and serotonergic signaling in reflex hyperventilation.

ACh is well-established as a key neurotransmitter in respiratory control, particularly in the carotid body, where it plays a crucial role in the ventilatory responses to hypoxia (Nurse, 2005). Our study further investigates this role in zebrafish by exploring the involvement of cholinergic signaling in cranial nerve ganglia involved in reflex hyperventilation. Using transgenic zebrafish expressing GCaMP6s, we examined changes in $[Ca^{2+}]_i$ in vagal nerve ganglia, the nodose ganglion and epibranchial ganglia, in response to nicotine and ACh. The nodose ganglion responded to both ACh and nicotine in a manner similar to its response during hypoxia, suggesting that cholinergic signaling from the gill influences central respiratory control centers. Further, a significant time delay was observed between hypoxia, ACh and nicotine activation of the epibranchial ganglia (directly above the gill arches) and the nodose ganglion.

This delay in activation suggests directionality of the hypoxic signal, from the gill to higher order centers,. This supports the idea that ACh released from the gill during hypoxia may facilitate signaling in higher-order centers that control ventilation, ultimately contributing to the hyperventilatory response.

While ACh plays a central role in ChN-mediated hypoxia signaling, 5-HT also appears to be involved in the hypoxic response, but in a manner independent of the ChN pathway. Our findings suggest that 5-HT operates through 5-$HT_3$ receptors, potentially in the gill, displaying activity in higher order centres involved in reflex hyperventilation. The presence of both ACh-positive and 5-HT-positive NECs in the gill indicates that these two pathways may function in parallel, with 5-HT influencing reflexes related to ventilation through its action on extrabranchial neurons, while ACh regulates ChN-mediated signaling within the gill (see Fig. 10). Future studies will need to focus on identifying the specific receptors and neuronal circuits involved in the serotonergic pathway to fully understand how 5-HT and ACh contribute to the hypoxic response.

### 4.5.4 Implications of A-type and S-type NECs

The existence of two distinct populations of NECs in fish gills, A-type and S-type, suggests a more complex hypoxia signaling system than previously thought. This dual pathway system for hypoxia detection and signaling has several possible implications.

One possibility is that these two NEC populations are activated under different hypoxic conditions: threshold-dependant activation and/or time-dependant activation. The current study's experimental design, using a single severe level of hypoxia for a set duration, may not have fully captured the complexity of natural hypoxic conditions. In natural environments, fish often

experience varying levels and durations of hypoxia. Perhaps one population of gill NECs is activated at moderate levels of hypoxia, serving as an early warning system, whereas the other may be recruited at more severe levels of hypoxia, providing a graduated response. Similarly, one population might respond to acute, short-term hypoxia, whereas the other is more sensitive to chronic, prolonged hypoxic conditions.

Another possibility of these two distinct hypoxia signaling pathways is that each is more specialized for different oxygen-sensing mechanisms. The position of A-type NECs and S-Type NECs in the epithelium above the filament artery (eFa) puts them in a position where they could be sensing changes in environmental and/or arterial $PO_2$. Perhaps the S-type NECs might be more attuned to environmental $PO_2$, similar to serotonergic neuroepithelial bodies (NEBs) in mammalian airways (Cutz et al., 1993), while the A-type NECs are more attuned to arterial $PO_2$ like the type 1 cells (reviewed by Ortega-Sáenz & López-Barneo, 2020). Due to the homology between the carotid body and the first gill arch in fish, NECs were believed to be homologues of type 1 cells (Milsom and Burleson, 2007); however, recent evidence has suggested they may have a closer evolutionary link to pulmonary NEBs (Hockman et al., 2017). The results of the present study suggest A-type NECs may be type 1 cell homologues.

The idea of a dual pathway system in fish gills provides a fascinating model for understanding the evolution and complexity of oxygen sensing mechanisms across vertebrates. Further research is needed to elucidate the specific roles and interactions of A-type and S-type NECs in hypoxia signaling and respiratory regulation

## 4.6 Conclusion

This study provides new insights into the cholinergic signaling mechanisms underlying hypoxia detection and response in zebrafish gills. We demonstrate that ACh is a key excitatory neurotransmitter involved in the activation of chain neurons during hypoxia and that this pathway may contribute to the reflex hyperventilation observed in response to low oxygen levels. Additionally, we identify two distinct populations of neurosecretory cells in the gill—ACh-positive and 5-HT-positive—that contribute hypoxia signaling by different postsynaptic neurons. Finally, our findings suggest that the regulation of nicotinic receptor subunits during hypoxia acclimation plays a critical role in adapting the cholinergic system to low-oxygen conditions, pointing to a conserved role for cholinergic signaling in hypoxia adaptation across vertebrates.

# Chapter 5

# General Discussion

This thesis is the first to show excitatory neurotransmission at the NEC-ChN synapse in the gill and mechanism by which presynaptic $D_2$Rs provide a feedback mechanism that attenuates the chemoreceptor response to hypoxia. The studies presented here provide novel insights into the role of dopamine, acetylcholine, and serotonin in regulating hypoxia signalling and respiratory control in the gills of zebrafish. By drawing comparisons to both mammalian and non-mammalian vertebrates, we deepen our understanding of the evolutionary conservation and diversification of these pathways, offering valuable perspectives on how complex respiratory systems evolved to meet the demands of different environments. In this discussion, I will synthesize the findings from these studies within a broader comparative framework, highlighting the shared mechanisms across vertebrate species and discussing future directions.

## 5.1 Dopamine as a Modulator of Oxygen Sensing in the Gills

Our first two studies established the presence of dopamine and its modulatory effects in the gills of zebrafish, identifying a presynaptic role for dopamine $D_2$ receptors ($D_2$Rs) in regulating the chemoreceptor response to hypoxia. The data presented here strongly suggest that dopamine functions as modulator in a feedback mechanism that attenuates the hypoxic response of neuroepithelial cells (NECs). We showed that dopamine is synthesized and stored in sensory nerve terminals that innervate NECs, where activation of $D_2$Rs dampens the hypoxic response, likely through inhibition of intracellular signaling pathways such as cyclic AMP (cAMP) production.

These results align with what is known about dopamine in other chemoreceptive tissues, but they also highlight a unique species-specific organization in zebrafish gills. In mammalian models, dopamine is released by type 1 cells and acts via G-protein-coupled $D_2$Rs located both

presynaptically and postsynaptically in the carotid body (Nurse, 2010; Zhang et al., 2018). In contrast, our zebrafish model reveals a presynaptic localization of $D_2$Rs, with tyrosine hydroxylase (TH) expression found exclusively within postsynaptic nerves. Even within fish species, this organization varies; for example, in catfish (*Ictalurus punctatus*), 5-HT-positive NECs are co-labeled with TH, suggesting dopamine and 5-HT may both be released from NECs (Burleson et al., 2006), while other species like goldfish and trout show a lack of TH labeling in gill tissues (Porteus et al., 2013; Zaccone et al., 2003). Despite this interspecies variability, our results indicate that the feedback mechanism mediated by dopamine is likely an ancient and conserved feature of vertebrate physiology arising early in evolution. This feedback system may be an evolutionary adaptation common to many vertebrates, with fine-tuning at the synaptic level that reflects specific ecological needs.

### 5.2 Dopamine During Development: Role in Skin vs. Gill Chemoreception

Zebrafish provide an exciting model for studying the ontogeny of chemoreception. Early in development, cutaneous NECs may serve as the primary oxygen sensors, but a dramatic shift occurs around 7 days post-fertilization (dpf), when the gills become fully innervated and functional. This transition, which involves a reduction in skin NECs, presents a unique opportunity to investigate the role of dopamine in oxygen sensing across developmental stages.

Exogenous dopamine application in zebrafish larvae has been shown to decrease ventilation frequency as early as 7 dpf (Shakarchi et al., 2013), suggesting a feedback mechanism for dopamine on the chemoreceptor response to hypoxia emerges early in development. One hypothesis is that skin NECs may be modulated by $D_2$Rs similarly to gill NECs, indicating a conserved mechanism across life stages. Alternatively, it is possible that the

modulation observed at 7 dpf originates from the developing gills, suggesting that the transition from skin to gill oxygen sensing is a gradual shift rather than an abrupt switch.

Although larval ventilation assays are useful for chemical screening, assessing ventilation via buccal cavity movements in early larvae is challenging due to the continued reliance on cutaneous respiration. However, our zebrafish model allows for the evaluation of skin chemoreceptor activity using dopamine agonists and antagonists, providing a much higher temporal resolution for developmental studies. Understanding how dopamine feedback mechanisms develop in response to hypoxia could provide key insights into hypoxic acclimation processes. Future research could examine how early-life exposure to hypoxia or manipulation of dopaminergic signaling affects both the development of the dopaminergic system and the animal's sensitivity to hypoxia, offering broader implications for vertebrate acclimation strategies in fluctuating environments.

### 5.3 5-HT and ACh as Dual Pathways for Hypoxic Signaling

In addition to dopamine, we identified ACh and 5-HT as critical neurotransmitters in the transmission of hypoxic signals via gill NECs. In chapter 4 we confirmed the presence of both neurotransmitters in these cells, and their effects on ganglia associated with the vagus nerve suggest that both play a significant role in coordinating the ventilatory response to hypoxia. However, the precise contributions of ACh and 5-HT, as well as the dynamics of their interactions, remain unclear.

The zebrafish model utilized in this study presents an excellent opportunity to probe the developmental emergence of 5-HT and ACh in hypoxic sensing. Previous ventilation assays have demonstrated that zebrafish larvae exhibit a response to 5-HT before ACh (Shakarchi et al.,

2013), which suggests that the serotonergic system plays a primary role in early developmental responses to hypoxia. One possible interpretation of this sequence is that 5-HT is involved in initiating hypoxic responses, with ACh becoming more integral at later developmental stages or during sustained hypoxic conditions. This is particularly intriguing when considering that serotonergic neuroepithelial bodies (NEBs) in neonatal mammals are essential for oxygen sensing before the carotid body is fully functional (Cutz & Jackson, 1999). It raises the hypothesis that 5-HT may serve as the primary neurotransmitter in oxygen sensing not only in primitive vertebrates but potentially also in mammals during early development.

The evolutionary relationship between early vertebrate oxygen-sensing cells and the mammalian carotid body remains a subject of debate. Historically, due to the anatomical and functional similarities between the carotid body and the first gill arch in fish, NECs were thought to be homologous to type 1 cells of the carotid body (Milsom and Burleson, 2007). However, more recent work by Hockman et al. (2017) has challenged this view, suggesting that NECs might share a closer evolutionary link with serotonergic pulmonary epithelial bodies (NEBs). Their study demonstrated that 5-HT-positive NECs in zebrafish gills are of endodermal origin, which further complicates the homology between NECs and type 1 cells. When we consider the neurotransmitter profiles of these oxygen-sensing cells, we observe a notable commonality: both gill NECs and mammalian airway NEBs express 5-HT, while type 1 cells in the carotid body are characterized by their use and storage of ACh. In Chapter 4, we present evidence for a novel cholinergic NEC-ChN pathway, which introduces a new layer of complexity to the discussion of NEC-NEB and NEC-Type 1 cell homology. This new data prompts the question of how these findings fit within the broader evolutionary context. My interpretation of this is that the serotonergic NECs may be homologues of NEBs while these novel ACh-containing NECs in the

NEC-ChN pathway may present more homology with carotid body type 1 cells. This new cholinergic pathway could suggest a closer evolutionary relationship between these cells than previously appreciated, supporting the hypothesis that certain aspects of oxygen-sensing mechanisms may have been conserved across vertebrate evolution.

### 5.4 Interplay between neurotransmitters in the gill

Although our studies have revealed the roles of dopamine, ACh, and 5-HT in regulating oxygen sensing in the gills, several important questions remain regarding how these pathways interact, and what other signaling components might contribute to the regulation of chemoreception. The mechanism proposed in Chapter 4 (Figure 4.10) suggests that dopamine modulates both populations of NECs, as indicated by our previous co-localization of SV2 and $D_2$ receptors. Given that 5-HT and ACh NECs are both SV2-positive, it is reasonable to infer that both populations of NECs express $D_2$Rs, making dopamine a central modulator in the signaling network. However, questions still remain regarding the precise role of dopamine in this context, particularly in terms of how it modulates the interaction between these neurotransmitters at different levels and durations of hypoxia.

Additionally, other signaling molecules identified in recent chemical screens, such as purinergic components (ATP and adenosine), provide exciting avenues for further research (Coe et al., 2017). In mammals, ATP is co-released with ACh by type 1 cells in the carotid body, contributing to postsynaptic neuron activation (Zhang et al., 2000; Nurse, 2005). Interestingly, qPCR analysis has revealed purinergic and adenosine receptor expression in isolated gill tissue, raising important questions about how ATP might modulate NEC-ChN activity in zebrafish gills (Figure S-1). The zebrafish isolated gill preparation presented here may be particularly useful in

exploring how ATP and ACh interact within the NEC-ChN synapse and could uncover additional layers of regulation and crosstalk that contribute to the overall function of oxygen sensing.

The diversity of neurotransmitters and neuromodulators involved in gill oxygen sensing is striking, and it raises important questions about the necessity of such complexity. One plausible explanation is that this intricate signaling network reflects the varying levels and durations of hypoxia that animals encounter in natural environments. In response to these fluctuations, organisms likely require a highly adaptable and finely tuned system to appropriately modulate their ventilatory responses. This need for precision could underlie the observed mechanisms of plasticity, acclimatization, and sensitivity to oxygen levels, which vary over time and across developmental stages. For example, the changes in receptor expression following hypoxic exposure—such as those we have observed in our studies—suggest that these signaling pathways are integral to the process of acclimation. The dynamic regulation of these receptors could enable organisms to adapt to hypoxic stress in a way that supports both immediate and long-term respiratory needs, thereby maintaining homeostasis across different environmental conditions.

## 5.5 Conclusion

The work presented here provides novel insights into the role of dopamine, acetylcholine, and serotonin in generating a hypoxic signal within the gill and link the signalling by these neurotransmitters in the hypoxic signal sent to the brain. Still, much remains to be learned about the mechanisms involved across different levels and durations of hypoxia. Moreover, while zebrafish serve as an excellent model for understanding the evolutionary origins of oxygen

sensing and signaling, they represent just one species in a broader evolutionary context. Comparative studies across different fish species are essential to uncover the diversity of neurotransmitter roles and receptor organizations across various ecological niches. Additionally, examining fish species that routinely encounter chronic hypoxia could provide important insights into adaptive mechanisms at the level of the oxygen sensory cell and signalling pathways and help us better understand how vertebrate species have evolved to cope with environmental stressors.

# Appendix A: Supplemental Results

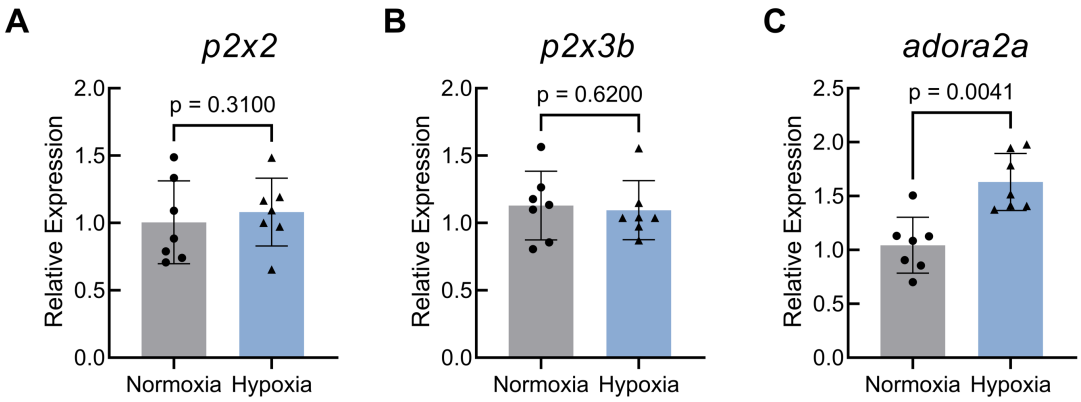


**Figure S-1. Relative gene expression of *p2x2, p2x3b*, and *adora2a* (encoding purinergic receptors P2X2, P2X3 and adenosine receptor) in isolated gill tissue.** Adenosine A2a receptor mRNA increased following 48 h of chronic hypoxia exposure. Data were normalized to the mRNA abundance of the reference gene, *ef1a*. Data were analyzed using a Mann–Whitney *U* test (n = 7).

# References

## Chapter 1 references


Bailly, Y., Dunel-Erb, S., Geffard, M., and Laurent, P. (1989). The vascular and epithelial serotonergic innervation of the actinopterygian gill filament with special reference to the trout, Salmo gairdneri. *Cell Tissue Res.* 258, 349–363.

Barnes, N. M., and Sharp, T. (1999). A review of central 5-HT receptors and their function. *Neuropharmacology* 38, 1083–1152.

Benot, A. R., and López-Barneo, J. (1990). Feedback Inhibition of Ca2+ Currents by Dopamine in Glomus Cells of the Carotid Body. *Eur. J. Neurosci.* 2, 809–812.

Booth, J. H. (1979). The Effects of Oxygen Supply, Epinephrine, and Acetylcholine on the Distribution of Blood Flow in Trout Gills. *J. Exp. Biol.* 83, 31–39.

Burleson M. L. (2009). Sensory innervation of the Gills: O2-sensitive chemoreceptors and mechanoreceptors. *Acta histochemica*, *111*(3), 196–206.

Burleson, M. L., Mercer, S. E., and Wilk-Blaszczak, M. A. (2006). Isolation and characterization of putative O2 chemoreceptor cells from the gills of channel catfish (Ictalurus punctatus). *Brain Res.* 1092, 100–107.

Burleson, M. L., and Milsom, W. K. (1995a). Cardio-ventilatory control in rainbow trout: I. Pharmacology of branchial, oxygen-sensitive chemoreceptors. *Respir. Physiol.* 100.

Burleson, M. L., and Milsom, W. K. (1995b). Cardio-ventilatory control in rainbow trout: II. Reflex effects of exogenous neurochemicals. *Respir. Physiol.* 101.

Burleson, M. L., and Smatresk, N. J. (1990). Evidence for Two Oxygen-Sensitive Chemoreceptor Loci in Channel Catfish, Ictalurus punctatus. *Physiol. Zool.* 63, 208–221.

Burnstock, G. (2018). Purine and purinergic receptors. *Brain Neurosci. Adv.* 2, 2398212818817494.

Caulfield, M. P. (1993). Muscarinic Receptors—Characterization, coupling and function. *Pharmacol. Ther.* 58, 319–379.

Coe, A. J., Picard, A. J., and Jonz, M. G. (2017). Purinergic and adenosine receptors contribute to hypoxic hyperventilation in zebrafish (Danio rerio). *Comp. Biochem. Physiol. -Part A Mol. Integr. Physiol.*

Dunel Erb, S., Bailly, Y., and Laurent, P. (1982). Neuroepithelial cells in fish gill primary lamellae. *J. Appl. Physiol. Respir. Environ. Exerc. Physiol.* 53.

Fu, X. W., Nurse, C. A., Wong, V., and Cutz, E. (2002). Hypoxia-induced secretion of serotonin from intact pulmonary neuroepithelial bodies in neonatal rabbit. *J. Physiol.* 539, 503–510.

Gonzalez, C., Almaraz, L., Obeso, A., and Rigual, R. (1994). Carotid body chemoreceptors: from natural stimuli to sensory discharges. *Physiol. Rev.* 74, 829–898.

Ho, T. N. T., Abraham, N., and Lewis, R. J. (2020). Structure-Function of Neuronal Nicotinic Acetylcholine Receptor Inhibitors Derived From Natural Toxins . *Front. Neurosci.* 14. Available at: https://www.frontiersin.org/article/10.3389/fnins.2020.609005.

Hockman, D., Burns, A. J., Schlosser, G., Gates, K. P., Jevans, B., Mongera, A., et al. (2017). Evolution of the hypoxia-sensitive cells involved in amniote respiratory reflexes. *Elife* 6, 1–28.

Hoyer, D., Hannon, J. P., and Martin, G. R. (2002). Molecular, pharmacological and functional diversity of 5-HT receptors. *Pharmacol. Biochem. Behav.* 71, 533–554.

Hughes, G. M. (1984). 1 general anatomy of the gills. In *Fish physiology* (Vol. 10, pp. 1-72). Academic Press.

Iturriaga, R., and Alcayaga, J. (2004). Neurotransmission in the carotid body: transmitters and modulators between glomus cells and petrosal ganglion nerve terminals. *Brain Res. Rev.* 47, 46–53.

Janvier, J. J., Peyraud-Waïtzenegger, M., and Soulier, P. (1996). Mediation of serotonin-induced hyperventilation via 5-HT3-receptor in European eel Anguilla anguilla. *J. Comp. Physiol. B* 165.

Jonz, M. G. (2018). Insights into the evolution of polymodal chemoreceptors. *Acta Histochem.* 120, 623–629.

Jonz, M. G., Fearon, I. M., and Nurse, C. A. (2004). Neuroepithelial oxygen chemoreceptors of the zebrafish gill. *J. Physiol.* 560, 737–752.

Jonz, M. G., and Nurse, C. A. (2003). Neuroepithelial cells and associated innervation of the zebrafish gill: A confocal immunofluorescence study. *J. Comp. Neurol.* 461, 1–17.

Jonz, M. G., & Nurse, C. A. (2008). New developments on gill innervation: insights from a model vertebrate. *The Journal of experimental biology*, *211*(Pt 15), 2371–2378.

Jonz, M. G., Zachar, P. C., Da Fonte, D. F., and Mierzwa, A. S. (2015). Peripheral chemoreceptors in fish: A brief history and a look ahead. *Comp. Biochem. Physiol. -Part A Mol. Integr. Physiol.* 186, 27–38.

Kalamida, D., Poulas, K., Avramopoulou, V., Fostieri, E., Lagoumintzis, G., Lazaridis, K., et al. (2007). Muscle and neuronal nicotinic acetylcholine receptors. *FEBS J.* 274, 3799–3845.

Kumar, P., and Prabhakar, N. R. (2012). Peripheral chemoreceptors: Function and plasticity of the carotid body. *Compr. Physiol.* 2, 141–219.

Laurent P (1984) Gill internal morphology. In: Hoar WS, Randall DJ (eds) Fish Physiology. vol XA, New York, Academic Press, pp 73–183.

Laurent P (1989) Gill structure and function: fish. In: Wood SC (ed) Comparative pulmonary physiology, New York, Marcel Dekker, pp 69–120.

Lauriano, E. R., Capillo, G., Icardo, J. M., Fernandes, J. M. O., Kiron, V., Kuciel, M., et al. (2021). Neuroepithelial cells (NECs) and mucous cells express a variety of neurotransmitters and neurotransmitter receptors in the gill and respiratory air-sac of the catfish Heteropneustes fossilis (Siluriformes, Heteropneustidae): a possible role in local immune defence. *Zoology* 148, 125958.

Lopez-Barneo, J., Lopez-Lopez, J. R., Urena, J., and Gonzalez, C. (1988). Chemotransduction in the carotid body: K+ current modulated by PO2 in type I chemoreceptor cells. *Science (80).* 241, 580–582.

Ma, K., Chen, Y., Zhou, L., Liu, Z., and Liu, Z. (2021). Cloning and characterization of nicotinic acetylcholine receptor γ-like gene in adult transparent Pristella maxillaris. *Gene* 769, 145193.

Martel, J. C., and Gatti McArthur, S. (2020). Dopamine Receptor Subtypes, Physiology and Pharmacology: New Ligands and Concepts in Schizophrenia. *Front. Pharmacol.* 11.

McDonald, M. D., Gilmour, K. M., Walsh, P. J., and Perry, S. F. (2010). Cardiovascular and respiratory reflexes of the gulf toadfish (Opsanus beta) during acute hypoxia. *Respir. Physiol. Neurobiol.* 170.

McKendry, J. E., Milsom, W. K., and Perry, S. F. (2001). Branchial CO(2) receptors and cardiorespiratory adjustments during hypercarbia in Pacific spiny dogfish (Squalus acanthias). *J. Exp. Biol.* 204, 1519–1527.

McKenzie, D. J., Taylor, E. W., Bronzi, P., and Bolis, C. L. (1995). Aspects of cardioventilatory

control in the adriatic sturgeon (Acipenser naccarii). *Respir. Physiol.* 100.

Milsom, W. K., and Burleson, M. L. (2007). Peripheral arterial chemoreceptors and the evolution of the carotid body. *Respir. Physiol. Neurobiol.* 157, 4–11.

Nurse, C. A. (2005). Neurotransmission and neuromodulation in the chemosensory carotid body. *Auton. Neurosci.* 120, 1–9.

Nurse, C. A. (2010). Neurotransmitter and neuromodulatory mechanisms at peripheral arterial chemoreceptors. *Exp. Physiol.* 95, 657–667.

Nurse, C. A. (2014). Synaptic and paracrine mechanisms at carotid body arterial chemoreceptors. *J. Physiol.* 592, 3419–3426.

Pan, Y. K., and Perry, S. F. (2020). Neuroendocrine control of breathing in fish. *Mol. Cell. Endocrinol.* 509, 110800.

Pan W, Godoy RS, Cook DP, Scott AL, Nurse CA, Jonz MG. (2022). Single-cell transcriptomic analysis of neuroepithelial cells and other cell types of the gills of zebrafish (*Danio rerio*) exposed to hypoxia. Scientific Reports

Peroutka, S. J., and Howell, T. A. (1994). The molecular evolution of G protein-coupled receptors: Focus on 5-hydroxytryptamine receptors. *Neuropharmacology* 33, 319–324.

Perry, S. F., Jonz, M. G., and Gilmour, K. M. (2009). "Chapter 5 Oxygen Sensing And The Hypoxic Ventilatory Response," in *Fish Physiology*.

Porteus, C. S., Brink, D. L., and Milsom, W. K. (2012). Neurotransmitter profiles in fish gills: Putative gill oxygen chemoreceptors. *Respir. Physiol. Neurobiol.* 184, 316–325.

Rahbar, S., Pan, W., and Jonz, M. G. (2016). Purinergic and Cholinergic Drugs Mediate Hyperventilation in Zebrafish: Evidence from a Novel Chemical Screen. *PLoS One* 11, e0154261.

Regan, K. S., Jonz, M. G., and Wright, P. A. (2011). Neuroepithelial cells and the hypoxia emersion response in the amphibious fish Kryptolebias marmoratus. *J. Exp. Biol.* 214.

Shakarchi, K., Zachar, P. C., and Jonz, M. G. (2013). Serotonergic and cholinergic elements of the hypoxic ventilatory response in developing zebrafish. *J. Exp. Biol.* 216, 869–880.

Stecyk, J. A. W., and Farrell, A. P. (2006). Regulation of the Cardiorespiratory System of Common Carp (Cyprinus carpio) during Severe Hypoxia at Three Seasonal Acclimation Temperatures. *Physiol. Biochem. Zool.* 79, 614–627.

Stensløkken, K.-O., Sundin, L., Renshaw, G. M. C., and Nilsson, G. E. (2004). Adenosinergic

and cholinergic control mechanisms during hypoxia in the epaulette shark (Hemiscyllium ocellatum), with emphasis on branchial circulation. *J. Exp. Biol.* 207, 4451–4461.

Sundin, L., Davison, W., Forster, M., and Axelsson, M. (1998). A role of 5-HT2 receptors in the gill vasculature of the antarctic fish Pagothenia borchgrevinki. *J. Exp. Biol.* 201, 2129–2138.

Wilson, J.M. and Laurent, P. (2002), Fish gill morphology: inside out. J. Exp. Zool., 293: 192-213.

Zachar, P. C., Pan, W., and Jonz, M. G. (2017). Characterization of ion channels and O2 sensitivity in gill neuroepithelial cells of the anoxia-tolerant goldfish (Carassius auratus). *J. Neurophysiol.* 118, 3014–3023.

Zhang, M., Zhong, H., Vollmer, C., and Nurse, C. A. (2000). Co-release of ATP and ACh mediates hypoxic signalling at rat carotid body chemoreceptors. *J. Physiol.* 525, 143–158.

Zhong, H., Zhang, M., and Nurse, C. A. (1999). Electrophysiological characterization of 5-HT receptors on rat petrosal neurons in dissociated cell culture. *Brain Res.* 816, 544–553.

## Chapter 2 references

Abdallah, S. J., Jonz, M. G. & Perry, S. F. (2015a) Extracellular H+ induces Ca2+ signals in respiratory chemoreceptors of zebrafish. Pflügers Archiv, 467, 399-413.

Abdallah, S. J., Thomas, B. S. & Jonz, M. G. (2015b). Aquatic surface respiration and Swimming behaviour in adult and developing zebrafish exposed to hypoxia. Journal of Experimental Biololgy, 218, 1777-1786.

Benot A & Lopez-Barneo J. (1990). Feedback inhibition of Ca2+ currents by dopamine in Glomus cells of the carotid body. European Journal of Neuroscience, 2, 809-812.

Boll., T., Lauweryns, J. M. & Lommel, A. V. (2000). Postnatal maturation of Neuroepithelial bodies and carotid body innervation: a quantitative investigation in the rabbit. Journal of Neurocytology, 29, 241-248.

Bradford, C. S., Sun, L., Collodi, P., & Barnes, D. W. (1994). Cell cultures from zebrafish embryos and adult tissues. Journal of Tissue Culture Methods, 16, 99-107.

Buckley, K., & Kelly, R. B. (1985). Identification of a transmembrane glycoprotein

specific for secretory vesicles of neural and endocrine cells. Journal of Cell Biology,100, 1284-1294.

Burleson, M. L., Mercer, S. E. & Wilk-Blaszczak, M. A. (2006). Isolation and characterization of putative O2 chemoreceptor cells from the gills of channel catfish (Ictalurus punctatus). Brain Research, 1092, 100-107.

Burleson, M. L. & Milsom, W. K. (1995). Cardio-ventilatory control in rainbow trout: II. Reflex effects of exogenous neurochemicals. Respiration Physiol, 101, 289-299.

Carroll, J. L., Boyle, K. M., Wasicko, M. J. & Sterni, L. M. (2005). Dopamine D2 receptor modulation of carotid body type 1 cell intracellular calcium in developing rats. American Journalof Physiology Lung Cell Molelcular Physiology, 288, L910-916.

Chen, Y. C., Priyadarshini, M. & Panula, P. (2009). Complementary developmental expression of the two tyrosine hydroxylase transcripts in zebrafish. Histochemistry and Cell Biology, 132,375-381.

Coe, A. J., Picard, A. J., & Jonz, M. G. (2017). Purinergic and adenosine receptors contribute to hypoxic hyperventilation in zebrafish (Danio rerio). Comparative Biochemistry and Physiology A Molecular and Integrative Physiology, 214, 50-57.

Fauquet, M. & Ziller, C. (1989). A monoclonal antibody directed against quail tyrosine hydroxylase: description and use in immunocytochemical studies on differentiating neural crest cells. Journal of Histochemistry and Cytochemistry, 37, 1197-1205.

Finley, J. C., Polak, J. & Katz, D. M. (1992). Transmitter diversity in carotid body afferent neurons: dopaminergic and peptidergic phenotypes. Neuroscience, 51, 973-987.

Gauda, E. B. (2002). Gene expression in peripheral arterial chemoreceptors. Microscopy Research and Technique, 59, 153-167.

Gonz.lez, C., Almaraz, L., Obeso, A. & Rigual, R. (1994) Carotid body chemoreceptors: from natural stimuli to sensory discharges. Physiological Reviews, 74, 829-898.

Huey, K. A. & Powell, F. L. (2000) Time-dependent changes in dopamine D2-receptor mRNA in the arterial chemoreflex pathway with chronic hypoxia. Molecular Brain Research, 75, 264-270.

Iturriaga, R., Alcayaga, J. & Gonzalez, C. (2009). Neurotransmitters in carotid body function: the case of dopamine-invited article. Advances in Experimental Medicine and Biology, 648.

Jonz, M. G. (2018). Insights into the evolution of polymodal chemoreceptors. Acta Histochemica, 120, 623-629.

Jonz, M. G., Fearon, I. M. & Nurse, C. A. (2004) Neuroepithelial oxygen chemoreceptors of the zebrafish gill. Journal of Physiology, 560, 737-752.

Jonz, M. G. & Nurse, C. A. (2003). Neuroepithelial cells and associated innervation of the zebrafish gill: A confocal immunofluorescence study. Journal of Comparative Neurology, 461:1-17.

Jonz, M. G. & Nurse, C. A. (2005). Development of oxygen sensing in the gills of zebrafish. Journal of Experimental Biology, 208, 1537-1549.

Kramer, D.L. & McClure, M. (1982). Aquatic surface respiration, a widespread adaptation to hypoxia in tropical freshwater fishes. Environmental Biology of Fishes, 7, 47-55.

Kumar, P. & Prabhakar, N. R. (2012) Peripheral chemoreceptors: Function and plasticity of the carotid body. Comprehensive Physiology, 2, 141-219.

Livak, K.J. & Schmittgen, T. D. (2001). Analysis of relative gene expression data using real-time quantitative PCR and the 2–DDCT Method. Methods, 25, 402-408.

Lopez-Barneo, J., L.pez-L.pez, J. R., Ure.a, J. & Gonz.lez, C. (1988) Chemotransduction in the carotid body: K+ current modulated by PO2 in type I chemoreceptor cells. Science, 241, 580-582.

Metcalfe, W. K, Myers, P. Z, Trevarrow, B., Bass, M. B. & Kimmel, C. B. (1990). Primary neurons that express the L2/HNK-1 carbohydrate during early development in the zebrafish. Development, 110, 491-504.

Milsom, W. K. & Burleson, M. L. (2007). Peripheral arterial chemoreceptors and the evolution of the carotid body. Respiratory Physiology and Neurobiology, 157, 4-11.

Mir, A. K., McQueen, D. S., Pallot, D. J. & Nahorski, S. R. (1984). Direct biochemical and neuropharmacological identification of dopamine D2-receptors in the rabbit carotid body. Brain Research, 291, 273-283.

Noble, S., Godoy, R., Affaticati, P. & Ekker, M. (2015). Transgenic zebrafish expressing mCherry in the mitochondria of dopaminergic neurons. Zebrafish, 12, 349-356.

Nurse, C. A. (2010). Neurotransmitter and neuromodulatory mechanisms at peripheral arterial chemoreceptors. Experimental Physiology, 95, 657-667.

Pan, W., Scott, A. L., Nurse, C. A. & Jonz, M. G. (2021). Identification of oxygen-sensitive

neuroepithelial cells through an endogenous reporter gene in larval and adult transgenic zebrafish. Cell and Tissue Research, 384, 35-47.

Pan W., Godoy, R. S., Cook, D. P., Scott, A. L., Nurse, CA & Jonz, M. G. (2022). Single-cell transcriptomic analysis of neuroepithelial cells and other cell types of the gills of zebrafish (Danio rerio) exposed to hypoxia. Scientific Reports, 12(1):10144.

Perry, S., Jonz, M.G. & Gilmour, K.M. (2009). Oxygen sensing and the hypoxic ventilatory response. In: Richards, J.G., Farrell, A.P., Brauner, C.J. (Eds.), Fish Physiology vol. 27. Academic Press, New York, pp. 193-253.

Porteus, C. S., Brink, D. L., Coolidge, E. H., Fong, A. Y. & Milsom, W. K. (2013). Distribution of acetylcholine and catecholamines in fish gills and their potential roles in the hypoxic ventilatory response. Acta Histochemica, 115, 158-169.

Powell, F., Milsom, W. & Mitchell, G. (1998). Time domains of the hypoxic ventilatory response. Respiration Physiology, 112, 123-134.

Qin, Z., Lewis, J. E. & Perry, S. F. (2010). Zebrafish (Danio rerio) gill neuroepithelial cells are sensitive chemoreceptors for environmental CO2. Journal of Physiology, 588, 861-872.

Rahbar, S., Pan, W. & Jonz, M. G. (2016). Purinergic and cholinergic drugs mediate hyperventilation in zebrafish: evidence from a novel chemical screen. PLoS One, 11(4):e0154261.

Schindelin, J., Arganda-Carreras, I., Frise, E., Kaynig, V., Longair, M., Pietzsch, T., Preibisch, S., Rueden, C., Saalfeld, S., Schmid, B., Tinevez, J. Y., White, D. J., Hartenstein, V., Eliceiri, K., Tomancak, P., & Cardona, A. (2012). Fiji: an open-source platform for biological-image analysis. Nature Methods, 9, 676-682.

Shakarchi, K., Zachar, P. C. & Jonz, M. G. (2013). Serotonergic and cholinergic elements of the hypoxic ventilatory response in developing zebrafish. Journal of Experimental Biology, 216, 869-880.

Timmerman, C. M. & Chapman, L. J. (2004). Behavioral and physiological compensation for chronic hypoxia in the sailfin molly (Poecilia latipinna). Physiological and Biochemical Zoology PBZ, 77, 601-610.

Tomares, S. M., Bamford, O. S., Sterni, L. M., Fitzgerald, R. S. & Carroll, J. L. (1994). Effects of domperidone on neonatal and adult carotid chemoreceptors in the cat. Journal of Applied Physiology, 77, 1274-1280.

Tom., M., Jim.nez, A. J., Richter, H., Vio, K., Berm.dez-Silva, F. J., Rodr.guez, E. M. & P.rez-F.gares, J. M. (2004). The subcommissural organ expresses D2, D3, D4, and D5 dopamine receptors. Cell and Tissue Research, 317, 65-77.

Trevarrow, B., Marks, D. L. & Kimmel, C. B. (1990). Organization of hindbrain segments in the zebrafish embryo. Neuron, 4, 669-679.

Wen, L., Wei, W., Gu, W., Huang, P., Ren, X., Zhang, Z., Zhu, Z., Lin, S. & Zhang, B. (2008). Visualization of monoaminergic neurons and neurotoxicity of MPTP in live transgenic zebrafish. Developmental Biology, 314, 84-92.

Westerfield, M. (2007). The zebrafish book. A guide for the laboratory use of zebrafish (Danio rerio) (5th ed.). Eugene, OR: University of Oregon Press.

Zaccone, G., Ainis, L., Mauceri, A., Lo Cascio, P., Lo Giudice, F. and Fasulo, S. (2003). NANC nerves in the respiratory air sac and branchial vasculature of the Indian catfish, Heteropneustes fossilis. Acta Histochemica, 105, 151-163.

Zachar, P. C. & Jonz, M. G. (2012). Neuroepithelial cells of the gill and their role in oxygen Sensing. Respiratory Physiology and Neurobiology, 184, 301-308.

Zachar, P. C., Pan, W. & Jonz, M. G. (2017a). Characterization of ion channels and O2 sensitivity in gill neuroepithelial cells of the anoxia-tolerant goldfish (Carassius auratus). Journal of Neurophysiology, 118, 3014-3023.

Zachar, P. C., Pan, W. & Jonz, M. G. (2017b). Distribution and morphology of cholinergic cells in the branchial epithelium of zebrafish (Danio rerio). Cell and Tissue Research, 367, 169-179.

## Chapter 3 references

Abdallah, S. J., Jonz, M. G., & Perry, S. F. (2015). Extracellular H+ induces $Ca^{2+}$ signals in respiratory chemoreceptors of zebrafish. *Pflügers Archiv*, 467, 399-413.

Almaraz, L., Wang, Z. Z., Stensaas, L. J., & Fidone, S. J. (1993). Release of dopamine from carotid sinus nerve fibers innervating type I cells in the cat carotid body. *Biological Signals*, 2(1), 16-26.

Bairam, A., & Carroll, J. L. (2005). Neurotransmitters in carotid body development. *Respiratory Physiology & Neurobiology*, 149(1-3), 217–232.

Bairam, A., Frenette, J., Dauphin, C., Carroll, J. L., & Khandjian, E. W. (1998). Expression of dopamine D1-receptor mRNA in the carotid body of adult rabbits, cats, and rats. *Neuroscience Research*, 31(2), 147–154.

Batuca, J. R., Monteiro, T. C., & Monteiro, E. C. (2003). Contribution of dopamine D2 receptors for the cAMP levels at the carotid body. In *Chemoreception: From Cellular Signaling to Functional Plasticity* (pp. 367-373). Springer US.

Beaulieu, J. M., & Gainetdinov, R. R. (2011). The physiology, signaling, and pharmacology of dopamine receptors. *Pharmacological reviews*, *63*(1), 182–217.

Benot, A., & López-Barneo, J. (1990). Feedback inhibition of $Ca^{2+}$ currents by dopamine in glomus cells of the carotid body. *European Journal of Neuroscience*, 2, 809-812.

Bisgard, G. E. (2000). Carotid body mechanisms in acclimatization to hypoxia. *Respiratory Physiology*, 121(2-3), 237-246.

Bradford, C. S., Sun, L., Collodi, P., & Barnes, D. W. (1994). Cell cultures from zebrafish embryos and adult tissues. *Journal of Tissue Culture Methods*, 16, 99–107.

Burleson, M. L., & Milsom, W. K. (1995). Cardio-ventilatory control in rainbow trout: II. Reflex effects of exogenous neurochemicals. *Respiration Physiology*, 101, 289-299.

Carroll, J. L., Boyle, K. M., Wasicko, M. J., & Sterni, L. M. (2005). Dopamine D2 receptor modulation of carotid body type 1 cell intracellular calcium in developing rats. *American Journal of Physiology: Lung Cellular and Molecular Physiology*, 288(5), L910-L916.

De Caro, R., Macchi, V., Sfriso, M. M., & Porzionato, A. (2013). Structural and neurochemical changes in the maturation of the carotid body. *Respiratory Physiology & Neurobiology*, 185(1), 9-19.

de Graaf, P.J.F. (1990). Innervation pattern of the gill arches and gills of the carp (*Cyprinus carpio*). J. Morphol., 206: 71-78.

Dunn, T. W., Mu, Y., Narayan, S., Randlett, O., Naumann, E. A., Yang, C. T., Schier, A. F., Freeman, J., Engert, F., & Ahrens, M. B. (2016). Brain-wide mapping of neural activity controlling zebrafish exploratory locomotion. *eLife*, 5, e12741.

Finley, J. C., Polak, J., & Katz, D. M. (1992). Transmitter diversity in carotid body afferent neurons: Dopaminergic and peptidergic phenotypes. *Neuroscience*, 51, 973–987.

Gauda, E. B. (2002). Gene expression in peripheral arterial chemoreceptors. *Microscopy Research and Technique*, 59(3), 153-167.

Gauda, E. B., Bamford, O. S., & Gerfen, C. R. (1996). Developmental expression of tyrosine hydroxylase, D2-dopamine receptor, and substance P genes in the carotid body of the rat. *Neuroscience*, 75, 969–977.

González, C., Almaraz, L., Obeso, A., & Rigual, R. (1994). Carotid body chemoreceptors: From natural stimuli to sensory discharges. *Physiological Reviews*, 74, 829-898.

Hockman, D., Burns, A. J., Schlosser, G., Gates, K. P., Jevans, B., Mongera, A., Fisher, S., Unlu, G., Knapik, E. W., Kaufman, C. K., Mosimann, C., Zon, L. I., Lancman, J. J., Dong, P. D. S., Lickert, H., Tucker, A. S., & Baker, C. V. (2017). Evolution of the hypoxia-sensitive cells involved in amniote respiratory reflexes. *eLife*, 6, e21231.

Huey, K. A., & Powell, F. L. (2000). Time-dependent changes in dopamine D2-receptor mRNA in the arterial chemoreflex pathway with chronic hypoxia. *Molecular Brain Research*, 75, 264–270.

Iturriaga, R., Alcayaga, J., & Gonzalez, C. (2009). Neurotransmitters in carotid body function: The case of dopamine-invited article. *Advances in Experimental Medicine and Biology*, 648, 137–143.

Jonz, M. G. (2018). Insights into the evolution of polymodal chemoreceptors. *Acta Histochemica*, 120, 623-629.

Jonz, M. G. (2024). Cell proliferation and regeneration in the gill. *Journal of Comparative Physiology B*. https://doi.org/10.1007/s00360-024-01548-2

Jonz, M. G., & Nurse, C. A. (2003). Neuroepithelial cells and associated innervation of the zebrafish gill: A confocal immunofluorescence study. *Journal of Comparative Neurology*, 461, 1-17.

Jonz, M. G., Fearon, I. M., & Nurse, C. A. (2004). Neuroepithelial oxygen chemoreceptors of the zebrafish gill. *Journal of Physiology*, 560, 737-752.

Kumar, P., & Prabhakar, N. R. (2012). Peripheral chemoreceptors: Function and plasticity of the carotid body. *Comprehensive Physiology*, 2, 141-219.

Leonard, E. M., Weaver, F. E., & Nurse, C. A. (2022). Lactate sensing by neuroepithelial cells isolated from the gills of killifish (Fundulus heteroclitus). *Journal of Experimental Biology*, 225(23), jeb245088.

Livermore, S., Zhou, Y., Pan, J., Yeger, H., Nurse, C. A., & Cutz, E. (2015). Pulmonary

neuroepithelial bodies are polymodal airway sensors: Evidence for $CO_2/H^+$ sensing. *American Journal of Physiology: Lung Cellular and Molecular Physiology*, 308(8), L807-L815.

López-Barneo, J., López-López, J. R., Ureña, J., & González, C. (1988). Chemotransduction in the carotid body: $K^+$ current modulated by PO2 in type I chemoreceptor cells. *Science*, 241, 580-582.

Montoro, R. J., Ureña, J., Fernández-Chacón, R., Alvarez de Toledo, G., & López-Barneo, J. (1996). Oxygen sensing by ion channels and chemotransduction in single glomus cells. *Journal of General Physiology*, 107(1), 133-143.

Milsom, W. K., & Burleson, M. L. (2007). Peripheral arterial chemoreceptors and the evolution of the carotid body. *Respiratory Physiology and Neurobiology*, 157, 4-11.

Mir, A. K., McQueen, D. S., Pallot, D. J., & Nahorski, S. R. (1984). Direct biochemical and neuropharmacological identification of dopamine $D_2$-receptors in the rabbit carotid body. *Brain Research*, 291, 273–283

Nilsson, S. (1984). 3 Innervation and Pharmacology of the Gills. In *Fish physiology* (Vol. 10, pp. 185-227). Academic Press.

Noble, S., Godoy, R., Affaticati, P., & Ekker, M. (2015). Transgenic zebrafish expressing mCherry in the mitochondria of dopaminergic neurons. *Zebrafish*, **12**, 349–356.

Nurse, C. A. (2010). Neurotransmitter and neuromodulatory mechanisms at peripheral arterial chemoreceptors. *Experimental Physiology*, 95, 657-667.

Pan, W., Godoy, R. S., Cook, D. P., Scott, A. L., Nurse, C. A., & Jonz, M. G. (2022). Single-cell transcriptomic analysis of neuroepithelial cells and other cell types of the gills of zebrafish (*Danio rerio*) exposed to hypoxia. *Scientific Reports*, 12(1), 10144.

Porteus, C. S., Abdallah, S. J., Pollack, J., Kumai, Y., Kwong, R. W., Yew, H. M., Milsom, W. K., & Perry, S. F. (2014). The role of hydrogen sulphide in the control of breathing in hypoxic zebrafish (*Danio rerio*). *Journal of Physiology*, 592(14), 3075-3088.

Powell, F. L. (2007). The influence of chronic hypoxia upon chemoreception. *Respiratory Physiology & Neurobiology*, 157(1), 154-161.

Qin, Z., Lewis, J. E., & Perry, S. F. (2010). Zebrafish (*Danio rerio*) gill neuroepithelial cells are sensitive chemoreceptors for environmental CO2. *Journal of Physiology*, 588, 861-872.

Reed, M., Pan, W., Musa, L., Arlotta, S., Mennigen, J. A., & Jonz, M. G. (2024). A role for

dopamine in control of the hypoxic ventilatory response via $D_2$ receptors in the zebrafish gill. *The Journal of Comparative Neurology*, 532(2), e25548.

Shakarchi, K., Zachar, P. C., & Jonz, M. G. (2013). Serotonergic and cholinergic elements of the hypoxic ventilatory response in developing zebrafish. *Journal of Experimental Biology*, 216, 869-880.

Sundin, L., & Nilsson, S. (2002). Branchial innervation. *Journal of Experimental Zoology*, 293(3), 232-248.

Usiello, A., Baik, J. H., Rougé-Pont, F., Picetti, R., Dierich, A., Le Meur, M., Piazza, P. V., & Borrelli, E. (2000). Distinct functions of the two isoforms of dopamine D2 receptors. *Nature*, 408(6809), 199–203.

Westerfield, M. (2007). *The zebrafish book: A guide for the laboratory use of zebrafish (Danio rerio)* (5th ed.). University of Oregon Press.

Zachar, P. C., & Jonz, M. G. (2012). Neuroepithelial cells of the gill and their role in oxygen sensing. *Respiratory Physiology and Neurobiology*, 184, 301-308.

Zachar, P. C., Pan, W., & Jonz, M. G. (2017). Characterization of ion channels and $O_2$ sensitivity in gill neuroepithelial cells of the anoxia-tolerant goldfish (Carassius auratus). *Journal of Neurophysiology*, 118, 3014-3023.

Zhang, L., Nurse, C. A., Jonz, M. G., & Wood, C. M. (2011). Ammonia sensing by neuroepithelial cells and ventilatory responses to ammonia in rainbow trout. *Journal of Experimental Biology*, 214(Pt 16), 2678-2689.

Zhang, M., Vollmer, C., & Nurse, C. A. (2018). Adenosine and dopamine oppositely modulate a hyperpolarization-activated current Ih in chemosensory neurons of the rat carotid body in co-culture. *Journal of Physiology*, 596(15), 3101-3117.

## Chapter 4 references

Bradford, C. S., Sun, L., Collodi, P., & Barnes, D. W. (1994). Cell cultures from zebrafish embryos and adult tissues. Journal of Tissue Culture Methods, 16, 99–107.

Burleson, M. L., & Milsom, W. K. (1995). Cardio-ventilatory control in rainbow trout: II. Reflex effects of exogenous neurochemicals. Respiration Physiology, 101, 289–299.

Cutz, E., Speirs, V., Yeger, H., Newman, C., Wang, D., & Perrin, D. G. (1993). Cell biology of

pulmonary neuroepithelial bodies--validation of an in vitro model. I. Effects of hypoxia and Ca2+ ionophore on serotonin content and exocytosis of dense core vesicles. *The Anatomical record*, *236*(1), 41–52.

Dinger, B., He, L., Chen, J., Stensaas, L., & Fidone, S. (2003). Oxygen Sensing: Responses and Adaptation to Hypoxia.

Dunn, T. W., Mu, Y., Narayan, S., Randlett, O., Naumann, E. A., Yang, C. T., Schier, A. F., Freeman, J., Engert, F., & Ahrens, M. B. (2016). Brain-wide mapping of neural activity controlling zebrafish exploratory locomotion. eLife, **5**, e12741

He, L., Dinger, B., & Fidone, S. (2005). Effect of chronic hypoxia on cholinergic chemotransmission in rat carotid body. *Journal of applied physiology (Bethesda, Md. : 1985)*, *98*(2), 614–619.

Jonz, M. G. & Nurse, C. A. (2003). Neuroepithelial cells and associated innervation of the zebrafish gill: A confocal immunofluorescence study. Journal of Comparative Neurology, 461:1-17.

Jonz, M. G. & Nurse, C. A. (2005). Development of oxygen sensing in the gills of zebrafish. Journal of Experimental Biology, 208, 1537-1549.

Jonz, M. G., Fearon, I. M., & Nurse, C. A. (2004). Neuroepithelial oxygen chemoreceptors of the zebrafish gill. *The Journal of physiology*, *560*(Pt 3), 737–752.

Kumar, P., & Prabhakar, N. R. (2012). Peripheral Chemoreceptors: Function and Plasticity of the Carotid Body. Compr. Physiol., 2, 141–219.

Lauriano, E. R., Capillo, G., Icardo, J. M., Fernandes, J. M. O., Kiron, V., Kuciel, M., et al. (2021). Neuroepithelial Cells (NECs) and Mucous Cells Express a Variety of Neurotransmitters and Neurotransmitter Receptors in the Gill and Respiratory Air-Sac of the Catfish Heteropneustes Fossilis (Siluriformes, Heteropneustidae): a Possible Role in Local Immune Defence. Zoology, 148, 125958.

Livak, K. J., & Schmittgen, T. D. (2001). Analysis of relative gene expression data using real-time quantitative PCR and the 2–ΔΔCT Method. Methods, 25, 402–408.

Nurse, C. A. (2005). Neurotransmission and Neuromodulation in the Chemosensory Carotid Body. Aut. Neurosci., 120, 1–9.

Nurse, C. A. (2010). Neurotransmitter and Neuromodulatory Mechanisms at Peripheral Arterial Chemoreceptors.

Ortega-Sáenz, P., & López-Barneo, J. (2020). Physiology of the Carotid Body: From Molecules to Disease. *Annual review of physiology*, *82*, 127–149.

Pan, W., Scott, A. L., Nurse, C. A., & Jonz, M. G. (2021). Identification of oxygen-sensitive neuroepithelial cells through an endogenous reporter gene in larval and adult transgenic zebrafish. Cell and Tissue Research, 384, 35–47.

Perry, S., Jonz, M.G. & Gilmour, K.M. (2009). Oxygen sensing and the hypoxic ventilatory response. In: Richards, J.G., Farrell, A.P., Brauner, C.J. (Eds.), Fish Physiology vol. 27. Academic Press, New York, pp. 193-253.

Porteus C. S., Brink D. L., Milsom W. K. (2012). Neurotransmitter Profiles in Fish Gills: Putative Gill Oxygen Chemoreceptors. Respir. Physiology Neurobiol. 184, 316–325.

Regan, K. S., Jonz, M. G., & Wright, P. A. (2011). Neuroepithelial Cells and the Hypoxia Emersion Response in the Amphibious fish Kryptolebias Marmoratus. J. Exp. Biol., 214, 2560–2568.

Shakarchi, K., Zachar, P. C., & Jonz, M. G. (2013). Serotonergic and cholinergic elements of the hypoxic ventilatory response in developing zebrafish. Journal of Experimental Biology, 216, 869–880.

Sundin, L., & Nilsson, S. (2002). Branchial innervation. *Journal of Experimental Zoology*, 293(3), 232-248.

Wen, L., Wei, W., Gu, W., Huang, P., Ren, X., Zhang, Z., Zhu, Z., Lin, S., & Zhang, B. (2008). Visualization of monoaminergic neurons and neurotoxicity of MPTP in live transgenic zebrafish. Developmental Biology, 314, 84–92.

Westerfield, M. (2007). *The zebrafish book: A guide for the laboratory use of zebrafish (Danio rerio) (5th ed.)*. University of Oregon Press

Whiteaker, P., Wilking, J. A., Brown, R. W., Brennan, R. J., Collins, A. C., Lindstrom, J. M., & Boulter, J. (2009). Pharmacological and immunochemical characterization of alpha2* nicotinic acetylcholine receptors (nAChRs) in mouse brain. *Acta pharmacologica Sinica*, *30*(6), 795–804.

Zhang, M., Zhong, H., Vollmer, C., & Nurse, C. A. (2000). Co-release of ATP and ACh mediates hypoxic signalling at rat carotid body chemoreceptors. The Journal of Physiology, 525, 143–158.

Zhong, H., Zhang, M., & Nurse, C. A. (1999). Electrophysiological Characterization of 5-HT

Receptors on Rat Petrosal Neurons in Dissociated Cell Culture. Brain Res., 816, 544–553.

Zachar, P. C., Pan, W., & Jonz, M. G. (2017). Characterization of ion channels and O2 sensitivity in gill neuroepithelial cells of the anoxia-tolerant goldfish (Carassius auratus). Journal of Neurophysiology, 118, 3014–3023.

## Chapter 5 references

Benot, A., & López-Barneo, J. (1990). Feedback inhibition of $Ca^{2+}$ currents by dopamine in glomus cells of the carotid body. *European Journal of Neuroscience*, 2, 809-812.

Burleson, M. L., Mercer, S. E., and Wilk-Blaszczak, M. A. (2006). Isolation and characterization of putative O2 chemoreceptor cells from the gills of channel catfish (Ictalurus punctatus). *Brain Res.* 1092, 100–107.

Carroll, J. L., Boyle, K. M., Wasicko, M. J. & Sterni, L. M. (2005). Dopamine D2 receptor modulation of carotid body type 1 cell intracellular calcium in developing rats. American Journalof Physiology Lung Cell Molelcular Physiology, 288, L910-916.

Coe, A. J., Picard, A. J., & Jonz, M. G. (2017). Purinergic and adenosine receptors contribute to hypoxic hyperventilation in zebrafish (Danio rerio). Comparative Biochemistry and Physiology A Molecular and Integrative Physiology, 214, 50-57.

Cutz E, Jackson A (1999) Neuroepithelial bodies as airway oxygen sensors. Respir Physiol 115:201–214.

Gauda, E. B. (2002). Gene expression in peripheral arterial chemoreceptors. *Microscopy Research and Technique*, 59(3), 153-167.

Iturriaga, R., Alcayaga, J. & Gonzalez, C. (2009). Neurotransmitters in carotid body function: the case of dopamine-invited article. Advances in Experimental Medicine and Biology, 648.

Mir, A. K., McQueen, D. S., Pallot, D. J. & Nahorski, S. R. (1984). Direct biochemical and neuropharmacological identification of dopamine D2-receptors in the rabbit carotid body. Brain Research, 291, 273-283.

Nurse, C. A. (2005). Neurotransmission and Neuromodulation in the Chemosensory Carotid Body. Aut. Neurosci., 120, 1–9.

Nurse, C. A. (2010). Neurotransmitter and Neuromodulatory Mechanisms at Peripheral Arterial Chemoreceptors.

Porteus, C. S., Brink, D. L., Coolidge, E. H., Fong, A. Y. & Milsom, W. K. (2013). Distribution of acetylcholine and catecholamines in fish gills and their potential roles in the hypoxic ventilatory response. Acta Histochemica, 115, 158-169.

Shakarchi, K., Zachar, P. C. & Jonz, M. G. (2013). Serotonergic and cholinergic elements of the hypoxic ventilatory response in developing zebrafish. Journal of Experimental Biology, 216, 869-880.

Zaccone, G., Ainis, L., Mauceri, A., Lo Cascio, P., Lo Giudice, F. and Fasulo, S. (2003). NANC nerves in the respiratory air sac and branchial vasculature of the Indian catfish, Heteropneustes fossilis. Acta Histochemica, 105, 151-163.

Zhang, M., Vollmer, C., & Nurse, C. A. (2018). Adenosine and dopamine oppositely modulate a hyperpolarization-activated current Ih in chemosensory neurons of the rat carotid body in co-culture. *Journal of Physiology*, 596(15), 3101-3117.

Zhang, M., Zhong, H., Vollmer, C., & Nurse, C. A. (2000). Co-release of ATP and ACh mediates hypoxic signalling at rat carotid body chemoreceptors. The Journal of Physiology, 525, 143.